MCR 74-474
NASA 8-30755

Volume I

Final Report

December 1974

Exhibit A

Payload/Orbiter Contamination Control Requirement Study

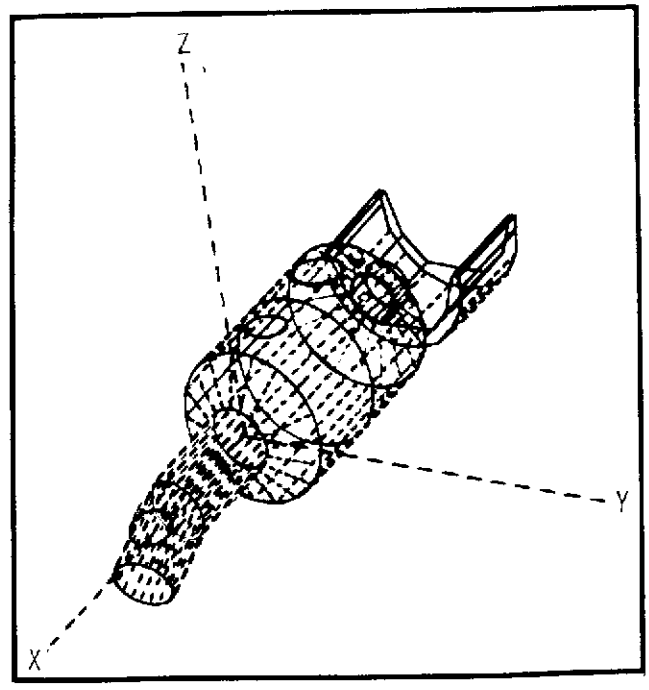

MARTIN MARIETTA

MCR-74-474
December 27, 1974

Technical Report

Volume I

Payload/Orbiter Contamination Control Requirement Study

Final Report
Exhibit A

Contract NAS8-30755

Authors

L. E. Bareiss
V. W. Hooper
R. O. Rantanen
E. B. Ress

Prepared for

George C. Marshall Space Flight Center
Marshall Space Flight Center, Alabama 35812

Martin Marietta Aerospace, Denver Division
Denver, Colorado 80201
P.O. Box 179

CONTENTS

CONTENTS (continued)

CONTENTS (continued)

CONTENTS (continued)

CONTENTS (continued)

CONTENTS (continued)

1. SCOPE

1.1 Purpose - The purpose of this study is to identify and quantify the expected molecular and particulate on orbit contaminant environment for selected Shuttle Payloads as a result of major Spacelab and Shuttle Orbiter contaminant sources. This study reviews individual Payload susceptibilities to contamination, identifies the combined induced environment, identifies the risk of Spacelab/Payload critical surface(s) degradation, and provides preliminary contamination recommendations. This study also establishes limiting factors which may depend upon operational activities associated with the Payloads, Spacelab, and the Shuttle Orbiter interface or upon independent Payload functional activities. This study will begin to support Spacelab Integrated Mission Planning and furnish a basis for Spacelab/Payload and Orbiter interface definition in the area of contamination control.

1.2 Scope - This report presents the development of a basic Spacelab contamination computer model which predicts the contaminant environment for three representative Spacelab configurations. The three configurations considered were:

a) a long module and short pallet;

b) a short module and long pallet; and

c) a long pallet.

In combination with an existing Shuttle Orbiter Contamination Model, the total induced environment for these configurations was predicted for the major contaminant sources considered.

The three Spacelab configurations have been synthesized by developing nodal descriptions of the important geometric surfaces. These nodal surfaces have been identified numerically and have been given an optical material characterization. The area of each nodal surface, the distance between nodal surfaces, the angular relationships, and geometric shadowing between nodal surfaces have been established. These relationships are presented as computer printout in Volume II of this report with a brief description of utilization. Based upon these geometrical considerations, nine lines-of-sight which encompass viewing requirements for both the contaminants and the anticipated Spacelab Payloads

have been established for the configurations a) and c) above. A comparison line-of-sight for configuration b) has also been developed to show the predicted induced environment variation as a function of the configurations.

Four major Spacelab contamination sources and flux characteristics based upon available data and experience/data from the Skylab Program have been identified and modeled consistent with the three Spacelab configurations. The principal Spacelab sources identified were outgassing and offgassing of the non-metallic material coatings, Spacelab module leakage (crew module and tunnel sections), and the Environmental Condensate Vent (ECV). Specific sources associated with the various experiments were not evaluated in this study.

Individual Spacelab/Payload configurations were reviewed to establish the contamination impact assessment on these configurations. Those Spacelab/Payload configurations reviewed were the:

a) Pallet/1.5 Meter Cryogenically Cooled Infrared Telescope;

b) Pallet/Deep Sky Ultraviolet Survey Telescope;

c) Pallet/1 Meter Ultraviolet Diffraction Limited Telescope;

d) Pallet/2.5 Meter Cryogenically Cooled Infrared Telescope;

e) Pallet/Apollo Telescope Mount Spacelab;

f) Pallet/Dedicated Solar Sortie Mission;

g) Module and Pallet/Scanning Spectroradiometer (Earth Observation); and

h) Module and Pallet/Atmospheric, Magnetospheric and Plasmas in Space (AMPS).

Two Payloads (one previously analyzed under NAS8-30452 - see Applicable Document MCR-74-93 and one called out in the

current study) were not assessed in this study. These are: 1) OA (Office of Applications) - this class of Payload has essentially been dropped and will be flown as portions of other Payload classes; and 2) CN-01-S Communications/Navigation Sortie Laboratory - this Payload has been removed from the Summarized NASA Payload Description - Sortie Payloads Level A and B Data Volumes dated July 1974.

In-Flight Contamination Control Criteria set forth in the above mentioned documentation for the Sortie Payloads and those stated in a memo from ES31/Bob Naumann to PM01/Bill Emanuel entitled "Definition of Contamination Monitor Requirements for Early Orbiter and Spacelab Missions" were used as the comparison basis for establishing the contamination impact upon the Spacelab/Payload combinations.

A qualitative assessment of the contaminant potential to typical Free Flying Payloads while stowed in the payload bay was made. An assessment of any potential contaminant impact such as deposition while stowed or during the operational phase when the Free Flying Payload is being deployed was made. A preliminary assessment of the torque and forces upon a typical Free Flying Payload was also established. In addition, an assessment of the Orbiter boost and reentry phase contaminant potential was made for these Payloads while stowed.

A review of ground control contamination measures was made to relate this potential particulate contaminant source to the on orbit induced environment. A review of ground control requirements established during the Skylab program for similar experiments/payloads was conducted. Cleanliness requirements were defined for Skylab where available with respect to different ground handling phases such that based upon types of clean room requirements, a relationship could be established for that particulate environment observed on Skylab. A review was also made of various manned and unmanned systems and available aircraft measurement programs for similar data. Results from these reviews were applied to establishing the potential of the particulate environment to be expected during on orbit operations as a result of ground handling. This particulate environment was related to those criteria set

forth for concerned Payloads. Recommendations are made where identifiable as to the ground control requirements necessary to minimize the on orbit particulate environment.

Based upon the defined flux levels and the locations of most sensitive Payload/operational surfaces, the types of contamination detection and monitoring instrumentation are discussed. Recommendations for the types of instrumentation are also discussed based upon the need to identify in real-time the contaminant level of the induced environment, the identification of the contaminant(s), and the impact of the contaminant upon the Payloads. For the types of detection instrumentation identified, preliminary contaminant levels were predicted which leads to the initial definition of the sensitivities and ranges of the particular contaminant detection instrumentation. Special interest was paid to those instruments which could provide real-time support of the Payloads and if necessary could provide supportive data for an experimenter or Payload system analyses with respect to any potential degradation of experimental data.

Conclusions and recommendations with respect to Payload risk, design, and operational aspects are presented. These recommendations are also presented with respect to support of the definition of the Orbiter interface and begin to develop a basis for overall Spacelab/Payload and Orbiter interface definition in the area of contamination control for Integrated Mission Planning.

1.3 Summary - This study was established to define and quantify the principle physical parameters and characteristics of the Spacelab and experiment surfaces which may be contaminant sources and/or susceptible to the Spacelab/Shuttle Orbiter induced environment. The results of the study begin to further define the requirements of Spacelab Payloads and experiments on Spacelab contamination control procedures. This study supports studies now being conducted and will furnish a continuing basis for Spacelab/experiment interface definition in the area of contamination control. The Spacelab configurations, sources, and supportive analyses contained in this report must be considered

preliminary since some program detail has not been identified to date. Where possible, anticipated conditions were assumed for completeness of analysis and are considered representative of expected situations. Many of the potential contamination impacts as identified by this study can be minimized by using alternate approaches, establishing operational constraints, and incorporating timely program controls. Additional studies will be required in those areas identified as potential contaminant problems in order to establish the necessary changes or improvements consistent to program requirements and objectives to minimize or eliminate the impact of the predicted contamination.

For those major Shuttle Orbiter and Spacelab steady state contamination sources modeled and under the assumptions used for this study, the predicted induced Shuttle Orbiter/Spacelab contaminant environment will be on the order of that anticipated and essentially observed on Skylab. Transient sources on the Shuttle Orbiter such as the RCS/VCS systems will produce higher predicted induced environments. The Skylab vehicle did not use an RCS/VCS system for primary attitude control. Certain Spacelab lines-of-sight may see momentarily higher induced environments depending upon the attitude and pointing control requirements for the particular Payload in question. A significant difference between the Shuttle Orbiter/Spacelab configuration is that on Skylab the majority of experiments viewed unidirectional and those sources which required venting could be positioned so as not to particularly impact any given line-of-sight. On the Shuttle Orbiter/Spacelab configuration, many of the Payloads will have off axis viewing requirements that encompass approximately 100 degrees of a 180 degree hemisphere. This may allow some lines-of-sight to be directly impacted by the flow field of a potential contamination source (e.g. VCS engines). In addition (due to reentry requirements for the Shuttle Orbiter), the present defined major vent type sources are all located on the top portion of the Orbiter and constrained to vent into the same hemisphere as the Payloads are looking.

One important aspect in establishing or defining the contamination control requirements for Spacelab/Payload configurations is identifying an acceptable environment. Although contamination controls were defined for the Skylab Program, on orbit criteria were not specifically identified because of the lack of total understanding of the induced environment. Skylab experience has brought additional technical insight into the

nature of the induced environment and its impact upon experiments such that it can be reasonably defined quantitatively. Subsequently, design criteria can now be established and used as a basis of evaluation as is in the case of this report where the criteria may apply.

The present induced environment definitions are specified in Volume X and summarized in Volume XIV of the JSC 07700 document and are stated as follows:

I. Purge gas will be 100 nominal, guaranteed class 5000, per FED-STD-209B with less than 15 ppm hydrocarbons (methane equivalent). Humidity will be less than $45 \pm 5\%$.

II. Internal surfaces maintained "visibly clean" which is interpreted to mean Class 300, per MIL-STD-1246A with non volatile residue (NVR) level A per JSC SN-C-0005.

III. No more than 1% absorption from IR through UV by condensibles on optical surfaces.

IV. Return flux of less than 10^{12} molecules/cm^2/second.

V. Background brightness from scattering or emission less than 20th magnitude/arc $second^2$ in the near ultraviolet.

VI. Fewer than 1 particle larger than 10 microns in a 4 arc minute half-angle field-of-view per orbit within 1 Km.

VII. Column density less than 10^{12} molecules/cm^2 for polar molecules.

The above specifications can be considered as design goals for contamination for the Shuttle Orbiter/Spacelab Program. They have been used in this study where possible for comparison where analysis can be related to each independent Payload to understand its relative susceptibility to contamination.

The following summary highlights those important contamination related conclusions and recommendations identified as a result of this study.

a) Selection of external Spacelab non-metallic material should be made with characteristic outgassing rates of no more than 1×10^{-9} g/cm^2/second at 100°C to meet the mass column density limits stated in Criteria VII. Currently stated materials criteria in Applicable Documents MSFC 50M02442 (0.04%/cm^2/hour) and JSC SO-R-0022 (total weight loss 1%) is approximately a factor of 6 greater than the recommended value. Specific surface thermal profiles, temperature dependence of the selected material, and external area of coverage will influence the final recommended outgassing rate.

b) Based upon the modeled Spacelab module leakage rates, leakage should present no problem to the induced environment. The total number column density exceeds Criteria VII but the dipole content of the leakage does not exceed the 10^{12} molecules/cm^2.

c) Either relocation of the Environmental Condensate Vent or changing specific vent characteristics (e.g. physical extent of vented plume) should be considered so that the vented plume would not be able to impinge upon any Shuttle Orbiter/Spacelab surfaces. Preliminary analysis has shown that clearing times similar to Skylab (approximately 15 minutes) can be established for the vented material once an acceptable location and/or specific vent characteristic have been selected.

d) Those Payloads which have been shown by this study to be especially sensitive to the predicted induced contaminant environment were the infrared, ultraviolet, and the AMPS Payloads.

    1) Infrared Payloads - For wavelengths greater than 3 micrometers, particles with radii greater than 300 microns will scatter a noise power in excess of that stated in Criteria V. For particles larger than 100 microns radii, the black body irradiance at the telescope focal plane will exceed the allowable limit. The basic question for infrared Payloads is the frequency of these

sightings. Based upon observed Skylab particle rates (1.3 particles/steradian/second), this would be approximately one every two or three orbits and should be no problem. Increased frequency of sighting could be of concern.

Molecular cloud absorption was calculated for the worst case predicted column densities and was determined to be less than 0.01 percent. The induced noise background from molecular scattering for worst case predicted column densities will present no significant noise contribution to the infrared Payloads.

The return flux deposition on the representative infrared telescope primary mirrors was calculated to be 0.23 microns (primarily for H_2O) resulting in less than a 2% absorption loss. The total deposition for a 30 day mission was approximately 0.98 microns resulting in approximately a 10% absorption loss. The increased surface scattering for the above deposition levels is expected to be negligible. Experimental programs have shown that deposition of H_2O on cryogenically cooled surfaces can significantly affect the surface emissivity and this effect should be evaluated further.

The major contributor to the predicted deposition is the Evaporator. The final Evaporator location has yet to be selected and the current baseline position used for this study could be considered as worst case. Final selection of the position of the Evaporator should significantly reduce the H_2O deposition potential to the infrared telescopes. The option may exist that the infrared Payloads could store the Evaporator effluents and then this particular source would not be an impact unless mission durations increased significantly and requiring orbital dumping of H_2O. Then, the impact of this vent would parallel that of the ECV from a contamination viewpoint.

2) Ultraviolet Payloads - For particle scattering, the 1 meter type telescope will see particles with radii greater than 1000 microns and the 0.75 meter telescope will see particles with radii greater than 100 microns. The impact of these particles upon these systems will depend upon their mode of operation and upon the particle size and dwell times in the field-of-view of the telescopes. For photographic surveys and imaging modes of operation, particles will appear as stars or as bright point sources and should not impact the resulting data. If the mode of operation is based upon long integration times for faint sources, then a particle of sufficient brightness and dwell time could influence the data being obtained. Particles on the order of 1 per orbit in the field-of-view or less should not affect these systems as in the case of the infrared telescopes unless the particle occurrence frequency increases.

For the molecular number column densities predicted in this study, both the scattering and the absorption appears to be of no concern for the two ultraviolet Payloads.

The ultraviolet Payloads as in the case of the infrared Payloads will be susceptible to deposition from the return flux. The reflectance loss for 100% exposure was calculated to reach the 1% maximum allowable of Criteria III at 2500Å for the 0.75 meter and the 1 meter systems in 2.5 and 3.5 days respectively. The outgassant contributions to the return flux contributed the most to the predicted values. The values of outgassing rates assumed for this study were based upon available data and the configuration considerations used. Tests currently under way at MSFC for simulated Orbiter tile configurations will present more specific data for evaluation. The above results must be weighed with this in mind.

3) Solar Oriented Payloads - The only instrument of this group that will be significantly susceptible to molecular and particulate cloud scattering will be the coronagraph type instrument. The molecular scattering was calculated for the worst case predicted number column density and was determined to be three orders of magnitude below the sensitivity of the coronagraph type instrumentation.

The photoheliograph and the scanning spectrometer type instruments are potentially susceptible to particle scattering but their fields-of-view are so small that the probability of a particle entering their fields-of-view is negligible. Particle scattering for the coronagraph instrument was assessed from the viewpoint of determining the minimum particle size required to produce a scattered light level of $B/B_{\odot} = 7x10^{-11}$ (the Skylab S052 sensitivity criteria). The analysis showed that particles in the near field ($d < 800$ meters) with radii greater than 1 micron will produce this equivalent scattering level. The Skylab S052 experiment observed particles on approximately 3% of its total data frames. If the Shuttle Orbiter/Spacelab configurations produce the same number of particles as Skylab, no significant data degradation is expected. However, if the Shuttle Orbiter/Spacelab particle production rate is greater than that of Skylab, then a degrading influence on the coronagraph data can be expected.

The return flux deposition was calculated for the primary optic of each of the analyzed solar physics class instruments. The analysis indicated that no significant instrument degradation will occur due to the return flux. Although these instruments are as susceptible as the ultraviolet telescopes, they have very limited physical acceptance angles for the contaminant (as contrasted to the much larger acceptance angles of ultraviolet telescopes).

Little detailed information is available for the high energy X-ray/ γ -ray instruments. They are not expected to be impacted by the contaminant induced environment.

4) AMPS Payload - The AMPS Payload instruments most likely to be effected are the ion probes and the mass spectrometers. Comparison of similar anticipated contaminant species with those of the ambient shows that the expected contaminant flux from the Shuttle Orbiter and Spacelab module leakage approaches the ambient N_2 and exceeds the O_2. H flux from the VCS exceeds the ambient as does A from offgassing. Under these conditions it may be difficult for the ion probes and the mass spectrometers to obtain representative data concerning the levels of ambient flux. The atmospheric science instruments on AMPS, in particular the ultraviolet measuring instruments, will see reflectance losses similar to those previously discussed for the ultraviolet Payloads. The induced environment is not anticipated to impact the subsatellite systems or those experiments which are designed to perturb the ambient environment.

e) The contamination potential of Free Flying Payloads was assessed based upon OMS engine burns for orbital considerations, the return flux of the induced environment, attitude control during deployment, stationkeeping, retrieval, and the potential impact of the 900 lb RCS engines to impart forces and torques upon a typical Free Flying Payload during retrieval. Geometric considerations indicate no direct line-of-sight exists between the Payloads and the OMS engines. The potential does exist that the Orbiter tail structure may reflect some material into the payload bay. Although there is no line-of-sight, the extensive flow fields of engines the size of the OMS must be closely evaluated for effects which may impact a Payload during these maneuvers. As these engines are developed and the final geometries become established, this potential problem should be

reassessed. A possible solution to this problem would be to close the payload bay doors during these firings.

The return flux deposition from the OMS engines for a 10 minute total burn could impact any thermal control surface in the payload bay. Changes in solar absorptivity could occur for thermal control paints like S13G. To eliminate this contaminant potential, the payload bay doors could be closed during the engine burn times or these burns could be timelined to a proper velocity vector orientation to allow minimum return flux deposition.

Once the desired orbit has been attained, the Free Flying Payload will reside in the payload bay for a time and be subjected to the return flux of the Shuttle Orbiter/Spacelab induced environment. For up to a seven day mission, return fluxes of the levels predicted should not detrimentally affect external operational surfaces of any Payload.

Applying the same type of analysis to the VCS engine (25 lb thrust) return flux, an orbital deposition rate of 1.3×10^{-10} g/cm^2/orbit is predicted for an engine firing once every 4.8 seconds for a 40 millisecond pulse. This is a worst case condition since the attitude and pointing requirements to fire the VCS at the above rate would not be required for Payload deployment periods. This yields a worst case return flux of 2.1×10^{-9} g/cm^2/day which should also be no problem for external Payload surface temperatures near 300^{o}K.

Approximately, a 12 minute period is required for a typical deployment mission (3A) of a Payload during which the manipulator arm deploys the Payload and attitude control is required. During this period, the Payload is susceptible to direct backflow contributions from the VCS engines. For a Payload

at 50 feet from the Orbiter X axis during deployment, the flux on a surface from the forward downward firing engines would be 3.1×10^{-14} g/cm^2/second and 2.9×10^{-13} g/cm^2/second for the aft outward firing engines (worst case for this configuration). The deposition rate resulting from these engines fluxes range from 6.2×10^{-17} to 5.8×10^{-16} g/cm^2/second and should be no problem. For distances closer than 50 feet, the deposition rate may increase slightly but still would be no problem because of the very low deposition levels. For small distances from the Orbiter, surface shadowing would block the engine backflow.

After deployment, the Shuttle Orbiter will remain in the vicinity (near 200 feet as stated for a 3A type mission) of the Payload for checkout and activation. During this time, the Payload will be susceptible to the normal contaminant sources of the Orbiter. Of these sources, outgassing will be the major source capable of depositing. The flux of the Orbiter outgassed materials at 200 feet is 2.3×10^{-11} g/cm^2/second for warm portions of the orbit. The total flux of all the sources is several orders of magnitude above the outgassing level but these are comprised of simple gases and will not deposit at the anticipated ambient Payload temperatures. For these temperatures, the anticipated outgassant deposition rate would be 1.2×10^{-11} g/cm^2/second. For short periods of checkout and activation on the order of hours, this rate should be no problem. However, for stationkeeping activities that may extend to periods of days, the potential deposition could accumulate to undesirable levels. Under these conditions, stationkeeping distances should be increased to distances on the order of a 1000 feet for maximum protection. The position of minimum contamination impact is forward and above the Orbiter providing the forward RCS engines are inhibited. This is also the best position for visual sighting by the Orbiter crew during this period.

During rendezvous with a Payload for retrieval, the 900 lb RCS engines on the Orbiter will be used for maneuvering and braking. In this case, there is the potential that the +Z firing 900 lb engines may be required for final rendezvous maneuvers. In this event, these engines could exhaust directly upon the Payload. For closing distances of 500 feet to 25 to 100 feet, a 10 second total firing from these engines could result in a change in solar absorptivity of a white thermal control paint. Depending upon the number of engine firings required to rendezvous, this could become a significant factor. A secondary factor is that under these conditions, these engines could impart a force or torque to the Payload which would result in increased attitude control requirements plus additional rendezvous maneuvers.

f) The on orbit contamination specifications, the contamination measurement requirements, the instrumentation requirements and location and positioning considerations of contamination monitors were evaluated. These evaluations covered a variety of instruments and their possible uses. The resulting recommended contamination monitoring instruments are summarized below:

1) Mass spectrometers;
2) Quartz Crystal Microbalances (QCMs);
3) Surface Material and Optical Element Samples;
4) Cameras;
5) Spectral Photoelectric Photometers;
6) Spectroreflectometer; and
7) Pressure Gages.

Ideally, from the standpoint of contamination investigation, multiple instruments of all the above should be considered and located within the payload bay and door areas with the exception of the mass spectrometer which should be located on the manipulator assembly to take advantage of spatial considerations. However, from economical and other practical

standpoints, at least one of all types should be used with two or more QCMs and cameras. If only a single package of instruments can be carried, it should be located as near the center and top of the payload bay as the particular mission payload will permit.

g) In comparison with the potential for contamination during on orbit operations (which can be at least semi-quantitatively treated) prelaunch contamination impact upon on orbit operations presents a much larger variable condition. Because of the enormous number of steps involved in selection of materials, design and manufacturing, fabrication, assembly, test, transportation, and storage of a complex spacecraft or Payload, it was found that it is extremely difficult to establish and perform systematic monitoring throughout these phases and treat them quantitatively.

Although quality control and protection procedures have been developed, identified, and generally implemented, a large spacecraft system such as Spacelab cannot be given the same degree of protection as a small individual laboratory developed Payload. In general, even with the best manufacturing control, the presence of a spacecraft in a clean room environment theoretically offers significant probability for particulate contamination of structural surfaces.

Those criteria which presently express an on orbit particle sighting or false star sighting tend to indicate that the Shuttle Orbiter/Spacelab Payload environment can be somewhat higher than that observed on Skylab. Criteria II translates to approximately 530 particles/second as compared to 16 particles/second observed by Skylab for particles of the same size class. Of all the criteria, this criteria may be the most difficult to relate to an effective control of on orbit particulate contamination.

An additional consideration is that from the Skylab Program and currently for the Shuttle/Spacelab Program, the molecular scattering does not appear to be a

significant contamination potential. How much submicron particles may add to the general scattering background is unknown. This may be answered eventually by the results of the T027 Photometer data analysis. Since the bonding strengths of submicron particles are very high in comparison to large particles and the probability of finding mechanical or electric forces on orbit to dislodge these particles is very small, surface cleanup techniques may tend to favor the larger particles. This indicates that special emphasis could be placed upon final cleanup as a way to minimize the potential on orbit particulate contamination in the 10 micron or larger size ranges. The most effective period for employing cleanup procedures of this nature would be as close as possible to final integration into the Shuttle Orbiter payload bay since any open storage of a Payload even in a clean room tends to add to the particulate potential. Where last minute cleanup is not practical, bagging and storage become an important consideration. Consideration could be given, prior to final closure of the Shuttle Orbiter payload bay, to performing a high degree of cleanup. This could eliminate the local particulate environment of the payload bay although the environment seen by the Shuttle Orbiter external surfaces just prior to launch and through boost may establish the final observed particulate environment.

This does not imply that the adequate and proper controls employed during other phases of ground development of a system or Payload are not necessary. It does imply that effective cleanup at the proper time may provide relief from final over restrictive and potentially timely final phases of Payload integration and still meet the criteria in limiting on orbit particulate contamination.

h) Contamination during launch, boost, and orbit insertion and during deorbit, reentry, and landing can occur from a number of sources as a result of a wide range of dynamic situations. The periods during which these contaminant sources can be an affect are either short lived or nothing can be done effectively to prevent their impact because of the existing conditions. Those sources which can be controlled to a certain degree are not considered severe. Although the cryogenically cooled infrared Payloads are recognized as potentially most susceptible, the anticipated employment of a Vacuum End Cap Assembly (VECA) and a vacuum external jacket should minimize any contaminant potential during these phases. Utilization of a VECA similar to that envisioned for the infrared Payloads could provide an effective contamination control measure for other classes of Payloads during these phases. Purging during these phases may also be an effective deterrent to contamination.

2. APPLICABLE DOCUMENTS

2.1 Program Documents - The following documents shown form a part of this report in the extent that they were used for Program information and/or are referenced for supporting technical material relevant to this study.

PROGRAM DOCUMENTS

MCR-74-93	"Payload/Orbiter Contamination Control Requirement Study," NAS8-30452, May 1974, Martin Marietta Aerospace - Denver Division.
Preliminary	"Summarized NASA Payload Descriptions - Sortie Payloads," Level A and B Data, July 1974, George C. Marshall Space Flight Center.
Preliminary	"Summarized NASA Payload Descriptions - Automated Payloads," Level A and B Data, July 1974, George C. Marshall Space Flight Center.
JSC 07700 Vol. X and XIV, Revision C	"Space Shuttle Program Space Shuttle System Payload Accommodations," July 3, 1974, Lyndon B. Johnson Space Center.
Rough Draft	"MRS Plume Test," R. Summerhays, LTV, Dallas, Texas.
Minutes	"Minutes from the 4th and 5th Particle and Gas Working Group Meetings," S. Jacobs, Lyndon B. Johnson Space Center.

Presentation	"European Spacelab Design and Development Effort," Parts A, C, and F, July 1974, ESRO/ESTEC.
Issue 3, Rev. 2	"Spacelab System Requirements (Level II)," Contract Document 8, October 15, 1973, ESRO/ESTEC.
RFP AO/600	"Proposal for the Spacelab Design and Development Contract to ESRO/ESTEC," April 16, 1974, ERNO.
SD 72-SH-0071B	"Orbiter Definition Handbook," Rockwell International, February 4, 1974.
Memo ES31/Bob Naumann to PM01/Bill Emanuel	"Definition of Contamination Monitor Requirements for Early Orbiter and Spacelab Missions," George C. Marshall Space Flight Center, September 19, 1974.
50M02442, Rev. W	"ATM Material Control for Contamination Due to Outgassing," George C. Marshall Space Flight Center, March 1, 1972.
SP-R-0022	"Specification Vacuum Stability Requirements of Polymeric Material for Spacecraft Application," Manned Spacecraft Center, Houston, Texas, December 12, 1969.

3. SPACELAB/ORBITER CONTAMINATION ANALYSIS

3.1 Modeling Considerations - The general modeling considerations and approach utilized in this study for the three Spacelab configurations modeled are identical to those used in establishing the Space Shuttle Orbiter Contamination Model reported in the MCR-74-93 report identified in the Applicable Documents Section. The following subsections treat specifically those considerations utilized for the three Spacelab configurations. A brief discussion is also presented to indicate the changes and status of the Orbiter configuration reflecting the most current available data identified and used for this study.

3.1.1 Spacelab Configurations - Three Spacelab configurations were selected to be representative of the largest majority of Spacelab/Payload configurations. The three configurations are schematically shown in Figures 1 through 3. For this study, the long module and short pallet, short module and long pallet, and the pallet only are referred to as the SL-1, SL-2, and SL-3 configurations respectively. The dimensions for the components of these configurations were obtained from the ESRO/ESTEC documents noted in the Applicable Documents Section.

The size envelope for the SL-1 configuration was directly obtained from these documents. The SL-1 configuration was placed in the Orbiter payload bay such that the end of the pallet would fall at the X_o= 1215.2 station. Positioning SL-1 in this manner allowed the remaining aft space of the payload bay to be compatible with the Orbital Maneuvering System (OMS) propulsion kit. The SL-2 and SL-3 configurations were both positioned to this envelope such that the aft portion of each of these configurations terminated at the X_o= 1215.2 station.

In the case of the SL-2 configuration, the forward tunnel was allowed to truncate at the Shuttle Orbiter forward bulkhead in order to insure a constant envelope for the OMS kit. This may have introduced a slight deviation from the actual structure, however, the resulting difference due to the tunnel length for the SL-2 configuration is felt to be very small in comparison to the total configuration.

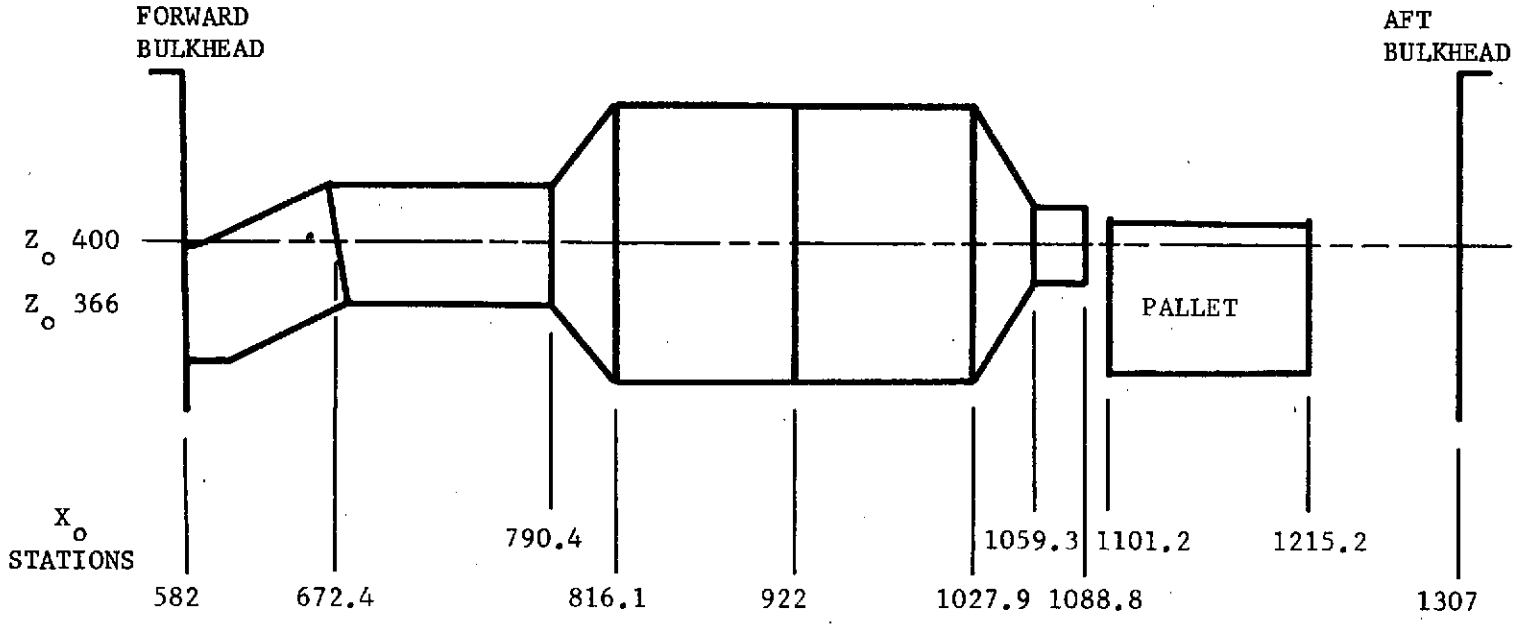

NOTE: FOR BREVITY THIS CONFIGURATION IS REFERRED TO AS SL-1 THROUGHOUT THIS REPORT AND SHOULD NOT BE CONFUSED WITH VARIOUS NUMBERING SYSTEMS USED FOR SPACELAB MISSIONS

Figure 1. Schematic Drawing of the Long Module/Short Pallet Spacelab Configuration (SL-1)

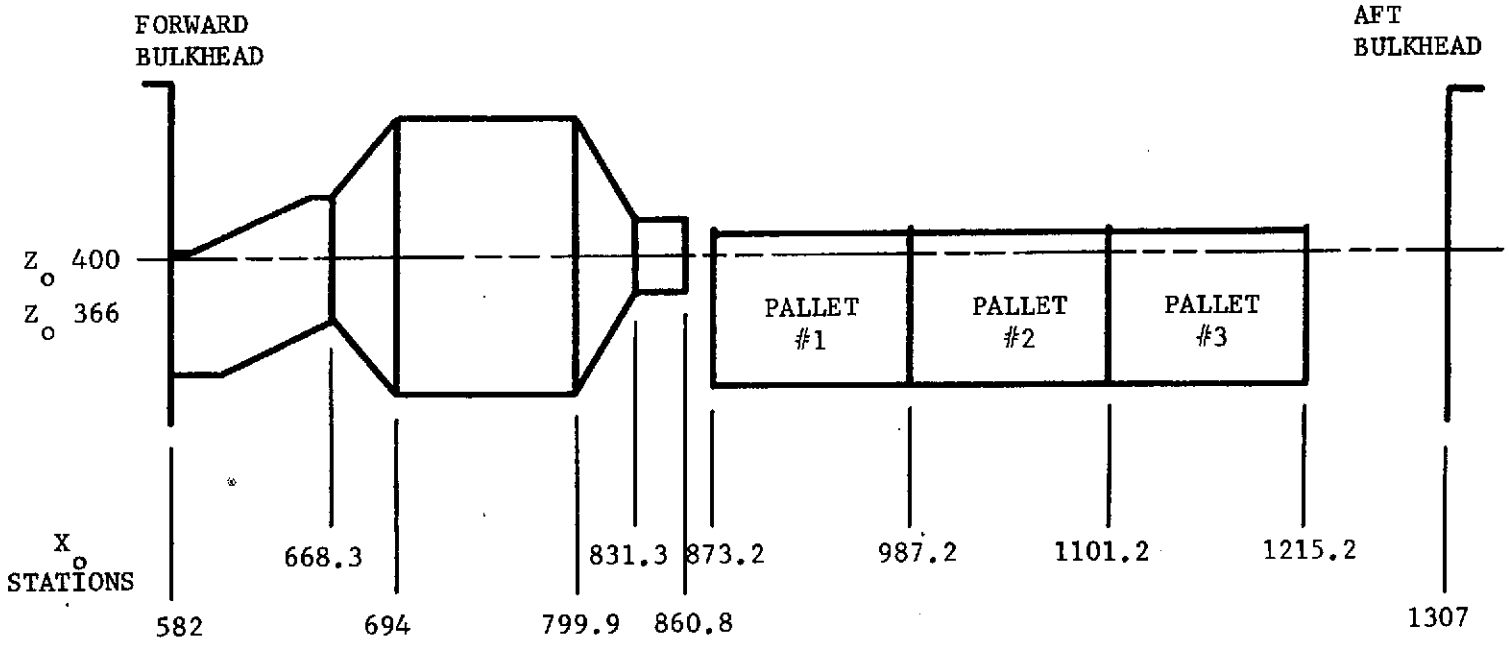

NOTE: FOR BREVITY THIS CONFIGURATION IS REFERRED TO AS SL-2 THROUGHOUT THIS REPORT & SHOULD NOT BE CONFUSED WITH VARIOUS NUMBERING SYSTEMS USED FOR SPACELAB MISSIONS

Figure 2. Schematic Drawing of the Short Module/Long Pallet Spacelab Configuration (SL-2)

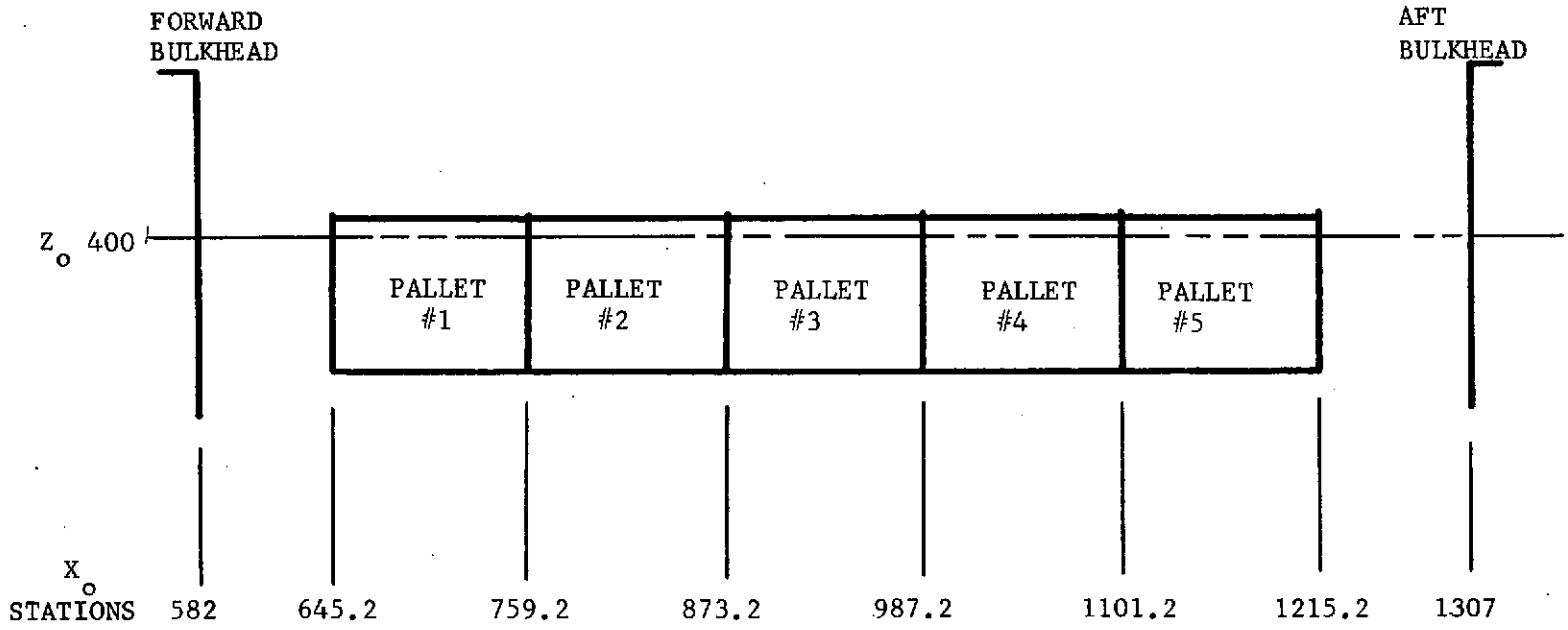

NOTE: FOR BREVITY THIS CONFIGURATION IS REFERRED TO AS SL-3 THROUGHOUT THIS REPORT & SHOULD NOT BE CONFUSED WITH VARIOUS NUMBERING SYSTEMS USED FOR SPACELAB MISSIONS

Figure 3. Schematic Drawing of the Pallet Only Spacelab Configuration (SL-3)

Figures 4 through 6 are computer drawn graphic displays of the modeled SL-1, SL-2, and SL-3 configurations respectively. The SL-1 configuration has been modeled by 29 geometric surfaces including the following major or critical surfaces/sources:

a) Environmental Condensate Vent;
b) experiment segment;
c) core segment;
d) aft airlock;
e) Extravehicular Activity (EVA) hatch;
f) core segment window;
g) experiment segment window;
h) aft viewing window; and
i) tunnel.

The SL-2 configuration has been modeled by 42 surfaces including the following major or critical surfaces/sources:

a) Environmental Condensate Vent;
b) core segment;
c) aft airlock;
d) core segment window;
e) aft viewing window; and
f) tunnel.

The SL-3 configuration has been modeled by 50 surfaces using 10 surfaces per pallet segment. The 10 surfaces per pallet segment were also used for each of the above configurations. Figure 7 shows a computer drawn graphic display of the SL-2 configuration integrated into the Shuttle Orbiter payload bay. The coordinate system used for the Spacelab configurations was based upon that currently in the Orbiter model and is representative of a system referenced to the main launch vehicle.

A number scheme was developed for the Spacelab configuration surfaces different than that of the Shuttle Orbiter Contamination Model. Presently, the Orbiter model uses a numbering system from 1 through 999 while each individual Spacelab configuration uses a numbering system from 1000 to 1999. For each Spacelab configuration where similar surfaces are identified, the similar surfaces are numbered alike. Volume II of this report presents the computer listings of these surfaces and the respective

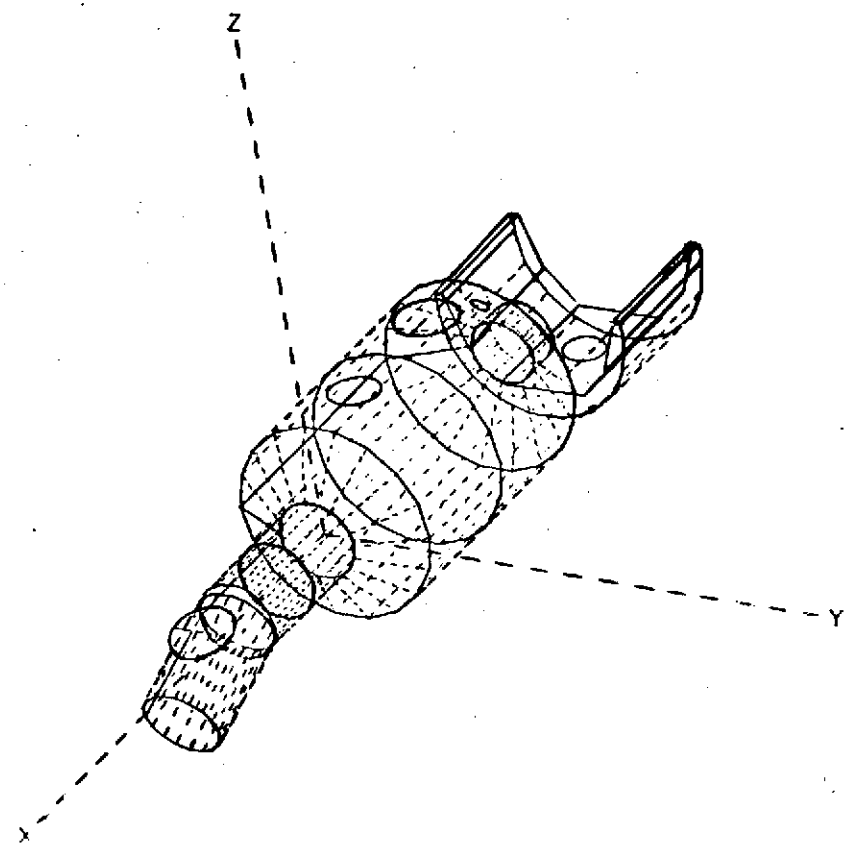

Figure 4. Computer Drawing of the Long Module/Short Pallet Spacelab Configuration (SL-1)

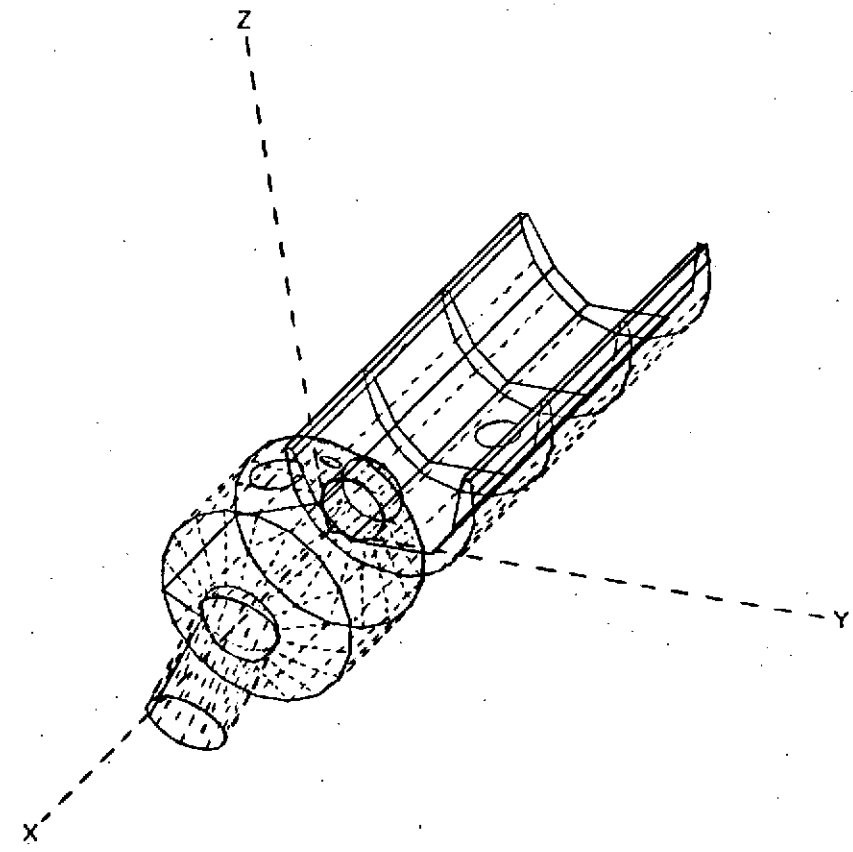

Figure 5. Computer Drawing of the Short Module/Long Pallet Spacelab Configuration (SL-2)

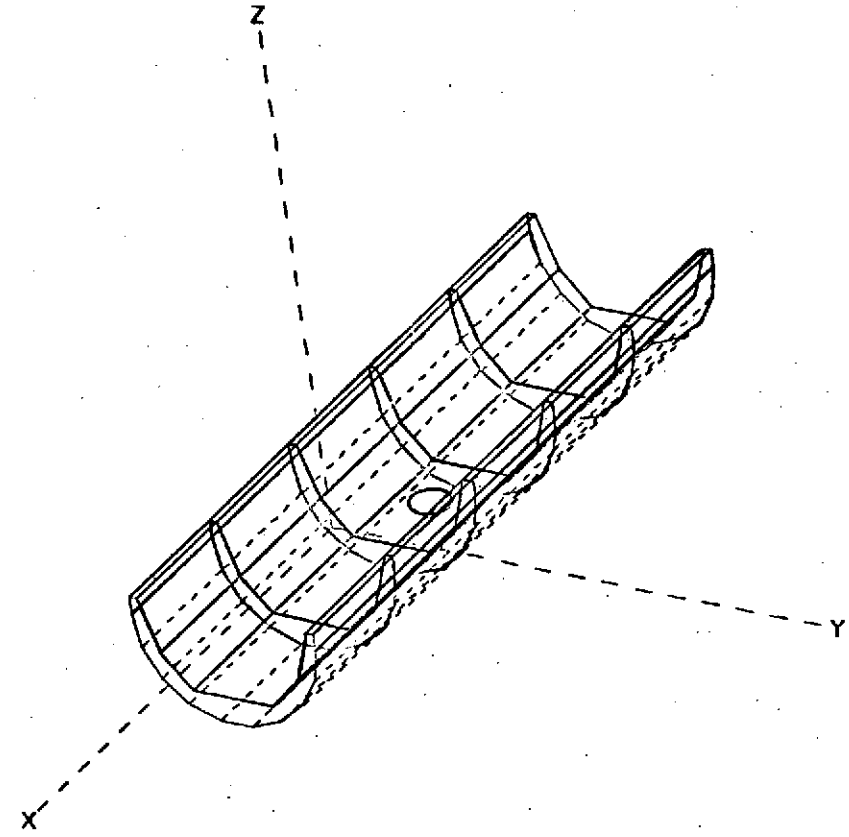

Figure 6. Computer Drawing of the Pallet Only Spacelab Configuration (SL-3)

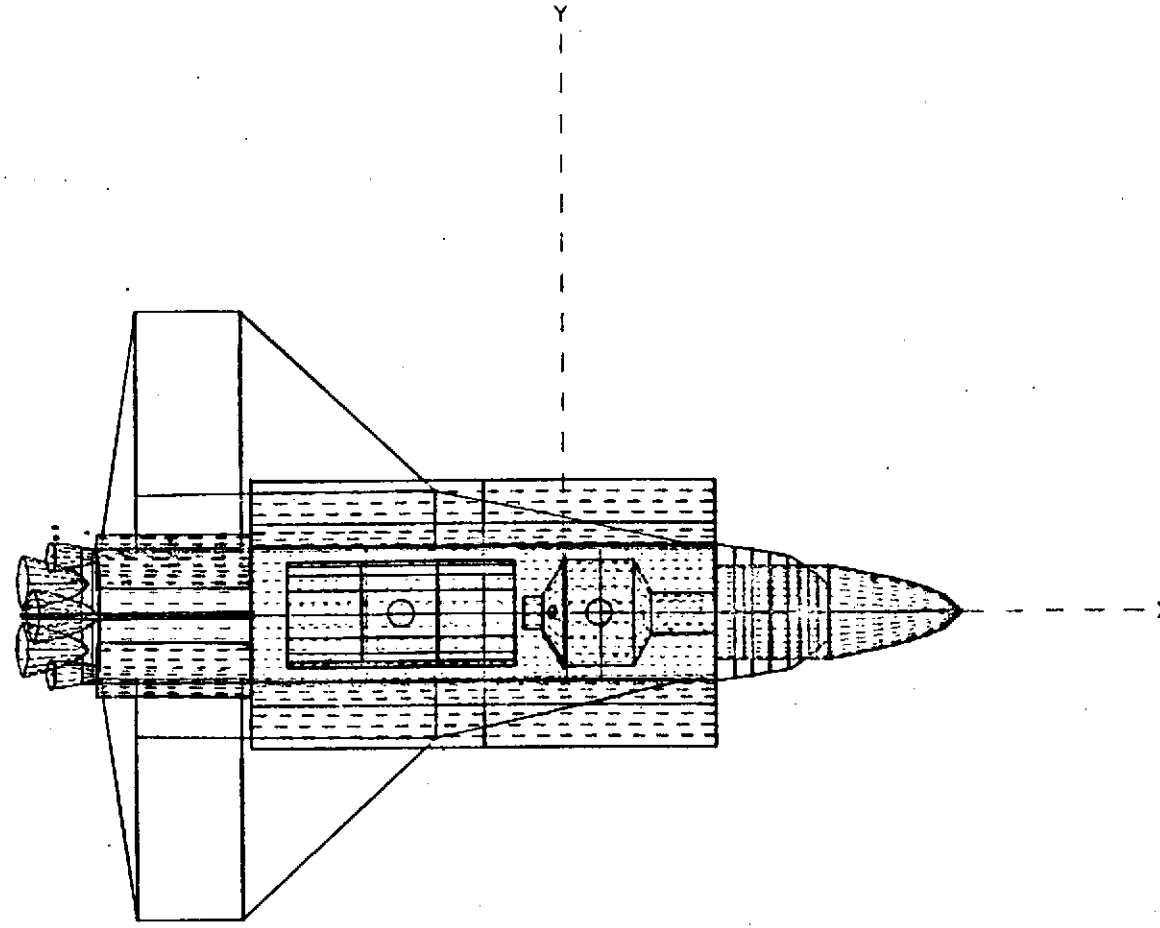

Figure 7. Computer Drawing of the Spacelab SL-2 Configuration Integrated into the Shuttle Orbiter Payload Bay

numbering system. This numbering system will allow future extension to a surface/material mapping capability if desired.

3.1.2 Modeled Spacelab Sources - Four major Spacelab sources were identified. These are outgassing and offgassing for the non-metallic thermal control surface coatings, Spacelab module leakage (crew modules and tunnel sections), and the Environmental Condensate Vent system. The latter two sources are of no consideration for the SL-3 configuration since they are associated with the man/module interface of the SL-1 and SL-2 configurations.

Review of the ESRO/ESTEC documents noted in the Applicable Document Section indicated that all solar oriented surfaces were coated with a white thermal control paint (S13G) while the anti solar surfaces were coated with a high reflective material. S13G is a soft, rubbery thermal control coating composed of zinc oxide and an RTV 602 binder which demonstrates a characteristic mass loss when exposed to vacuum. A steady state outgassing rate of $1x10^{-8}g/cm^2$/second at $100^{o}C$ was assumed for the S13G paint. This was based upon data available from pre-Skylab testing and results gained from Skylab flight experience. A corresponding offgassing rate for the first 100 hours was assumed to be $2.5x10^{-7}g/cm^2$/second at $100^{o}C$ at the 10 hour point in the decay curve for offgassing. The 10 hour point was chosen to be indicative of that time after launch when early on orbit checkout and operational activities can be expected to commence. Figure 8 depicts graphically the relationships used in modeling these sources. This data was developed from materials typical of those used for thermal control materials.

The Spacelab module leakage (crew modules and tunnel sections) was taken to be 1.35 kg/day for both the SL-1 and SL-2 module based upon the given maximum leak rate as identified in the European Spacelab Design and Development Effort Part F. This source was assumed to leak uniformly from all top side module surfaces. The Environmental Condensate Vent has not been adequately defined to date. Since this vent apparently will be similar to that established for Skylab (e.g. operational usage and nozzle/orifice design and size), values developed through the Skylab Contamination Ground Test Program for the Skylab contingency ECV were assumed for this source. Table I presents a summary of the major Spacelab sources considered and their characteristics. No experiment sources were considered.

In this study, potential sources from any experiment or Payload were not considered since sufficient detail is not available for the experiments in general.

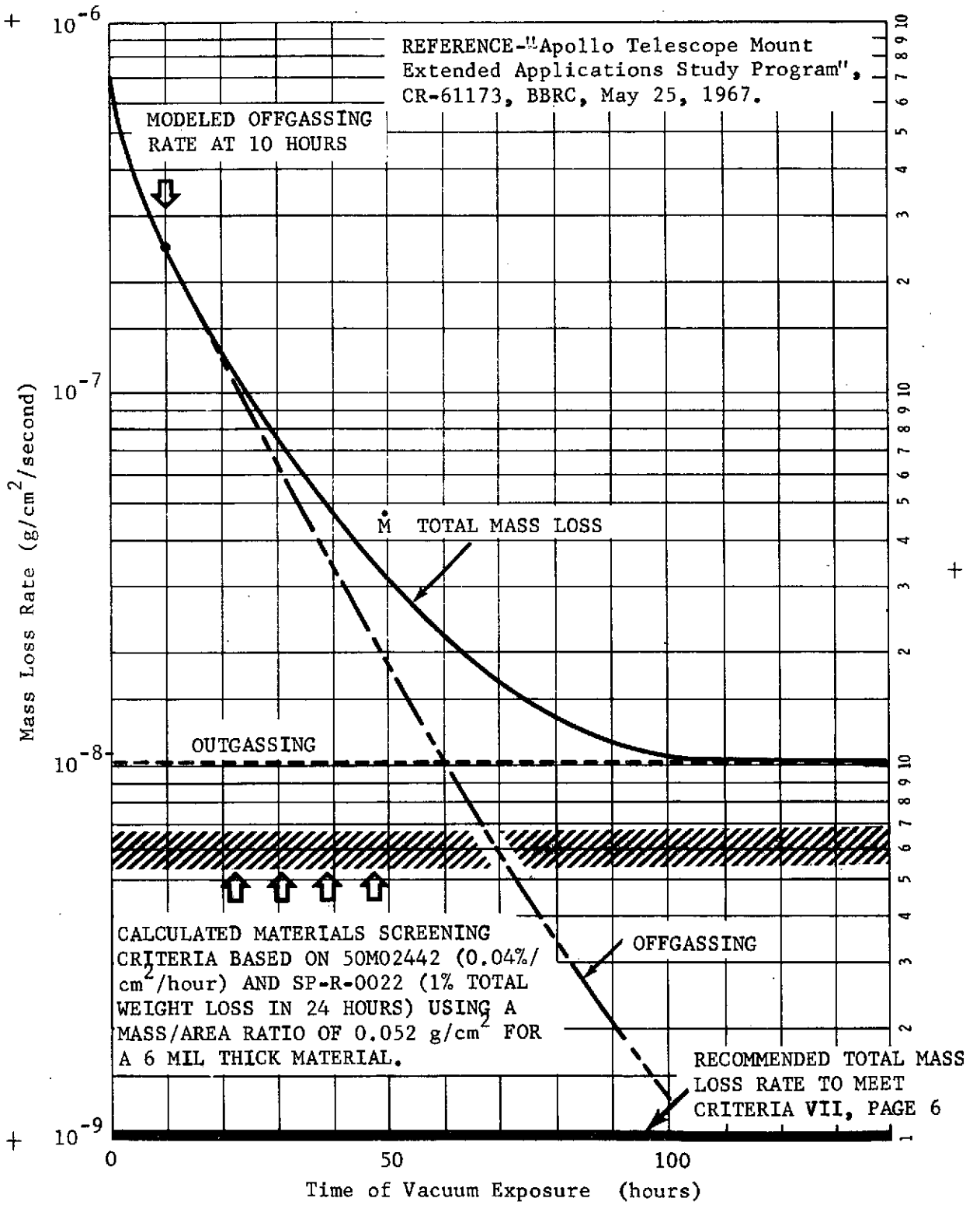

Figure 8. Modeled Outgassing and Offgassing Mass Loss Decay Curves as a Function of Time

Table I. Summary Table for Major Spacelab Sources

MAJOR SOURCES	DURATION/ FREQUENCY	FLOWRATE	CONSTITUENTS	PLUME SHAPE FUNCTION	VELOCITY	SIZE PARAMETER
Outgassing	Continuous	$1 \times 10^{-8} e^{-t/4100} e^{(T-100)/29}$ $g/cm^2/second$	Hydrocarbon chain fragments, RTV's, etc.	$\cos\theta/r^2$	$12.9 \sqrt{T}$ m/second	Molecular average M=100
Offgassing	Continuous for the first 100 hours on orbit	$[3.87e^{-0.14\ t} + 3.0\ e^{-0.055\ t}]\ e^{(T-100)/29} \times 10^{-7}$ $g/cm^2/second$	Water Light Gases Volatiles	$\cos\theta/r^2$	$30.4 \sqrt{T}$ m/second	Molecular average M=18
Cabin Atmosphere Leakage	Continuous	1.35 kg/day	O_2 N_2 CO_2 H_2O	$\cos\theta/r^2$	$2220 \sqrt{\frac{1}{M}}$ m/second	Molecular average M=29
Environmental Condensate Vent	Once every seven days for 28 minutes	2 lb/minute	Water	Empirical 65° half angle	7 m/second	30μ to 900μ radius

3.1.3 Modeled Spacelab Lines-of-Sight - In order to define the mass and number column densities and the return flux of the contaminants, lines-of-sight were developed for each of the Spacelab configurations consistent with those developed previously for the Orbiter. This allows a comparison to be drawn for each Spacelab configuration and/or each Spacelab/Orbiter configuration independently.

Nine lines-of-sight were established with respect to the +Z axis for the SL-1 and SL-3 configurations. These two configurations were considered the principle configurations to be flown with the Payloads being evaluated in this study. It is recognized that the SL-2 and SL-3 configurations will be flown with the majority of the Sortie Payloads. However, the SL-1 configuration was better known dimensionally than that of the SL-2 and SL-3 configurations. Therefore, the SL-1 and SL-3 configurations were selected to be the most representative while presenting the maximum contrast for the configurations modeled. The SL-2 configuration is physically very similar to that of the SL-1 configuration and the resultant mass column and number column densities are very close. Only the +Z , the zero degree line-of-sight was established for comparison purposes for the SL-2 configuration.

For each configuration, the center of the pallet configuration whether one, three, or five segments was chosen as the representative point for evaluation. Until more definitive information is available concerning operational requirements of the various Spacelab/Payload configurations, the nature and extent of the sources are better defined, and the geometries associated with the Payloads are better known; Spacelab/Payload lines-of-sight for this one representative position will only be considered. The lines-of-sight considered encompass a 100 degree cone of the available hemisphere in the +Z direction above the Shuttle Orbiter. This 100 degree cone encompasses the viewing requirements of the majority of Spacelab Payloads to be flown.

The specific lines-of-sight established for the SL-1 and SL-3 configurations are schematically depicted in Figure 9 using the SL-1 configuration for illustration. These lines-of-sight are the:

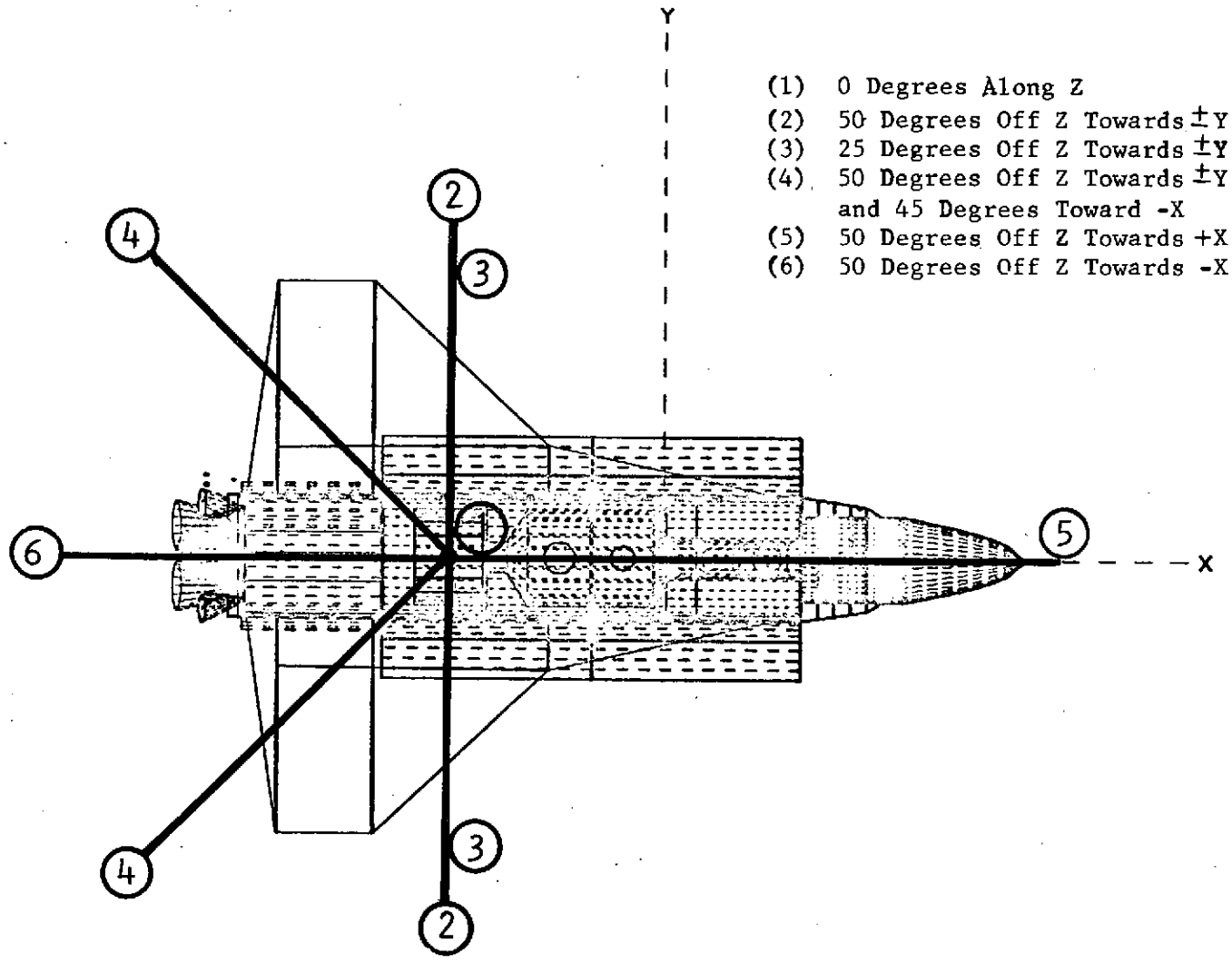

Figure 9. Computer Drawn Graphic Display of the Top View of the Orbiter/SL-1 Configuration Showing the Location of the Lines-of-Sight

a) zero degree line-of-sight (in the +Z direction);

b) fifty degree lines-of-sight (4 directions, forward in the (+Z, +X), aft in the (+Z, -X), port in the (+Z, +Y), and starboard in the (+Z, -Y) directions);

c) twenty-five degree lines-of-sight (2 directions, port in the (+Z, +Y), and starboard in the (+Z, -Y) direction); and

d) forty-five degrees to the aft (2 directions both port and starboard and fifty degrees from the normal or +Z direction).

As mentioned previously, only one line-of-sight was established for the SL-2 configuration and this was the zero degree line-of-sight in the +Z direction.

An additional line-of-sight was considered for the SL-1 configuration. This line-of-sight was placed one meter above the Shuttle Orbiter skinline in the (X, Z) plane parallel to the Orbiter X axis. This particular line-of-sight was established to include Payload viewing requirements into the Orbiter velocity vector such as that of proposed AMPS Payload instruments. This line-of-sight is graphically presented in Figure 10 and represents the worst case condition of a sensor which would be located close to the Orbiter skinline viewing in the +X direction.

3.1.4 Modeled Shuttle Orbiter Configuration Changes - Concurrent with activities performed for this study, changes to the basic Shuttle Orbiter Contamination Assessment Model have been made to improve the fidelity of the original configuration. These changes have been reflected in this study. The contamination impact analysis for the Spacelab/Payload configurations to be presented in the following subsection uses the updated evaluations based upon the changes that have been incorporated. Those changes to the Orbiter contamination model which are presently reflected in this study are:

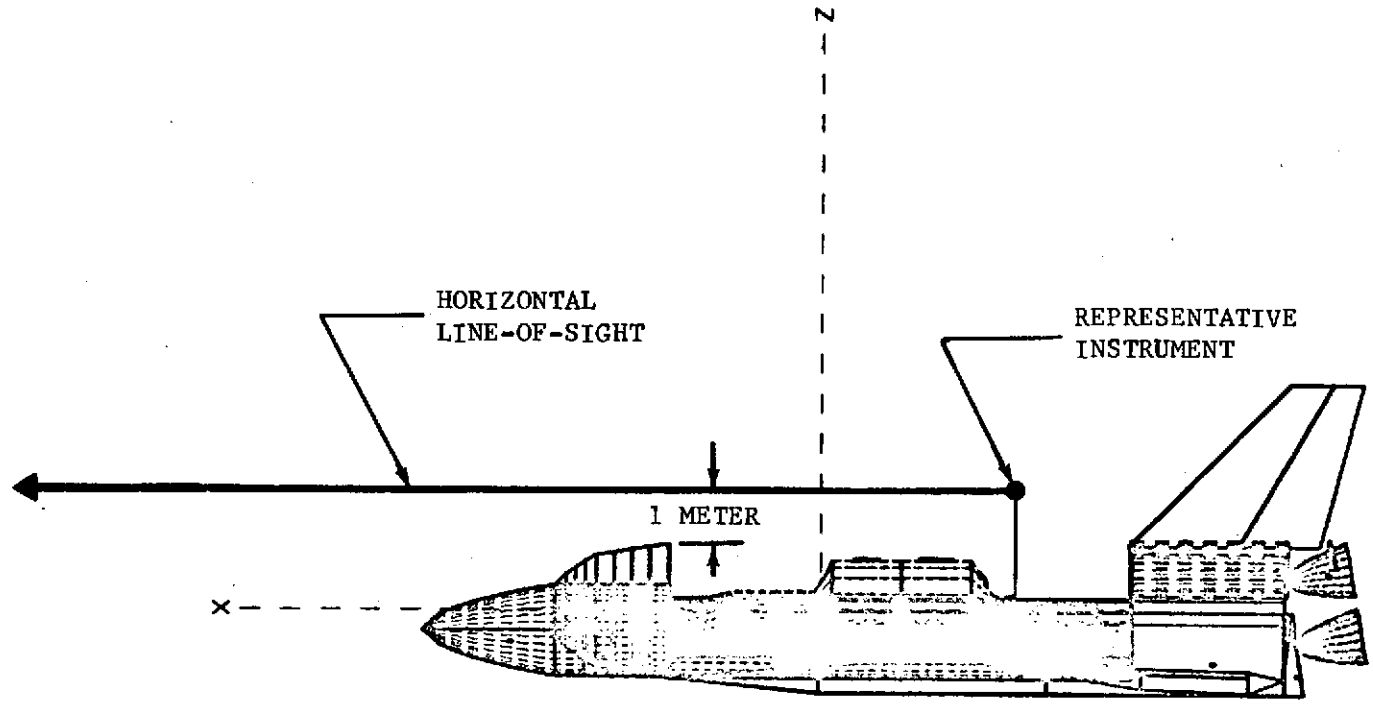

Figure 10. Computer Drawn Graphic Display of the Side View of the Orbiter/SL-1 Configuration Showing the Parallel Line-of-Sight Considered for the AMPS Payload

a) modification of the payload bay door geometry to the full open position;

b) modification of the Orbiter wing geometry to represent the downward slope of the +Z wing surfaces;

c) incorporation of the canted forward Vernier Control System (VCS) 25 lb thrust engines with the scarfed nozzle;

d) extension of the interaction spheres out to 1000 feet from the Shuttle Orbiter;

e) redefinition of the flow field descriptions for the 900 lb Reaction Control System (RCS) engines; and

f) redefinition of evaporator plume distribution.

3.1.5 Modeled Shuttle Orbiter Sources - For completeness, Table II is presented to summarize the major Shuttle Orbiter sources used for the definition of the Orbiter induced environment. These sources plus those defined for the Spacelab configurations establish the combined induced environments presented in the following subsections. The duration of the return flux as indicated in Table II is approximately 10 minutes/orbit. This is an integrated sine function over an orbit considering the optical instrument physical acceptance angle and variation of the vehicle velocity vector with respect to the optical axis of the instruments. The encounter point on orbit for the return flux will be dependent upon the type of mission to be flown (e.g. at orbital sunrise for solar physics payloads or at orbital sunset for deep sky payloads).

3.2 Comparison of Spacelab/Orbiter Induced Environment Predictions - This subsection presents a series of tabular comparisons of the various Spacelab configuration induced environment predictions along with the updated Shuttle Orbiter induced environment predictions. The individual and the combined induced environment predictions as a result of outgassing and offgassing, leakage, evaporator, and the VCS (25 lb thrust engines) are tabulated for the various configurations and lines-of-sight. Two summary tables are presented to show independently the variations of the induced environment predictions between the three individual Spacelab configurations and the maximum and minimum induced environment predictions from the combined configurations.

Table II. Major Orbiter Sources Summary

Major Sources	Duration/ Frequency	Flowrate	Constituents	Plume Shape Function	Velocity	Size Parameter
Outgassing	Continuous	$\left[5.0e^{-t/4100} + e^{(T-100)/29} \times 10^{-10}\right]$ g/cm^2/sec	Hydrocarbon chain fragments RTV's,etc.	$\cos\theta / r^2$	12.9 $\sqrt{T}$ m/sec	Molecular Avg. M = 100
Offgassing	Continuous for first 100 hours on-orbit	$\left[3.87e^{-0.14t} + 3.0e^{-.055t} + e^{(T-100)/29} \times 10^{-9}\right]$ g/cm^2/sec	Water light gases Volatiles	$\cos\theta / r^2$	30.4 $\sqrt{T}$ m/sec	Molecular Avg. M = 18.
* Evaporator (2)	~60% of on-orbit Time	5.5 lb/hr/vent	Water	$\cos^6(1.01\,\theta)/r^2$ $[0° \leq \theta \leq 36.8°]$ $\frac{e^{-.0773(\theta-36.8°)}}{r^2}$ $[36.8° < \theta \leq 148°]$	1012 m/sec	Molecular M = 18
Cabin Atmos Leakage	Continuous	7 lb/day	O_2 N_2 CO_2 H_2O	$\cos\theta / r^2$	2220 $\sqrt{\frac{1}{M}}$ m/sec	Molecular Avg. M = 29
RCS Vernier Engines**	As Reqd.	.09 lb/min Avg. 40 msec pulse ea. 4.8 sec--Y-POP attitude at 200 km	H_2O N_2 H_2 CO CO_2 H	$\frac{(\cos \frac{\pi}{2} \cdot \frac{\theta}{\theta_1})^{8.65}}{r^2}$ $[0° \leq \theta \leq 40°]$ $\frac{e^{-.0467(\theta-40°)}}{r^2}$ $[40° < \theta \leq 140°]$ $\frac{e^{-4.67}}{r^2}$ $[140° < \theta \leq 180°]$	3505 m/sec	Molecular
Ambient Reflection	~10 min per orbit	Varies with above sources & orbital attitude	Any of the above sources	$\cos\theta/r^2$ from collision points	Varies with all above sources Max = 7.65 km/sec	Varies with all above sources

* Plume reflections off of structural surfaces (e.g. wings, experiment bay doors) are equivalent to a source equal to the plume impingement rate with a $\cos\theta/r^2$ distribution and a velocity of 30.4 $\sqrt{T}$ m/sec from the surface where T = surface temp.

** RCS plume reflections off of structural surfaces are assumed to have a rate equal to the plume impingement rate with a $\cos\theta/r^2$ distribution and a velocity equal to 129 $\sqrt{\frac{T}{M}}$ where T = surface temperature.

The predictions in the following subsections are for the Spacelab SL-1 and SL-3 configurations since these two Spacelab configurations were chosen to be representative of the various Payloads to be assessed. The SL-2 configuration induced environment prediction data is summarized in subsection 3.2.4 to show comparisons for the zero degree line-of-sight for all three analyzed Spacelab configurations. The minor differences between SL-1 and the SL-2 configurations do not impact the individual induced environments sufficiently merit inclusion of this configuration in all the presented tables.

3.2.1 Outgassing Induced Environment Predictions - Table III presents a summary of the outgassing induced environment predictions for the SL-1 and SL-3 configurations. For the nine major lines-of-sight, the mass and number column densities and the return flux for the orbital altitudes of 700, 435, and 200 Km are presented. The return flux numbers are based upon an acceptance relationship at the Shuttle Orbiter of 0.2 steradians. Depending upon the nature of the surface or system to be analyzed, the return flux is further modified to account for the proper involved geometries. The maximum and minimum values are also presented for beta angles of 0, 60, and 73 degrees. Although these beta angles may not be unique for the Payloads being analyzed, the corresponding surface temperatures at these beta angles do present a range of outgassing levels that can be expected as a function of the time in sunlight for the various Payloads.

Based upon the outgassing rate assumed in this study of $1x10^{-8}$ g/cm^2/second at 100°C for the solar oriented non-metallic Spacelab surfaces, the SL-1 configuration has predicted number column densities from 10^{10} to 10^{12} molecules/cm^2. Depending upon the line-of-sight in question for SL-1, the number column density limit of $1x10^{12}$ molecules/cm^2 stated in Applicable Document JSC 07700 Volume XIV Revision C is slightly exceeded. However, the assumed outgassing rate is characteristic of an S13G type thermal control paint. Depending upon the selection of thermal control paint or material, this must be considered preliminary. It does point out that to meet the above stated criteria the outgassing rate of the thermal control paint or

Table III. Outgassing Induced Environment Predictions for the Spacelab SL-1 and SL-3 Configurations

PREDICTED PARAMETERS / LINE-OF-SIGHT & BETA ANGLE	SPACELAB-1					SPACELAB-3				
	M.C.D. g/cm^2	N.C.D. $mol./cm^2$	RETURN FLUX (MAX.) $g/cm^2/second$			M.C.D. g/cm^2	N.C.D. $mol./cm^2$	RETURN FLUX (MAX.) $g/cm^2/second$		
			700 Km	435 Km	200 Km			700 Km	435 Km	200 Km
0° + Z										
0° MAX	2.3(-10)*	1.5(+12)	4.1(-12)	1.1(-10)	0	2.9(-11)	1.8(+11)	5.2(-13)	1.4(-11)	0
MIN	4.2(-12)	2.6(+10)	7.5(-14)	2.0(-12)	0	1.3(-11)	7.8(+10)	2.2(-13)	6.0(-12)	0
60° MAX	2.3(-10)	1.5(+12)	4.1(-12)	1.1(-10)	0	2.9(-11)	1.8(+11)	5.2(-13)	1.4(-11)	0
MIN	5.1(-12)	3.2(+10)	9.1(-14)	2.5(-12)	0	1.5(-11)	9.6(+10)	2.7(-13)	7.4(-12)	0
73° MAX	2.3(-10)	1.5(+12)	4.1(-12)	1.1(-10)	0	2.9(-11)	1.8(+11)	5.2(-13)	1.4(-11)	0
50° ± Y										
0° MAX	1.4(-10)	8.8(+11)	2.5(-12)	6.7(-11)	0	2.0(-11)	1.3(+11)	3.6(-13)	9.6(-12)	0
MIN	2.5(-12)	1.6(+10)	4.5(-14)	1.2(-12)	0	1.3(-11)	8.5(+10)	2.3(-13)	6.2(-12)	0
60° MAX	1.4(-10)	8.8(+11)	2.5(-12)	6.7(-11)	0	2.0(-11)	1.3(+11)	3.6(-13)	9.6(-12)	0
MIN	3.1(-12)	1.9(+10)	5.5(-14)	1.5(-12)	0	1.5(-11)	9.8(+10)	2.7(-13)	7.2(-12)	0
73° MAX	1.4(-10)	8.8(+11)	2.5(-12)	6.7(-11)	0	2.0(-11)	1.3(+11)	3.6(-13)	9.6(-12)	0
25° ± Y										
0° MAX	1.7(-10)	1.0(+12)	3.0(-12)	8.0(-11)	0	2.5(-11)	1.6(+11)	4.5(-13)	1.2(-11)	0
MIN	3.4(-12)	2.1(+10)	6.1(-14)	1.6(-12)	0	1.3(-11)	8.5(+10)	2.3(-13)	6.2(-12)	0
60° MAX	1.7(-10)	1.0(+12)	3.0(-12)	8.0(-11)	0	2.5(-11)	1.6(+11)	4.5(-13)	1.2(-11)	0
MIN	4.2(-12)	2.6(+10)	7.4(-14)	2.0(-12)	0	1.6(-11)	1.0(+11)	2.9(-13)	7.7(-12)	0
73° MAX	1.7(-10)	1.0(+12)	3.0(-12)	8.0(-11)	0	2.5(-11)	1.6(+11)	4.5(-13)	1.2(-11)	0
50° ± Y, 45° -X										
0° MAX	1.0(-10)	6.2(+11)	1.8(-12)	4.8(-11)	0	2.6(-11)	1.7(+11)	4.6(-13)	1.2(-11)	0
MIN	3.0(-12)	1.8(+10)	5.3(-14)	1.4(-12)	0	1.1(-11)	7.2(+10)	2.0(-13)	5.3(-12)	0
60° MAX	1.0(-10)	6.2(+11)	1.8(-12)	4.8(-11)	0	2.6(-11)	1.7(+11)	4.6(-13)	1.2(-11)	0
MIN	3.6(-12)	2.3(+10)	6.5(-14)	1.7(-12)	0	1.3(-11)	8.5(+10)	2.3(-13)	6.2(-12)	0
73° MAX	1.0(-10)	6.2(+11)	1.8(-12)	4.8(-11)	0	2.6(-11)	1.7(+11)	4.6(-13)	1.2(-11)	0
50° + X										
0° MAX	3.6(-10)	2.2(+12)	6.3(-12)	1.7(-10)	0	3.7(-11)	2.4(+11)	6.6(-13)	1.8(-11)	0
MIN	2.9(-12)	1.8(+10)	5.2(-14)	1.4(-12)	0	1.0(-11)	6.5(+10)	1.8(-13)	4.8(-12)	0
60° MAX	3.6(-10)	2.2(+12)	6.3(-12)	1.7(-10)	0	3.7(-11)	2.4(+11)	6.6(-13)	1.8(-11)	0
MIN	3.4(-12)	2.1(+10)	6.0(-14)	1.6(-12)	0	1.2(-11)	7.8(+10)	2.1(-13)	5.7(-12)	0
73° MAX	3.6(-10)	2.2(+12)	6.3(-12)	1.7(-10)	0	3.7(-11)	2.4(+11)	6.6(-13)	1.8(-11)	0
50° -X										
0° MAX	9.7(-11)	6.0(+11)	1.7(-12)	4.6(-11)	0	3.7(-11)	2.4(+11)	6.6(-13)	1.8(-11)	0
MIN	3.2(-12)	2.0(+10)	5.6(-14)	1.5(-12)	0	1.0(-11)	6.5(+10)	1.8(-13)	4.8(-12)	0
60° MAX	9.7(-11)	6.0(+11)	1.7(-12)	4.6(-11)	0	3.7(-11)	2.4(+11)	6.6(-13)	1.8(-11)	0
MIN	3.9(-12)	2.4(+10)	6.9(-14)	1.9(-12)	0	1.2(-11)	7.8(+10)	2.1(-13)	5.7(-12)	0
73° MAX	9.7(-11)	6.0(+11)	1.7(-12)	4.6(-11)	0	3.7(-11)	2.4(+11)	6.6(-13)	1.8(-11)	0

* (-10) = 10^{-10}

material should be on the order of $1x10^{-9}g/cm^2$/second at 100°C. This would allow adequate margin such that the resulting number column density would fall below the stated criteria under any circumstances. This value is approximately a factor of 6 less than the maximum acceptable mass loss rate stated in Applicable Documents MSFC 50M02442 (0.04%/cm^2/hour) and JSC SP-R-0022 (total weight loss 1% in 24 hours). Specific surface thermal profiles, temperature dependence of rates of the selected material, and Spacelab external area of coverage will influence the final recommended maximum allowable rate.

This is also true for the return fluxes at 435 Km where the predictions slightly exceed the $10^{-10}g/cm^2$/second ($\sim 10^{12}$ molecules/cm^2/second) criteria stated in the above referenced document. The return flux at 200 Km is approximately zero since the mean free path of outgassing molecules (molecular weights typically 100 and diameters assumed near 30Å) at this altitude is less than a meter and the outgassed molecules essentially are not able to travel into the velocity vector far enough to be considered as being reflected back to the Payload.

Table IV presents the outgassing environment predictions for the Shuttle Orbiter excluding Spacelab for the same physical considerations used for the Spacelab configurations. The number column density of the Orbiter ranges from a high 10^9 to a low 10^{11} molecules/cm^2 and does not exceed the stated criteria as is the case with the return flux for the Orbiter. The outgassing rate assumed for the Orbiter based on the RSI tile configuration is $5x10^{-10}g/cm^2$/second. The validity of this assumed rate will be established through vacuum testing currently being conducted at MSFC which is using a simulated RSI tile configuration of the Orbiter.

Table V presents the combined outgassing induced environment predictions for the SL-1 and SL-3 Spacelab configurations and the Orbiter configuration for the lines-of-sight and conditions considered.

3.2.2 Offgassing Induced Environment Predictions - Table VI presents a summary of the offgassing induced environment predictions for the SL-1 and SL-3 configurations. The data contained in Table VI and in the subsequent tables (Tables VII and VIII) are formatted consistent with those of the previous tables of subsection 3.2.1.

Table IV. Outgassing Induced Environment Predictions for the Shuttle Orbiter Configuration

PREDICTED PARAMETERS / LINE-OF-SIGHT & BETA ANGLE	M.C.D. g/cm^2	N.C.D. $mol./cm^2$	RETURN FLUX (MAX) $g/cm^2/second$		
			700 Km	435 Km	200 Km
0° + Z					
0° MAX	2.9(-11)*	1.8(+11)	5.2(-13)	1.4(-11)	0
MIN	1.4(-12)	8.8(+9)	2.5(-14)	6.7(-13)	0
60° MAX	3.0(-11)	1.9(+11)	5.3(-13)	1.4(-11)	0
MIN	1.9(-12)	1.2(+10)	3.4(-14)	9.1(-13)	0
73° MAX	3.1(-11)	2.0(+11)	5.5(-13)	1.5(-11)	0
$50^\circ \pm$ Y					
0° MAX	2.0(-11)	1.3(+11)	3.6(-13)	9.6(-12)	0
MIN	1.4(-12)	8.8(+9)	2.5(-14)	6.7(-13)	0
60° MAX	2.1(-11)	1.3(+11)	3.7(-13)	1.0(-11)	0
MIN	1.9(-12)	1.2(+10)	3.4(-14)	9.1(-13)	0
73° MAX	2.2(-11)	1.4(+11)	3.9(-13)	1.1(-11)	0
$25^\circ \pm$ Y					
0° MAX	2.5(-11)	1.6(+11)	4.4(-13)	1.2(-11)	0
MIN	1.4(-12)	8.8(+9)	2.5(-14)	6.7(-13)	0
60° MAX	2.6(-11)	1.6(+11)	4.6(-13)	1.3(-11)	0
MIN	2.0(-12)	1.3(+10)	3.6(-14)	9.6(-13)	0
73° MAX	2.7(-11)	1.7(+11)	4.8(-13)	1.3(-11)	0
$50^\circ \pm$ Y, 45° -X					
0° MAX	2.7(-11)	1.7(+11)	4.8(-13)	1.3(-11)	0
MIN	1.2(-12)	7.2(+9)	2.1(-14)	5.8(-13)	0
60° MAX	2.7(-11)	1.7(+11)	4.8(-13)	1.3(-11)	0
MIN	1.7(-12)	1.1(+10)	3.0(-14)	8.1(-13)	0
73° MAX	2.8(-11)	1.7(+11)	5.0(-13)	1.3(-11)	0
50° + X					
0° MAX	2.1(-11)	1.3(+11)	3.8(-13)	1.0(-11)	0
MIN	1.3(-12)	8.1(+9)	2.3(-14)	6.2(-13)	0
60° MAX	2.4(-11)	1.5(+11)	4.2(-13)	1.1(-11)	0
MIN	1.8(-12)	1.2(+10)	3.3(-14)	8.9(-13)	0
73° MAX	2.4(-11)	1.5(+11)	4.4(-13)	1.2(-11)	0
50° - X					
0° MAX	3.7(-11)	2.3(+11)	6.6(-13)	1.8(-11)	0
MIN	1.1(-12)	6.6(+9)	1.9(-14)	5.1(-13)	0
60° MAX	3.7(-11)	2.3(+11)	6.6(-13)	1.8(-11)	0
MIN	1.5(-12)	9.1(+9)	2.6(-14)	7.0(-13)	0
73° MAX	3.8(-11)	2.4(+11)	6.7(-13)	1.8(-11)	0

* (-11) = 10^{-11}

Table V. Outgassing Induced Environment Predictions for the Combined Spacelab/Orbiter Configurations

PREDICTED PARAMETERS / LINE-OF-SIGHT & BETA ANGLE	SPACELAB-1/ORBITER					SPACELAB-3/ORBITER				
	M.C.D. g/cm^2	N.C.D. $mol./cm^2$	RETURN FLUX (MAX.) $g/cm^2/second$ 700 Km	435 Km	200 Km	M.C.D. g/cm^2	N.C.D. $mol./cm^2$	RETURN FLUX (MAX.) $g/cm^2/second$ 700 Km	435 Km	200 Km
$0^\circ + Z$										
0° MAX	2.5(-10)*	1.6(+12)	4.4(-12)	1.2(-10)	0	4.9(-11)	3.1(+11)	8.8(-13)	2.4(-11)	0
MIN	5.4(-12)	3.4(+10)	9.6(-14)	2.6(-12)	0	1.4(-11)	8.5(+10)	2.4(-13)	6.6(-12)	0
60° MAX	2.5(-10)	1.6(+12)	4.5(-12)	1.2(-10)	0	5.0(-11)	3.1(+11)	8.9(-13)	2.4(-11)	0
MIN	6.8(-12)	4.3(+10)	1.2(-13)	3.3(-12)	0	1.7(-11)	1.1(+11)	3.0(-13)	8.2(-12)	0
73° MAX	2.5(-10)	1.6(+12)	4.5(-12)	1.2(-10)	0	5.1(-11)	3.1(+11)	9.0(-13)	2.4(-11)	0
$50^\circ \pm Y$										
0° MAX	1.5(-10)	9.7(+11)	2.7(-12)	7.4(-11)	0	3.5(-11)	2.2(+11)	6.2(-13)	1.7(-11)	0
MIN	3.8(-12)	2.4(+10)	6.7(-14)	1.8(-12)	0	1.4(-11)	8.5(+10)	2.4(-13)	6.6(-12)	0
60° MAX	1.6(-10)	9.8(+11)	2.8(-12)	7.4(-11)	0	3.6(-11)	2.3(+11)	6.4(-13)	1.7(-11)	0
MIN	4.9(-12)	3.0(+10)	8.7(-14)	2.4(-12)	0	1.7(-11)	1.1(+11)	3.0(-13)	8.2(-12)	0
73° MAX	1.6(-10)	9.8(+11)	2.8(-12)	7.5(-11)	0	3.6(-11)	2.3(+11)	6.4(-13)	1.7(-11)	0
$25^\circ \pm Y$										
0° MAX	1.9(-10)	1.1(+12)	3.3(-12)	8.8(-11)	0	4.2(-11)	2.6(+11)	7.5(-13)	2.0(-11)	0
MIN	4.6(-12)	2.9(+10)	8.3(-14)	2.2(-12)	0	1.4(-11)	8.5(+10)	2.4(-13)	6.6(-12)	0
60° MAX	1.9(-10)	1.1(+12)	3.3(-12)	8.9(-11)	0	4.3(-11)	2.7(+11)	7.6(-13)	2.1(-11)	0
MIN	5.9(-12)	3.7(+10)	1.1(-14)	2.8(-12)	0	1.8(-11)	1.1(+11)	3.2(-13)	8.7(-12)	0
73° MAX	1.9(-10)	1.1(+12)	3.4(-12)	8.9(-11)	0	4.4(-11)	2.8(+11)	7.8(-13)	2.1(-11)	0
$50^\circ \pm Y$, 45° -X										
0° MAX	1.2(-10)	7.6(+11)	2.2(-12)	5.9(-11)	0	4.8(-11)	3.0(+11)	8.5(-13)	2.3(-11)	0
MIN	4.1(-12)	2.5(+10)	7.3(-14)	1.9(-12)	0	1.2(-11)	7.6(+10)	2.1(-13)	5.8(-12)	0
60° MAX	1.2(-10)	7.6(+11)	2.2(-12)	5.9(-11)	0	4.9(-11)	3.1(+11)	8.7(-13)	2.4(-11)	0
MIN	5.2(-12)	3.3(+10)	9.3(-14)	2.5(-12)	0	1.4(-11)	8.5(+10)	2.4(-13)	6.6(-12)	0
73° MAX	1.3(-10)	7.7(+11)	2.2(-12)	5.9(-11)	0	5.0(-11)	3.1(+11)	8.9(-13)	2.4(-11)	0
$50^\circ + Y$										
0° MAX	3.7(-10)	2.3(+12)	6.5(-12)	1.7(-10)	0	4.8(-11)	3.0(+11)	8.5(-13)	2.3(-11)	0
MIN	4.0(-12)	2.5(+10)	7.1(-14)	1.9(-12)	0	1.1(-11)	6.9(+10)	2.0(-13)	5.3(-12)	0
60° MAX	3.7(-10)	2.3(+12)	6.5(-12)	1.8(-10)	0	5.0(-11)	3.1(+11)	8.9(-13)	2.4(-11)	0
MIN	5.0(-12)	3.1(+10)	8.8(-14)	2.4(-12)	0	1.4(-11)	8.5(+10)	2.4(-13)	6.6(-12)	0
73° MAX	3.8(-10)	2.3(+12)	6.6(-12)	1.8(-10)	0	5.1(-11)	3.2(+11)	9.1(-13)	2.5(-11)	0
$50^\circ - X$										
0° MAX	1.3(-10)	8.1(+11)	2.3(-12)	6.2(-11)	0	7.0(-11)	4.4(+11)	1.2(-12)	3.4(-11)	0
MIN	4.2(-12)	2.6(+10)	7.3(-14)	2.0(-12)	0	1.1(-11)	6.9(+10)	2.0(-13)	5.3(-12)	0
60° MAX	1.3(-10)	8.1(+11)	2.3(-12)	6.2(-11)	0	7.0(-11)	4.4(+11)	1.2(-12)	3.4(-11)	0
MIN	5.3(-12)	3.3(+10)	9.3(-14)	2.6(-12)	0	1.3(-11)	8.2(+10)	2.3(-13)	6.3(-12)	0
73° MAX	1.3(-10)	8.1(+11)	2.3(-12)	6.2(-11)	0	7.1(-11)	4.5(+11)	1.3(-12)	3.4(-11)	0

* $(-10) = 10^{-10}$

Table VI. Offgassing Induced Environment Predictions for the Spacelab SL-1 and SL-3 Configurations

PREDICTED PARAMETERS / LINE-OF-SIGHT & BETA ANGLE	SPACELAB-1					SPACELAB-3				
	M.C.D. g/cm^2	N.C.D. $mol./cm^2$	RETURN FLUX (MAX) g/cm^2/second 700 Km	435 Km	200 Km	M.C.D. g/cm^2	N.C.D. $mol./cm^2$	RETURN FLUX (MAX) g/cm^2/second 700 Km	435 Km	200 Km
0° + Z										
0° MAX	2.5(-9)*	8.0(+13)	1.5(-12)	4.2(-11)	2.2(-9)	3.1(-10)	1.0(+13)	1.9(-13)	5.5(-12)	2.8(-10)
MIN	4.5(-11)	1.5(+12)	2.7(-14)	7.5(-13)	4.1(-11)	1.4(-10)	4.4(+12)	8.0(-14)	2.3(-12)	1.2(-10)
60° MAX	2.5(-9)	8.0(+13)	1.5(-12)	4.2(-11)	2.2(-9)	3.1(-10)	1.0(+13)	1.9(-13)	5.5(-12)	2.8(-10)
MIN	5.5(-11)	1.8(+12)	3.3(-14)	9.0(-13)	4.9(-11)	1.7(-10)	5.5(+12)	1.0(-13)	2.8(-12)	1.5(-10)
73° MAX	2.5(-9)	8.0(+13)	1.5(-12)	4.2(-11)	2.2(-9)	3.1(-10)	1.0(+13)	1.9(-13)	5.5(-12)	2.8(-10)
$50^\circ \pm Y$										
0° MAX	1.5(-9)	4.9(+13)	9.0(-13)	2.6(-11)	1.4(-9)	2.3(-10)	7.6(+12)	1.4(-13)	4.1(-12)	2.1(-10)
MIN	2.7(-11)	9.0(+11)	1.6(-14)	4.6(-13)	2.4(-11)	1.4(-10)	4.4(+12)	8.0(-14)	2.3(-12)	1.2(-10)
60° MAX	1.5(-9)	4.9(+13)	9.0(-13)	2.6(-11)	1.4(-9)	2.3(-10)	7.6(+12)	1.4(-13)	4.1(-12)	2.1(-10)
MIN	3.3(-11)	1.1(+12)	2.0(-14)	5.5(-13)	2.9(-11)	1.7(-10)	5.6(+12)	1.0(-13)	3.0(-12)	1.5(-10)
73° MAX	1.5(-9)	4.9(+13)	9.0(-13)	2.6(-11)	1.4(-9)	2.3(-10)	7.6(+12)	1.4(-13)	4.1(-12)	2.1(-10)
$25^\circ \pm Y$										
0° MAX	1.8(-9)	6.0(+13)	1.1(-12)	3.0(-11)	1.6(-9)	2.7(-10)	8.9(+12)	1.6(-13)	4.8(-12)	2.4(-10)
MIN	3.7(-11)	1.2(+12)	2.2(-14)	6.0(-13)	3.3(-11)	1.4(-10)	4.4(+12)	8.0(-14)	2.3(-12)	1.2(-10)
60° MAX	1.8(-9)	6.0(+13)	1.1(-12)	3.0(-11)	1.6(-9)	2.7(-10)	8.9(+12)	1.6(-13)	4.8(-12)	2.4(-10)
MIN	4.5(-11)	1.5(+12)	2.7(-14)	7.5(-13)	4.0(-11)	1.7(-10)	5.6(+12)	1.0(-13)	3.0(-12)	1.5(-10)
73° MAX	1.8(-9)	6.0(+13)	1.1(-12)	3.0(-11)	1.6(-9)	2.7(-10)	8.9(+12)	1.6(-13)	4.8(-12)	2.4(-10)
$50^\circ \pm Y$, 45° -X										
0° MAX	1.1(-9)	3.5(+13)	6.5(-13)	1.8(-11)	9.5(-10)	2.9(-10)	9.6(+12)	1.7(-13)	5.1(-12)	2.6(-10)
MIN	3.2(-11)	1.1(+12)	1.9(-14)	5.5(-13)	2.9(-11)	1.2(-10)	4.0(+12)	7.2(-14)	2.1(-12)	1.1(-10)
60° MAX	1.1(-9)	3.5(+13)	6.5(-13)	1.8(-11)	9.5(-10)	2.9(-10)	9.6(+12)	1.7(-13)	5.1(-12)	2.6(-10)
MIN	3.9(-11)	1.3(+12)	2.3(-14)	6.5(-13)	3.5(-11)	1.5(-10)	5.0(+12)	9.0(-14)	2.7(-12)	1.4(-10)
73° MAX	1.1(-9)	3.5(+13)	6.5(-13)	1.8(-11)	9.5(-10)	2.9(-10)	9.6(+12)	1.7(-13)	5.1(-12)	2.6(-10)
50° + X										
0° MAX	3.8(-9)	1.3(+14)	2.3(-12)	6.5(-11)	3.4(-9)	3.8(-10)	1.3(+13)	2.3(-13)	6.7(-12)	3.4(-10)
MIN	3.1(-11)	1.0(+12)	1.9(-14)	5.5(-13)	2.8(-11)	1.0(-10)	3.3(+12)	6.0(-14)	1.8(-12)	9.0(-11)
60° MAX	3.8(-9)	1.3(+14)	2.3(-12)	6.5(-11)	3.4(-9)	3.8(-10)	1.3(+13)	2.3(-13)	6.7(-12)	3.4(-10)
MIN	3.6(-11)	1.2(+12)	2.2(-14)	6.0(-13)	3.2(-11)	1.7(-10)	5.6(+12)	1.0(-13)	3.0(-12)	1.5(-10)
73° MAX	3.8(-9)	1.3(+14)	2.3(-12)	6.5(-11)	3.4(-9)	3.8(-10)	1.3(+13)	2.3(-13)	6.7(-12)	3.4(-10)
50° -X										
0° MAX	1.0(-9)	3.4(+13)	6.0(-13)	1.8(-11)	9.0(-9)	3.8(-10)	1.3(+13)	2.3(-13)	6.7(-12)	3.4(-10)
MIN	3.4(-11)	1.2(+12)	2.1(-14)	6.0(-13)	3.1(-11)	1.0(-10)	3.3(+12)	6.0(-14)	1.8(-12)	9.0(-11)
60° MAX	1.0(-9)	3.4(+13)	6.0(-13)	1.8(-11)	9.0(-9)	3.8(-10)	1.3(+13)	2.3(-13)	6.7(-12)	3.4(-10)
MIN	4.2(-11)	1.4(+12)	2.5(-14)	7.0(-13)	3.7(-11)	1.7(-10)	5.6(+12)	1.0(-13)	3.0(-12)	1.5(-10)
73° MAX	1.0(-9)	3.4(+13)	6.0(-13)	1.8(-11)	9.0(-9)	3.8(-10)	1.3(+13)	2.3(-13)	6.7(-12)	3.4(-10)

* $(-9) = 10^{-9}$

As discussed earlier in the report, the offgassing source is assumed to have a duration of 100 hours. Since this is difficult to treat in a continuous fashion for presentation of data, a 10 hour point in the offgassing decay curve was selected to be representative of the offgassing contribution to the induced environment. The 10 hour point was selected since it is representative of that time frame on orbit when operational activities may be expected to begin. The offgassing rate under this assumption is 2.5×10^{-7} g/cm^2/second at 100°C and will fall below that of the assumed near steady state outgassing rate of 1×10^{-8} g/cm^2/second before the 100 hour point.

Based upon the above assumptions, the number column density of offgassing ranged from 10^{12} to 10^{14} molecules/cm^2. This range exceeds the stated criteria and indicates a potential problem for some Payloads if operations are anticipated to begin very early on orbit. This is particularly true for systems which may be corona susceptible from high voltage power supplies.

This is also true for the return flux contaminants which ranged from 10^{-14} to 10^{-9} g/cm^2/second (10^{8} to 10^{13} molecules/cm^2/second). Generally the very light constituents of the offgassing will not condense upon normal spacecraft surfaces. However for those Payloads which utilize open cryogenic surfaces, offgassing represents an early threat contributing to the total contaminant environment as seen by these Payload types.

Offgassing as opposed to outgassing will demonstrate a return flux capability at the lower orbital altitudes (200 Km) since the mean free path for the offgassants at these altitudes is considerably larger than that of the heavier outgassing molecules. The average molecular weight and offgassing molecule size have been assumed to be 18 and 3Å respectively.

Table VII presents the offgassing environment predictions for the Shuttle Orbiter for the same physical considerations used for the Spacelab configurations. The assumed offgassing rate for the Orbiter surfaces at the 10 hour point was 2.5×10^{-9} g/cm^2/second at 100°C. The number column density predictions for the Orbiter range from 10^{11} to the low 10^{12} molecules/cm^2 which is close to the stated criteria. The return flux

Table VII. Offgassing Induced Environment Predictions for the Shuttle Orbiter Configuration

PREDICTED PARAMETERS / LINE-OF-SIGHT & BETA ANGLE	M.C.D. g/cm^2	N.C.D. $mol./cm^2$	RETURN FLUX (MAX) $g/cm^2/second$		
			700 Km	435 Km	200 Km
0° + Z					
0° MAX	6.0(-11)*	2.0(+12)	3.6(-14)	1.1(-12)	5.4(-11)
MIN	3.0(-12)	9.9(+10)	1.8(-15)	5.3(-14)	2.7(-12)
60° MAX	6.5(-11)	2.1(+12)	3.9(-14)	1.2(-12)	5.9(-11)
MIN	4.1(-12)	1.4(+11)	2.5(-15)	7.3(-14)	3.7(-12)
73° MAX	6.5(-11)	2.1(+12)	3.9(-14)	1.2(-12)	5.9(-11)
$50^\circ \pm$ Y					
0° MAX	4.3(-11)	1.4(+12)	2.6(-14)	7.7(-13)	3.9(-11)
MIN	2.9(-12)	9.6(+10)	1.7(-15)	5.2(-14)	2.6(-12)
60° MAX	4.5(-11)	1.5(+12)	2.7(-14)	8.0(-13)	4.1(-11)
MIN	4.1(-12)	1.4(+11)	2.5(-15)	7.3(-14)	3.7(-12)
73° MAX	4.7(-11)	1.6(+12)	2.8(-14)	8.4(-13)	4.2(-11)
$25^\circ \pm$ Y					
0° MAX	5.5(-11)	1.8(+12)	3.3(-14)	9.8(-13)	5.0(-11)
MIN	3.0(-12)	9.9(+10)	1.8(-15)	5.3(-14)	2.7(-12)
60° MAX	5.5(-11)	1.8(+12)	3.3(-14)	9.8(-13)	5.0(-11)
MIN	4.2(-12)	1.4(+11)	2.5(-15)	7.5(-14)	3.8(-12)
73° MAX	5.5(-11)	1.8(+12)	3.3(-14)	9.8(-13)	5.0(-11)
$50^\circ \pm$ Y, 45° -X					
0° MAX	5.5(-11)	1.8(+12)	3.4(-14)	9.5(-13)	5.0(-11)
MIN	2.6(-12)	8.5(+10)	1.6(-15)	4.4(-14)	2.3(-12)
60° MAX	6.0(-11)	1.9(+12)	3.5(-14)	1.0(-12)	5.0(-11)
MIN	3.6(-12)	1.2(+11)	2.2(-15)	6.0(-14)	3.2(-12)
73° MAX	6.0(-11)	2.0(+12)	3.6(-14)	1.0(-12)	5.5(-11)
50° +X					
0° MAX	4.6(-11)	1.5(+12)	2.8(-14)	8.0(-13)	4.1(-11)
MIN	2.8(-12)	9.0(+10)	1.7(-15)	4.7(-14)	2.5(-12)
60° MAX	5.0(-11)	1.6(+12)	3.0(-14)	8.5(-13)	4.6(-11)
MIN	3.9(-12)	1.3(+11)	2.4(-15)	6.5(-14)	3.5(-12)
73° MAX	5.0(-11)	1.7(+12)	3.1(-14)	9.0(-13)	4.7(-11)
50° -X					
0° MAX	8.0(-11)	2.6(+12)	4.7(-14)	1.4(-12)	7.0(-11)
MIN	2.3(-12)	7.5(+10)	1.4(-15)	3.8(-14)	2.0(-12)
60° MAX	8.0(-11)	2.6(+12)	4.8(-14)	1.4(-12)	7.0(-11)
MIN	3.1(-12)	1.0(+11)	1.9(-15)	5.5(-14)	2.8(-12)
73° MAX	8.0(-11)	2.7(+12)	4.8(-14)	1.4(-12)	7.0(-11)

* $(-11) = 10^{-11}$

varies from 10^{-15} to the high 10^{-11} g/cm^2/second (10^7 to 10^{12} molecules/cm^2/second) which again is very close to the stated criteria. As in the outgassing case, the testing being performed at MSFC on the RSI tile configurations should help to establish an offgassing characteristic for the Shuttle Orbiter.

Table VIII presents the combined offgassing induced environment predictions of the SL-1 and SL-3 Spacelab configurations and the Orbiter configuration for the lines-of-sight and conditions considered.

3.2.3 Leakage Induced Environment Predictions - Table IX presents the leakage induced environment predictions for the combined SL-1/Orbiter and the SL-3/Orbiter configurations. Unlike outgassing and offgassing, leakage is not dependent upon orbital conditions such as the beta angle. Table IX identifies the total mass and total number column densities for the leakage. Number column densities of the principal constituents of the leakage (O_2, N_2, CO_2, and H_2O) are also identified along with the return flux for 700, 435, and 200 Km.

Since the SL-3 configuration (Pallet Only) does not have a manned module associated with it, the predicted induced environment for the leakage will be that of the Orbiter only. However, both SL-1 and SL-2 will contribute to the total environment through leakage. The total number column density contributions due to either the Orbiter or each of the SL-1 and SL-2 configurations exceed the 10^{12} molecules/cm^2 by an order of magnitude. However, the amount of available polar molecules (H_2O, CO_2, etc.) which are the principle contaminants are slightly below the stated criteria and should present no problem.

Table VIII. Offgassing Induced Environment Predictions for the Combined Spacelab/Orbiter Configurations

PREDICTED PARAMETERS / LINE-OF-SIGHT & BETA ANGLE	SPACELAB-1/ORBITER					SPACELAB-3/ORBITER				
	M.C.D. g/cm^2	N.C.D. $mol./cm^2$	RETURN FLUX (MAX) $g/cm^2/second$			M.C.D. g/cm^2	N.C.D. $mol./cm^2$	RETURN FLUX (MAX) $g/cm^2/second$		
			700 Km	435 Km	200 Km			700 Km	435 Km	200 Km
$0^\circ + Z_o$										
0° MAX	2.5(-9)*	8.2(+13)	1.5(-12)	4.3(-11)	2.3(-9)	3.6(-10)	1.2(+13)	2.1(-13)	6.5(-12)	3.2(-10)
MIN	4.8(-11)	1.6(+12)	2.9(-14)	8.0(-13)	4.3(-11)	1.4(-10)	4.5(+12)	8.0(-14)	2.3(-12)	1.2(-10)
60° MAX	2.5(-9)	8.2(+13)	1.5(-12)	4.3(-11)	2.3(-9)	3.6(-10)	1.2(+13)	2.1(-13)	6.5(-12)	3.2(-10)
MIN	6.0(-11)	1.9(+12)	3.5(-14)	8.5(-13)	5.0(-11)	1.7(-10)	5.5(+12)	1.0(-13)	2.9(-12)	1.5(-10)
73° MAX	2.5(-9)	8.2(+13)	1.5(-12)	4.3(-11)	2.3(-9)	3.6(-10)	1.2(+13)	2.2(-13)	6.5(-12)	3.2(-10)
$50^\circ \pm Y$										
0° MAX	1.5(-9)	5.0(+13)	9.2(-13)	2.6(-11)	1.4(-9)	2.6(-10)	8.6(+12)	1.6(-13)	4.6(-12)	2.3(-10)
MIN	3.0 (-11)	1.0(+12)	1.8(-14)	5.0(-13)	2.7(-11)	1.4(-10)	4.5(+12)	8.0(-14)	2.3(-12)	1.2(-10)
60° MAX	1.5(-9)	5.1(+13)	9.2(-13)	2.6(-11)	1.4(-9)	2.6(-10)	8.6(+12)	1.6(-13)	4.6(-12)	2.3(-10)
MIN	3.7(-11)	1.3(+12)	2.2(-14)	6.0(-13)	3.3(-11)	1.8(-10)	5.9(+12)	1.1(-13)	3.2(-12)	1.6(-10)
73° MAX	1.6(-9)	5.2(+13)	9.2(-13)	2.6(-11)	1.4(-9)	2.7(-10)	8.9(+12)	1.6(-13)	4.8(-12)	2.4(-10)
$25^\circ \pm Y$										
0° MAX	1.8(-9)	6.1(+13)	1.1(-12)	3.1(-11)	1.7(-9)	3.1(-10)	1.0(+13)	1.9(-13)	5.5(-12)	2.8(-10)
MIN	4.0(-11)	1.3(+12)	2.4(-14)	6.5(-13)	3.5(-11)	1.4(-10)	4.5(+12)	8.0(-14)	2.3(-12)	1.2(-10)
60° MAX	1.8(-9)	6.2(+13)	1.1(-12)	3.1(-11)	1.7(-9)	3.1(-10)	1.0(+13)	1.9(-13)	5.5(-12)	2.8(-10)
MIN	4.9(-11)	1.6(+12)	2.9(-14)	8.0(-13)	4.3(-11)	1.8(-10)	5.9(+12)	1.1(-13)	3.2(-12)	1.6(-10)
73° MAX	1.8(-9)	6.2(+13)	1.1(-12)	3.1(-11)	1.7(-9)	3.1(-10)	1.0(+13)	1.9(-13)	5.5(-12)	2.8(-10)
$50^\circ \pm Y$, 45° -X										
0° MAX	1.1(-9)	3.7(+13)	6.8(-13)	1.9(-11)	1.0(-9)	3.4(-10)	1.1(+13)	2.0(-13)	6.1(-12)	3.1(-10)
MIN	3.5(-11)	1.2(+12)	2.1(-14)	6.0(-13)	3.1(-11)	1.2(-10)	4.0(+12)	7.2(-14)	2.1(-12)	1.1(-10)
60° MAX	1.1(-9)	3.7(+13)	6.8(-13)	1.9(-11)	1.0(-9)	3.4(-10)	1.1(+13)	2.0(-13)	6.1(-12)	3.1(-10)
MIN	4.2(-11)	1.4(+12)	2.5(-14)	7.0(-13)	3.8(-11)	1.5(-10)	5.0(+12)	9.0(-14)	2.7(-12)	1.4(-10)
73° MAX	1.1(-9)	3.7(+13)	6.8(-13)	1.9(-11)	1.0(-9)	3.4(-10)	1.1(+13)	2.0(-13)	6.1(-12)	3.1(-10)
$50^\circ + X$										
0° MAX	3.8(-9)	1.3(+14)	2.3(-12)	6.5(-11)	3.4(-9)	4.0(-10)	1.3(+13)	2.4(-13)	7.1(-12)	3.6(-10)
MIN	3.4(-11)	1.1(+12)	2.0(-14)	6.0(-13)	3.0(-11)	1.0(-10)	3.3(+12)	6.0(-14)	1.8(-12)	9.0(-11)
60° MAX	3.8(-9)	1.3(+14)	2.3(-12)	6.6(-11)	3.5(-9)	4.1(-10)	1.4(+13)	2.5(-13)	7.3(-12)	3.7(-10)
MIN	3.9(-11)	1.3(+12)	2.4(-14)	6.5(-13)	3.5(-11)	1.7(-10)	5.5(+12)	1.0(-13)	2.9(-12)	1.5(-10)
73° MAX	3.8(-9)	1.3(+14)	2.3(-12)	6.6(-11)	3.5(-9)	4.1(-10)	1.4(+13)	2.5(-13)	7.3(-12)	3.7(-10)
50° -X										
0° MAX	1.1(-9)	3.6(+13)	6.4(-13)	1.9(-11)	9.5(-10)	5.2(-10)	1.7(+13)	3.1(-13)	9.3(-12)	4.7(-10)
MIN	3.6(-11)	1.2(+12)	2.2(-14)	6.5(-13)	3.3(-11)	1.0(-10)	3.3(+12)	6.0(-14)	1.8(-12)	9.0(-11)
60° MAX	1.1(-9)	3.6(+13)	6.5(-13)	1.9(-11)	9.5(-10)	5.2(-10)	1.7(+13)	3.1(-13)	9.3(-12)	4.7(-10)
MIN	4.5(-11)	1.5(+12)	2.7(-14)	7.5(-13)	4.0(-11)	1.7(-10)	5.5(+12)	1.0(-13)	2.9(-12)	1.5(-10)
73° MAX	1.1(-9)	3.6(+13)	6.5(-13)	1.9(-11)	9.5(-10)	5.2(-10)	1.7(+13)	3.1(-13)	9.3(-12)	4.7(-10)

* (-9) = 10^{-9}

Table IX. Leakage Induced Environment Predictions for the Combined Spacelab/Orbiter Configurations

PREDICTED PARAMETERS / LINE-OF-SIGHT & CONFIGURATION	M.C.D. g/cm^2	N.C.D. Total $mol./cm^2$	N.C.D. O_2 $mol./cm^2$	N.C.D. N_2 $mol./cm^2$	N.C.D. CO_2 $mol./cm^2$	N.C.D. H_2O $mol./cm^2$	RETURN $_2$ FLUX (MAX) $g/cm^2/second$		
							700 Km	435 Km	200 Km
0° + Z									
SL-1/ORBITER	1.11(-9)*	2.4(+13)	5.1(+12)	1.9(+13)	1.6(+11)	4.3(+11)	6.7(-13)	1.9(-11)	9.9(-10)
SL-3/ORBITER	1.0(-9)	2.2(+13)	4.6(+12)	1.7(+13)	1.5(+11)	3.9(+11)	6.0(-13)	1.7(-11)	9.0(-10)
$50^\circ \pm$ Y									
SL-1/ORBITER	1.09(-9)	2.4(+13)	5.0(+12)	1.9(+13)	1.6(+11)	4.2(+11)	6.5(-13)	1.9(-11)	9.8(-10)
SL-3/ORBITER	9.9(-10)	2.2(+13)	4.5(+12)	1.7(+13)	1.4(+11)	3.8(+11)	5.9(-13)	1.7(-11)	8.9(-10)
$25^\circ \pm$ Y									
SL-1/ORBITER	1.21(-9)	2.7(+13)	5.6(+12)	2.1(+13)	1.8(+11)	4.7(+11)	7.3(-13)	2.1(-11)	1.1(-9)
SL-3/ORBITER	1.1(-9)	2.4(+13)	5.1(+12)	1.9(+13)	1.6(+11)	4.3(+11)	6.6(-13)	1.9(-11)	9.9(-10)
$50^\circ \pm$ Y, 45° -X									
SL-1/ORBITER	9.5(-10)	2.1(+13)	4.4(+12)	1.6(+13)	1.4(+11)	3.7(+11)	5.7(-13)	1.6(-11)	8.5(-10)
SL-3/ORBITER	8.8(-10)	1.9(+13)	4.0(+12)	1.5(+13)	1.3(+11)	3.4(+11)	5.3(-13)	1.5(-11)	7.9(-10)
50° + X									
SL-1/ORBITER	1.8(-9)	4.0(+13)	8.3(+12)	3.0(+13)	2.6(+11)	7.1(+11)	1.1(-12)	3.1(-11)	1.6(-9)
SL-3/ORBITER	1.6(-9)	3.5(+13)	7.4(+12)	2.7(+13)	2.3(+11)	6.2(+11)	9.6(-13)	2.7(-11)	1.4(-9)
50° -X									
SL-1/ORBITER	9.1(-10)	2.0(+13)	4.2(+12)	1.6(+13)	1.3(+11)	3.5(+11)	5.5(-13)	1.5(-11)	8.2(-10)
SL-3/ORBITER	8.6(-10)	1.9(+13)	4.0(+12)	1.5(+13)	1.2(+11)	3.3(+11)	5.2(-13)	1.5(-11)	7.7(-10)

* $(-9) = 10^{-9}$

3.2.4 Evaporator Induced Environment Predictions - Although the Shuttle Orbiter Evaporator is not a Spacelab source uniquely, it contributes to the total environment and is presented in Table X for completeness. The location of the Evaporator has not been specifically established. A number of possible locations have been studied for contamination impact as is reported in the Applicable Document MCR 74-93. However, for this study, the present baseline position of X_o = 1392, Y_o = $\pm$113, and Z_o = 323 was used (see Figure 11).

For this baseline position, both the number column density and the resulting return flux exceed the stated criteria. Preliminary consideration for relocating this source under the payload bay door has indicated that the stated criteria could be met. Testing is being planned at JSC to establish the physical characteristics (plume shape, particle characteristics, and deposition characteristics) of the Evaporator taking into consideration various geometrical configurations. Until results are available from this test, the current baseline will be used for the subsequent analysis and should be considered preliminary.

3.2.5 Vernier Control System (25 lb Thrust Engines) Induced Environment Predictions - As in the case of the Evaporator, the VCS induced environment is not a direct result of the Spacelab configurations. However, it is a function of attitude and pointing requirements for each Payload. Two basic attitude and pointing modes have been identified. These are VCS for primary attitude control and VCS for desaturation of a Control Moment Gyro (CMG) attitude control system. In either case, the induced environment prediction from the VCS is basically constant per second of operation with the frequency required to be identified depending upon the mode. With CMG control and VCS desaturation, the anticipated usage is on the order of 4.7 to 5.6 lbs per desaturation which would occur approximately once every 9 orbits.

VCS attitude and pointing requirements have been identified in JSC 07700 Vol. XIV to require up to 3 lbs per orbit (approximately one firing every 4.8 seconds) for pointing accuracies comparable to those required for the analyzed Payloads. VCS pulses are anticipated to be on the order of 0.040 seconds which results in VCS firings on the order of 1% of the time on orbit. With

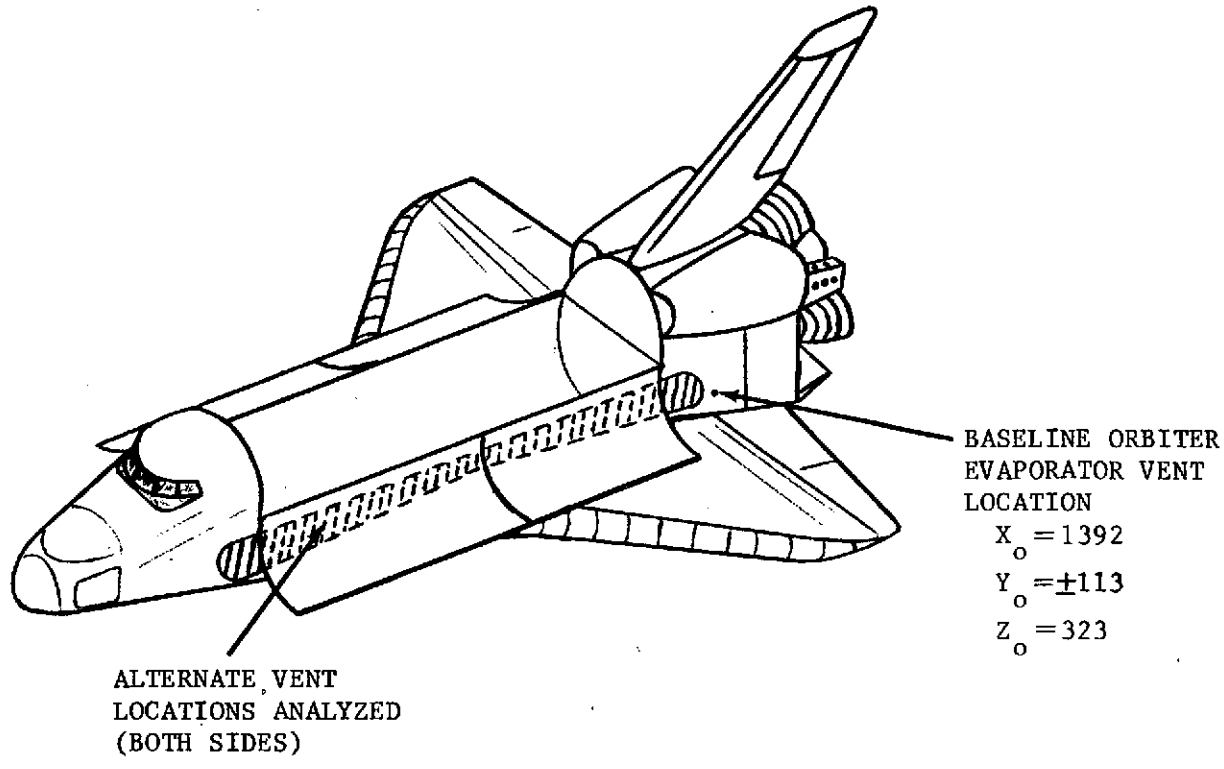

Figure 11. Shuttle Orbiter Baseline Evaporator Vent Location

Table X. Shuttle Orbiter Evaporator Induced Environment Predictions

PREDICTED PARAMETERS / LINE-OF-SIGHT & EVAPORATOR(S)	M.C.D. g/cm^2			N.C.D. mol./cm^2	RETURN FLUX g/cm^2/second		
	DIRECT IMPINGMT.	WING REFLECTION	TOTAL	TOTAL	700 Km	435 Km	200 Km
0° +Z							
+Y EVAP.	0	9.7(-10)*	9.7(-10)	3.2(+13)	5.8(-13)	1.6(-11)	8.7(-10)
-Y EVAP.	0	9.7(-10)	9.7(-10)	3.2(+13)	5.8(-13)	1.6(-11)	8.7(-10)
BOTH	0	1.9(-9)	1.9(-9)	6.3(+13)	1.1(-12)	3.2(-11)	1.7(-9)
50° +Y							
+Y EVAP.	1.2(-9)	2.3(-9)	3.5(-9)	1.2(+14)	2.1(-12)	6.0(-11)	3.1(-9)
-Y EVAP.	0	9.5(-12)	9.5(-12)	3.1(+11)	5.7(-15)	1.6(-13)	8.5(-12)
BOTH	1.2(-9)	2.3(-9)	3.5(-9)	1.2(+14)	2.1(-12)	6.0(-11)	3.1(-9)
25° +Y							
+Y EVAP.	1.7(-10)	2.3(-9)	2.5(-9)	8.3(+13)	1.5(-12)	4.3(-11)	2.2(-9)
-Y EVAP.	0	1.8(-10)	1.8(-10)	5.9(+12)	1.1(-13)	3.1(-12)	1.6(-10)
BOTH	1.7(-10)	2.5(-9)	2.7(-9)	8.9(+13)	1.6(-12)	4.6(-11)	2.4(-9)
50° +Y, 45° -X							
+Y EVAP.	6.1(-10)	3.6(-9)	4.2(-9)	1.4(+14)	2.5(-12)	7.1(-11)	3.8(-9)
-Y EVAP.	0	1.6(-12)	1.6(-12)	5.3(+10)	9.6(-16)	2.7(-14)	1.4(-12)
BOTH	6.1(-10)	3.6(-9)	4.2(-9)	1.4(+14)	2.5(-12)	7.1(-11)	3.8(-9)
50° +X							
+Y EVAP.	0	4.6(-10)	4.6(-10)	1.5(+13)	2.8(-13)	7.8(-12)	4.1(-10)
-Y EVAP.	0	4.6(-10)	4.6(-10)	1.5(+13)	2.8(-13)	7.8(-12)	4.1(-10)
BOTH	0	9.2(-10)	9.2(-10)	3.0(+13)	5.5(-13)	1.6(-11)	8.2(-10)
50° -X							
+Y EVAP.	0	8.9(-10)	8.9(-10)	2.9(+13)	5.3(-13)	1.5(-11)	8.0(-10)
-Y EVAP.	0	8.9(-10)	8.9(-10)	2.9(+13)	5.3(-13)	1.5(-11)	8.0(-10)
BOTH	0	1.8(-9)	1.8(-9)	5.9(+13)	1.1(-12)	3.1(-11)	1.6(-9)

* $(-10) = 10^{-10}$

potential firing frequencies of this nature, the VCS must be considered a near continuous source and a direct contributor to the induced environment predictions. Table XI presents the contribution to the various lines-of-sight that the aft Y and -Z firing engines and the forward Y/Z firing engines generate. In all cases, the VCS engines exceed the stated criteria in both number column density and return flux for the lower orbital altitudes of 435 and 200 Km. The interaction mechanisms for the VCS engines are from engine backflow, wing reflection, and forward flow for some lines-of-sight. Depending upon the sensitivity of a Payload to number column densities and return flux levels of this nature and the particular attitude and pointing control requirements, the need for CMG control may be a consideration for these Payloads.

Analytical treatment of the flow fields for the VCS uses empirical and analytical data developed by a variety of engine evaluators. The VCS plume definition used in this study is the same approach as established in the Applicable Document MCR-74-93. This is a modified Simons[1] approach for angles off the engine axis up to 140 degrees. From 140 degrees to 180 degrees, the plume definition described by test data of Chirivella and Simons[2] was used. These approaches are consistent with engine evaluators who are concerned with these flow fields during pre-engine design and development phases. As these engines are designed and tested, the improved definition and subsequent impact of the flow fields must be reassessed.

(1) Simons, G. A.: "Effect of Nozzle Boundary Layers on Rocket Exhaust Plumes," AIAA Journal, Vol. 10, No. 11 November 1972.

(2) Chirivella, J. E. and Simon, E.: "Molecular Flux Measurements in the Back Flow Region of a Nozzle Plume," J.P.L., JANNAF 7th Plume Technology Meeting, April 1973.

Table XI. Shuttle Orbiter VCS (25 Lb. Thrust) Induced Environment Predictions

PREDICTED PARAMETERS / LINE-OF-SIGHT & ENGINE FLUX DIRECTION	M.C.D. g/cm^2			N.C.D. mol./cm^2	RETURN FLUX g/cm^2/second		
	DIRECT IMPINGMT.	WING REFLECTION	TOTAL	TOTAL	700 Km	435 Km	200 Km
0^o + Z							
AFT -Z*	2.4(-10)***	1.8(-8)	1.8(-8)	4.4(+14)	1.1(-11)	3.1(-10)	1.6(-8)
AFT Y*	1.9(-9)	6.3(-9)	8.2(-9)	2.0(+14)	4.9(-12)	1.4(-10)	7.3(-9)
FWD Y/Z*	1.6(-10)	0	1.6(-10)	3.9(+12)	9.6(-14)	2.7(-12)	1.4(-10)
$50^o \pm$ Y							
AFT -Z	7.3(-10)	3.3(-8)	3.4(-8)	8.3(+14)	2.0(-11)	5.8(-10)	3.0(-8)
AFT -Z_o**	0	3.0(-10)	3.0(-10)	7.3(+12)	1.8(-13)	5.1(-12)	2.7(-10)
AFT Y	2.0(-8)	1.0(-8)	3.0(-8)	7.3(+14)	2.8(-11)	5.1(-10)	2.7(-8)
AFT Y_o	0	2.9(-10)	2.9(-10)	7.1(+12)	1.7(-13)	4.9(-12)	2.6(-10)
FWD Y/Z	1.3(-9)	0	1.3(-9)	3.2(+13)	7.8(-13)	2.2(-11)	1.2(-9)
FWD Y/Z_o	0	0	0	0	0	0	0
$25^o \pm$ Y							
AFT -Z	3.4(-10)	3.4(-8)	3.4(-8)	8.3(+14)	2.0(-11)	5.8(-10)	3.0(-8)
AFT -Z_o**	0	2.7(-9)	2.7(-9)	6.6(+13)	1.6(-12)	4.6(-11)	2.4(-9)
AFT Y	6.2(-9)	8.9(-9)	1.5(-8)	3.7(+14)	9.0(-12)	2.6(-10)	1.3(-8)
AFT Y_o	0	3.5(-9)	3.5(-9)	8.5(+13)	2.1(-12)	6.0(-11)	3.1(-9)
FWD Y/Z	4.5(-10)	0	4.5(-10)	1.1(+13)	2.7(-13)	7.7(-12)	4.0(-10)
FWD Y/Z_o	0	0	0	0	0	0	0
$50^o \pm$ Y, 45^o -X							
AFT -Z	5.4(-10)	5.8(-8)	5.9(-8)	1.4(+15)	3.5(-11)	1.0(-9)	5.3(-8)
AFT -Z_o**	0	7.9(-11)	7.9(-11)	1.9(+12)	4.7(-14)	1.3(-12)	7.1(-11)
AFT Y	2.2(-8)	1.3(-8)	3.5(-8)	8.5(+14)	2.1(-11)	6.0(-10)	3.1(-8)
AFT Y_o	0	6.3(-11)	6.3(-11)	1.5(+12)	3.8(-14)	1.1(-12)	5.6(-11)
FWD Y/Z	6.4(-10)	0	6.4(-10)	1.6(+13)	3.8(-13)	1.1(-11)	5.7(-10)
FWD Y/Z_o	0	0	0	0	0	0	0
50^o +X							
AFT -Z*	2.1(-11)	7.4(-9)	7.4(-9)	1.8(+14)	4.4(-12)	1.3(-10)	6.6(-9)
AFT Y*	2.9(-10)	3.0(-9)	3.3(-9)	8.1(+13)	2.0(-12)	5.6(-11)	3.0(-9)
FWD Y/Z*	1.1(-10)	0	1.1(-10)	2.7(+12)	6.6(-14)	1.9(-12)	9.9(-11)
50^o -X							
AFT -Z*	1.4(-10)	3.2(-8)	3.2(-8)	7.8(+14)	1.9(-11)	5.4(-10)	2.9(-8)
AFT Y*	3.1(-9)	7.1(-9)	1.0(-8)	2.4(+14)	6.0(-12)	1.7(-10)	9.0(-9)
FWD Y/Z*	0	0	0	0	0	0	0

* Due to symmetry of this Line-of-Sight with respect to verniers, contributions to it from opposite side verniers are equal to values presented.

** Contribution to Line-of-Sight from vernier on opposite side of vehicle (Z_o, Y_o, Y/Z_o)

*** (-10) = 10^{-10}

3.2.6 Horizontal Line-of-Sight Induced Environment Predictions - The lines-of-sight previously considered had an origin at the geometric center of each of the different pallet configurations and extended outward encompassing a 100 degree cone in the +Z direction. For the AMPS Payload, an additional line-of-sight was developed (see Figure 10). This line-of-sight is parallel to the (X, Z) plane and positioned one meter above the Shuttle Orbiter skinline along the X axis or major axis of the Orbiter. This line-of-sight was constructed for a manned Spacelab Orbiter configuration since this has been identified as one of the modes of operation for the Spacelab/AMPS configuration. Table XII presents the induced environment predictions for this line-of-sight for all modeled Spacelab/Orbiter sources.

3.2.7 Induced Environment Predictions Comparison for the Spacelab SL-1, SL-2, and SL-3 Configurations - Zero Degree Line-of-Sight - Although three Spacelab configurations were modeled, only two (SL-1 and SL-3) were considered to develop the contaminant impact assessment upon the evaluated Payloads. Since SL-2 and SL-1 are similar in that they both use a module and pallet configuration, the resulting mass column densities along any given line-of-sight are comparable with small differences. Only the zero degree or +Z line-of-sight was modeled for the SL-2 configuration. Table XIII presents a comparison of the induced environment predictions for the zero degree line-of-sight for the sources and the three Spacelab configurations modeled.

3.2.8 Combined Induced Environment Predictions - Table XIV presents the combined maximum and minimum induced environment predictions for the two Spacelab/Orbiter configurations. The predictions are based upon those conditions which result from either operational activities (e.g. beta angle) or from Payload requirements (e.g. use of CMGs or VCS). The maximum predictions incorporate the following considerations:

a) contributions from peak outgassing and offgassing (at 10 hrs) as a result of beta angle;
b) leakage;
c) Evaporator; and
d) VCS (25 lb thrust) when used for attitude and pointing control.

The minimum predictions are based upon the following considerations:

Table XII. Horizontal Line-of-Sight Induced Environment Predictions

PREDICTED PARAMETERS / SOURCE & CONDITIONS	M.C.D. g/cm^2	N.C.D. $mol./cm^2$	RETURN FLUX AT 435 Km* $g/cm^2/second$
OUTGASSING			
$\beta = 0^\circ$ MAX	5.4(-10)**	3.4(+12)	4.3(-9)
MIN	1.5(-11)	9.6(+10)	1.2(-10)
$\beta = 60^\circ$ MAX	6.4(-10)	4.0(+12)	5.1(-9)
MIN	2.3(-11)	1.4(+11)	1.8(-10)
$\beta = 73^\circ$ MAX	6.5(-10)	4.1(+12)	5.2(-9)
OFFGASSING			
$\beta = 0^\circ$ MAX	1.1(-9)	3.6(+13)	3.1(-10)
MIN	3.3(-11)	1.1(+12)	9.4(-12)
$\beta = 60^\circ$ MAX	1.4(-9)	4.6(+13)	4.0(-10)
MIN	4.8(-11)	1.6(+12)	1.4(-11)
$\beta = 73^\circ$ MAX	1.4(-9)	4.6(+13)	4.0(-10)
LEAKAGE			
	2.2(-10)	4.8(+12)	6.2(-11)
VCS ENGINES			
FWD Y/Z	1.0(-9)	7.9(+13)***	2.8(-10)
AFT Y	1.2(-9)	9.5(+13)	3.4(-10)
AFT -Z	9.2(-10)	7.4(+13)	2.6(-10)
EVAPORATOR			
	6.2(-11)	2.0(+12)	1.8(-11)

* Based on π steradian Field-of-View
** (-10) = 10^{-10}
*** Based on individual constituents rather than M avg = 18

TAble XIII. Induced Environment Prediction Comparison for Spacelab
SL-1, SL-2, and SL-3 Configurations Zero Degree Line-of-Sight

PREDICTED PARAMETERS / SOURCE & BETA ANGLE	SPACELAB-1					SPACELAB-2					SPACELAB-3				
	M.C.D. g/cm^2	N.C.D. $mol./cm^2$	RETURN FLUX (MAX) $g/cm^2/second$ 700 Km	435 Km	200 Km	M.C.D. g/cm^2	N.C.D. $mol./cm^2$	RETURN FLUX (MAX) $g/cm^2/second$ 700 Km	435 Km	200 Km	M.C.D. g/cm^2	N.C.D. $mol./cm^2$	RETURN FLUX (MAX) $g/cm^2/second$ 700 Km	435 Km	200 Km
OUTGASSING															
0^o MAX	2.3(-10)*	1.5(+12)	4.1(-12)	1.1(-10)	0	1.4(-10)	8.6(+11)	2.5(-12)	6.6(-11)	0	2.9(-11)	1.8(+11)	5.2(-13)	1.4(-11)	0
MIN	4.2(-12)	2.6(+10)	7.5(-14)	2.0(-12)	0	7.7(-12)	4.9(+10)	1.4(-13)	3.7(-12)	0	1.3(-11)	7.8(+10)	2.2(-13)	6.0(-12)	0
60^o MAX	2.3(-10)	1.5(+12)	4.1(-12)	1.1(-10)	0	1.4(-10)	8.6(+11)	2.5(-12)	6.6(-11)	0	2.9(-11)	1.8(+11)	5.2(-13)	1.4(-11)	0
MIN	5.1(-12)	3.2(+10)	9.1(-14)	2.5(-12)	0	9.5(-12)	6.0(+10)	1.7(-13)	4.6(-12)	0	1.5(-11)	9.6(+10)	2.7(-13)	7.4(-12)	0
73^o MAX	2.3(-10)	1.5(+12)	4.1(-12)	1.1(-10)	0	1.4(-10)	8.6(+11)	2.5(-12)	6.6(-11)	0	2.9(-11)	1.8(+11)	5.2(-13)	1.4(-11)	0
OFFGASSING															
0^o MAX	2.5(-9)	8.0(+13)	1.5(-12)	4.2(-11)	2.2(-9)	1.5(-9)	4.9(+13)	9.0(-13)	2.5(-11)	1.3(-9)	3.1(-10)	1.0(+13)	1.9(-13)	5.5(-12)	2.8(-10)
MIN	4.5(-11)	1.5(+12)	2.7(-14)	7.5(-13)	4.1(-11)	8.0(-11)	2.7(+12)	5.0(-14)	1.4(-12)	7.5(-11)	1.4(-10)	4.4(+12)	8.0(-14)	2.3(-12)	1.2(-10)
60^o MAX	2.5(-9)	8.0(+13)	1.5(-12)	4.2(-11)	2.2(-9)	1.5(-9)	4.9(+13)	9.0(-13)	2.5(-11)	1.3(-9)	3.1(-10)	1.0(+13)	1.9(-13)	5.5(-12)	2.8(-10)
MIN	5.5(-11)	1.8(+12)	3.3(-14)	9.0(-13)	4.9(-11)	1.0(-10)	3.4(+12)	6.0(-14)	1.7(-12)	9.0(-11)	1.7(-10)	5.5(+12)	1.0(-13)	2.8(-12)	1.5(-10)
73^o MAX	2.5(-9)	8.0(+13)	1.5(-12)	4.2(-11)	2.2(-9)	1.5(-9)	4.9(+13)	9.0(-13)	2.5(-11)	1.3(-9)	3.1(-10)	1.0(+13)	1.9(-13)	5.5(-12)	2.8(-10)
LEAKAGE	1.1(-10)	2.5(+12)	6.7(-14)	1.9(-12)	1.0(-10)	1.2(-10)	2.6(+12)	7.1(-14)	2.0(-12)	1.1(-10)	0	0	0	0	0

* (-10) = 10^{-10}

TABLE XIV. MAXIMUM - MINIMUM RANGE OF INDUCED ENVIRONMENT PREDICTIONS

PREDICTED PARAMETERS / LINE-OF-SIGHT & MAX/MIN CONDITIONS	SPACELAB-1/ORBITER					SPACELAB-3/ORBITER				
	M.C.D. g/cm^2	N.C.D. $mol./cm^2$	RETURN FLUX $g/cm^2/second$ 700 Km	435 Km	200 Km	M.C.D. g/cm^2	N.C.D. $mol./cm^2$	RETURN FLUX $g/cm^2/second$ 700 Km	435 Km	200 Km
$0^\circ + Z$										
MAX**	2.4(-8)*	6.1(+14)	1.8(-11)	5.2(-10)	2.1(-8)	2.1(-8)	5.4(+14)	1.4(-11)	3.8(-10)	1.9(-8)
	1.5(-8)	4.2(+14)	1.3(-11)	3.7(-10)	1.2(-8)	1.2(-8)	3.5(+14)	9.5(-12)	2.3(-10)	1.1(-8)
MIN*** (EVAP-ON)	3.1(-9)	8.9(+13)	1.9(-12)	5.4(-11)	2.7(-9)	3.1(-9)	9.0(+13)	2.0(-12)	5.8(-11)	2.7(-9)
	2.0(-9)	6.5(+13)	1.2(-12)	3.6(-11)	1.8(-9)	2.1(-9)	6.8(+13)	1.4(-12)	4.1(-11)	1.8(-9)
(EVAP-OFF)	1.2(-9)	2.6(+13)	8.0(-13)	2.2(-11)	1.0(-9)	1.2(-9)	2.7(+13)	9.2(-13)	2.6(-11)	1.0(-9)
	7.5(-11)	2.1(+12)	1.4(-13)	3.8(-12)	6.3(-11)	1.7(-10)	5.0(+12)	3.3(-13)	9.2(-12)	1.4(-10)
$50^\circ \pm Y$										
MAX	4.0(-8)	1.0(+15)	2.6(-11)	7.6(-10)	3.5(-8)	3.9(-8)	9.8(+14)	2.3(-11)	6.8(-10)	3.4(-8)
	2.4(-8)	7.0(+14)	1.7(-11)	4.8(-10)	2.1(-8)	2.3(-8)	6.5(+14)	1.4(-11)	4.0(-10)	2.0(-8)
MIN (EVAP-ON)	4.6(-9)	1.5(+14)	2.8(-12)	8.1(-11)	4.1(-9)	4.6(-9)	1.5(+14)	3.0(-12)	8.6(-11)	4.1(-9)
	3.6(-9)	1.2(+14)	2.2(-12)	6.3(-11)	3.1(-9)	3.7(-9)	1.3(+14)	2.4(-12)	6.9(-11)	3.2(-9)
(EVAP-OFF)	1.1(-9)	2.5(+13)	7.4(-13)	2.1(-11)	1.0(-9)	1.1(-9)	2.7(+13)	9.1(-13)	2.6(-11)	1.0(-9)
	5.6(-11)	1.5(+12)	9.8(-14)	2.7(-12)	4.7(-11)	1.7(-10)	5.0(+12)	3.3(-13)	9.2(-12)	1.4(-10)
$25^\circ \pm Y$										
MAX	4.0(-8)	1.0(+15)	2.7(-11)	7.7(-10)	3.5(-8)	3.8(-8)	9.5(+14)	2.3(-11)	6.7(-10)	3.3(-8)
	2.3(-8)	6.8(+14)	1.7(-11)	4.9(-10)	2.1(-8)	2.2(-8)	6.2(+14)	1.4(-11)	3.9(-10)	1.9(-8)
MIN (EVAP-ON)	3.9(-9)	1.2(+14)	2.4(-12)	7.0(-11)	3.5(-9)	4.0(-9)	1.2(+14)	2.6(-12)	7.4(-11)	3.5(-9)
	2.8(-9)	9.1(+13)	1.7(-12)	4.9(-11)	2.5(-9)	2.9(-9)	9.4(+13)	1.9(-12)	5.5(-11)	2.5(-9)
(EVAP-OFF)	1.2(-9)	2.8(+13)	8.4(-13)	2.4(-11)	1.1(-9)	1.3(-9)	2.9(+13)	1.0(-12)	2.8(-11)	1.1(-9)
	6.9(-11)	1.9(+12)	1.2(-13)	3.3(-12)	5.7(-11)	1.8(-10)	5.1(+12)	3.3(-13)	9.3(-12)	1.4(-10)
$50^\circ \pm Y$, $45^\circ -X$										
MAX	6.5(-8)	1.6(+15)	4.1(-11)	1.2(-9)	5.9(-8)	6.4(-8)	1.6(+15)	3.9(-11)	1.1(-9)	5.8(-8)
	3.8(-8)	1.1(+15)	2.5(-11)	7.0(-10)	3.4(-8)	3.7(-8)	1.0(+15)	2.3(-11)	6.5(-10)	3.3(-8)
MIN (EVAP-ON)	5.2(-9)	1.6(+14)	3.2(-12)	9.0(-11)	4.7(-9)	5.2(-9)	1.6(+14)	3.3(-12)	9.4(-11)	4.7(-9)
	4.3(-9)	1.4(+14)	2.6(-12)	7.4(-11)	3.8(-9)	4.4(-9)	1.4(+14)	2.8(-12)	7.9(-11)	3.9(-9)
(EVAP-OFF)	1.0(-9)	2.2(+13)	6.6(-13)	1.9(-11)	8.8(-10)	1.0(-9)	2.3(+13)	8.1(-13)	2.3(-11)	9.0(-10)
	5.8(-11)	1.6(+12)	1.1(-13)	2.8(-12)	4.8(-11)	1.5(-10)	4.5(+12)	2.9(-13)	8.2(-12)	1.3(-10)
$50^\circ + X$										
MAX	1.4(-8)	3.8(+14)	1.5(-11)	4.2(-10)	1.3(-8)	1.0(-8)	2.6(+14)	6.9(-12)	2.1(-10)	9.2(-9)
	9.2(-9)	2.8(+14)	1.2(-11)	3.3(-10)	8.0(-9)	5.5(-9)	1.6(+14)	4.0(-12)	1.2(-10)	4.8(-9)
MIN (EVAP-ON)	2.8(-9)	7.1(+13)	1.7(-12)	5.0(-11)	2.5(-9)	2.6(-9)	6.8(+13)	1.8(-12)	5.0(-11)	2.3(-9)
	9.9(-10)	3.2(+13)	6.6(-13)	1.9(-11)	8.8(-10)	1.1(-9)	3.4(+13)	8.3(-13)	2.3(-11)	9.4(-10)
(EVAP-OFF)	1.8(-9)	4.1(+13)	1.2(-12)	3.4(-11)	1.6(-9)	1.7(-9)	3.8(+13)	1.2(-12)	3.4(-11)	1.5(-9)
	7.4(-11)	1.9(+12)	1.1(-13)	3.1(-12)	6.2(-11)	1.4(-10)	4.1(+12)	2.8(-13)	7.4(-12)	1.2(-10)
$50^\circ - X$										
MAX	3.6(-8)	9.0(+14)	2.4(-11)	6.7(-10)	3.2(-8)	3.5(-8)	8.8(+14)	2.2(-11)	6.3(-10)	3.2(-8)
	2.1(-8)	5.9(+14)	1.5(-11)	4.1(-10)	1.9(-8)	2.0(-8)	5.7(+14)	1.3(-11)	3.7(-10)	1.8(-8)
MIN (EVAP-ON)	2.8(-9)	8.0(+13)	1.7(-12)	4.9(-11)	2.5(-9)	2.8(-9)	8.1(+13)	1.9(-12)	5.3(-11)	2.5(-9)
	1.9(-9)	6.1(+13)	1.2(-12)	3.4(-11)	1.7(-9)	1.9(-9)	6.3(+13)	1.4(-12)	3.8(-11)	1.7(-9)
(EVAP-OFF)	1.0(-9)	2.1(+13)	6.5(-13)	1.8(-11)	8.5(-10)	1.0(-9)	2.2(+13)	7.8(-13)	2.2(-11)	8.6(-10)
	5.8(-11)	1.6(+12)	1.1(-13)	3.0(-12)	4.9(-11)	1.3(-10)	3.7(+12)	2.7(-13)	7.4(-12)	1.1(-10)

* $(-8) = 10^{-8}$

** Maximum outgassing, offgassing at 10 hrs. leakage, evaporator, and VCS

*** Minimum outgassing, offgassing at 10 hrs. leakage with and without evaporator

____ Polar molecules

a) contributions from minimum outgassing and off-gassing (at 10 hrs) as a result of beta angle;
b) leakage; and
c) with and without the Evaporator.

In this case, CMG attitude and pointing control was assumed to be the mode of operation and desaturation of the CMGs by VCS could be timelined such that critical experiments would be protected during CMG desaturation.

3.2.9 Environmental Condensate Vent Induced Environment Predictions - The Spacelab Environmental Condensate Vent (ECV) was treated differently than that of the previously discussed sources. The previous sources are basically molecular sources while the ECV will vent liquid overboard with same vapor. However, the predominant contaminant from this vent is ice particles that result from phase change of the condensate when it is vented into space. Skylab employed a similar system as a contingency overboard vent for condensate while the prime mode of storage was in a water tank (which was dumped into the waste tank at the end of each mission). Considerable testing was conducted on the Skylab condensate vent to establish a plume of vented material which would clear the spacecraft through a definable trajectory if vented overboard. This testing established particle distributions, sizes, shapes, and velocities for the vent system. In this manner, predictable clearing times of the vented material could be established to identify any potential operational constraints to be employed for sensitive experiments.

The similarities that exist operationally between the Skylab and the Spacelab ECV indicate that the same approach should be considered for the Spacelab ECV. Operationally, the Spacelab ECV is planned to be activated near the end of a seven day mission. However, if mission durations extend to 30 days and/or operationally the need arises to vent at a higher frequency, the requirement to identify similar clearing time constraints as was established on Skylab becomes important.

Indications are that the double tapered 0.050 inch orifice nozzle employed on Skylab will be used for Spacelab. The following induced environment predictions for particle clearing times will be based upon performance characteristics of the similar Skylab vent obtained during extensive pre-Skylab ground testing.

The Environmental Condensate Vent is located on the Spacelab core module forward taper in the (X, Z) plane oriented ~ 45 degrees from the +Z axis toward the +X axis (see Figure 12). With the ECV located in this position and with the 0.05 inch orifice nozzle full plume angle of 130 degrees, a portion of the vented condensate will impinge upon the Shuttle Orbiter forward payload bay bulkhead. For any position on the forward taper of the module, the full plume angle would have to be less than 90^{o} to provide total clearing. This could be difficult to achieve for vents of this type. Therefore, relocation of this vent may be a prime consideration. This impingement will tend to retain particles in and/or near the payload bay. Consideration should be given to relocating this nozzle to minimize any surface impingement from the vented material to insure maximum particulate clearing. Although the present configuration shows the potential of impingement, the following clearing time analysis was conducted to ascertain what might be expected operationally in establishing clearing times for particles at various orbital altitudes from this vent. It was assumed that the Spacelab condensate holding tank will vent 56 lbs of liquid every seven days (8 lbs/3men/day x 7 days). An experiment line-of-sight in the +Z direction (zero degree) was selected to be representative of the Payloads.

Vent clearing time was defined as the time, measured from vent termination, required for the last particle to intersect the selected line-of-sight. This criteria corresponds to a number column density of zero resulting in a worst case condition (longest clearing time), with the exception of reencounter during successive orbits. The determination of number column densities as a function of time for the numerous variables involved and for a large number of lines-of-sight was not felt to be appropriate at this time due to the complexity of the calculations required and the extent of the present unknowns. The detailed impact of reencounter was not assessed for the same reasons. To further simplify the calculations, the vent axis and the line-of-sight were assumed to be contained in the orbital plane reducing the trajectory calculations to two dimensions. As further Spacelab Payload and system definitions become available, the analysis can be extended, as required, to assess the total combined effect of these phenomena on specific Payloads and lines-of-sight.

Molecular cloud clearing was not analyzed in depth since Skylab analyses have shown that molecular cloud clearing times, due to ambient molecular interactions, are negligible compared to particulate clearing times.

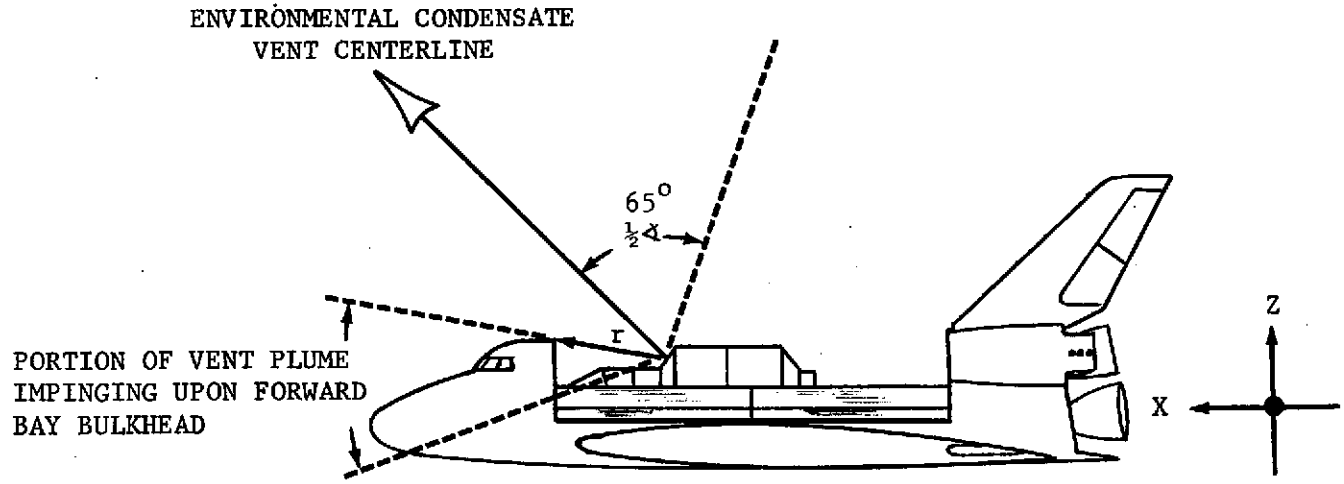

NOTE: $r \simeq 216"$ AT $\sim 75^{\circ}$ OFF Z TOWARDS X FOR SL-1 (ILLUSTRATED); $r \simeq 110"$ AT $\sim 58^{\circ}$ OFF Z TOWARDS X FOR SL-2

Figure 12. Spacelab Overboard Condensate Vent Plume Geometry

A computer program, NOMAD, was used to determine the trajectories of spherical particles emitted from an orbiting spacecraft. The program accounts for the atmospheric drag effects and the orbital mechanics effects acting on the particles.

The program input variables are particle size, particle density, particle ejection velocity, particle ejection angle with respect to the spacecraft velocity vector, particle drag coefficient, and spacecraft orbital altitude. The program calculates the position of individual particles with respect to the spacecraft as a function of time after emission for both a local vertical (ZLV) attitude and an inertial attitude. The program also provides plots of the particle trajectory in the orbital plane for both attitudes.

The Spacelab ECV parameters were assumed to be the same as the Skylab Contingency Condensate Vent (SCCV) parameters even though the driving pressure and the subsequent velocity and plume angles will be different. This should not greatly impact establishing a representative clearing time for this vent. The SCCV parameters were obtained from the Skylab Contamination Ground Test Program data. The SCCV operated with a pressure of 4.8 psia and flowed at approximately 2 lb/minute through a 0.050 inch diameter double tapered orifice nozzle.

The SCCV vent parameters are:

a) particle size range (10 to 1800 microns diameter);
b) mean particle size (110 microns diameter);
c) plume half angle (65 degrees);
d) mean particle velocity (7 m/second); and
e) flow rate (2 lbs/minute).

An inertial Shuttle Orbiter attitude was selected for the analysis since experiments most sensitive to scattering, such as stellar telescopes, will be operated in this mode.

Parametric analyses were performed for orbital altitudes of 200 Km, 435 Km, and 700 Km; particle sizes of 10, 110, and 1800 microns; and various nozzle orientations with respect to the Shuttle Orbiter velocity vector. All clearing time data is for the condition of the vent axis and the line-of-sight in the orbital plane. Typical computer generated trajectory plots are shown in Figures 13 and 14 for a ZLV and inertial spacecraft attitude, respectively. Three of the typical ZLV plots are superimposed in Figure 15 to show the geometry of a particle plume as a function of time. This example is for an initial vent axis orientation of 90 degrees with respect to the velocity vector, a plume half angle of 65 degrees, and an orbital altitude of 435 Km.

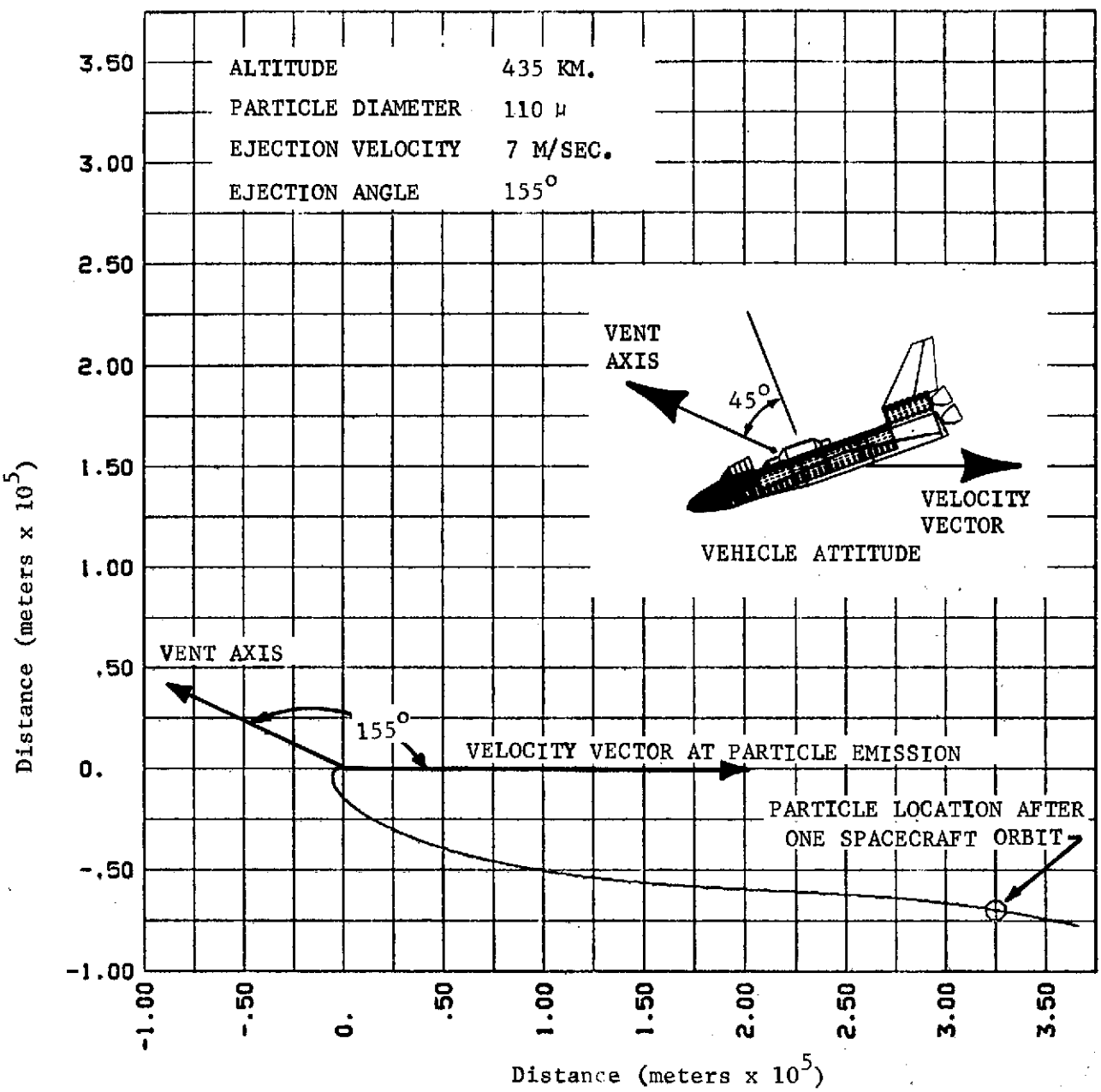

Figure 13. Typical Particle Trajectory for a ZLV Attitude at 435 km Altitude

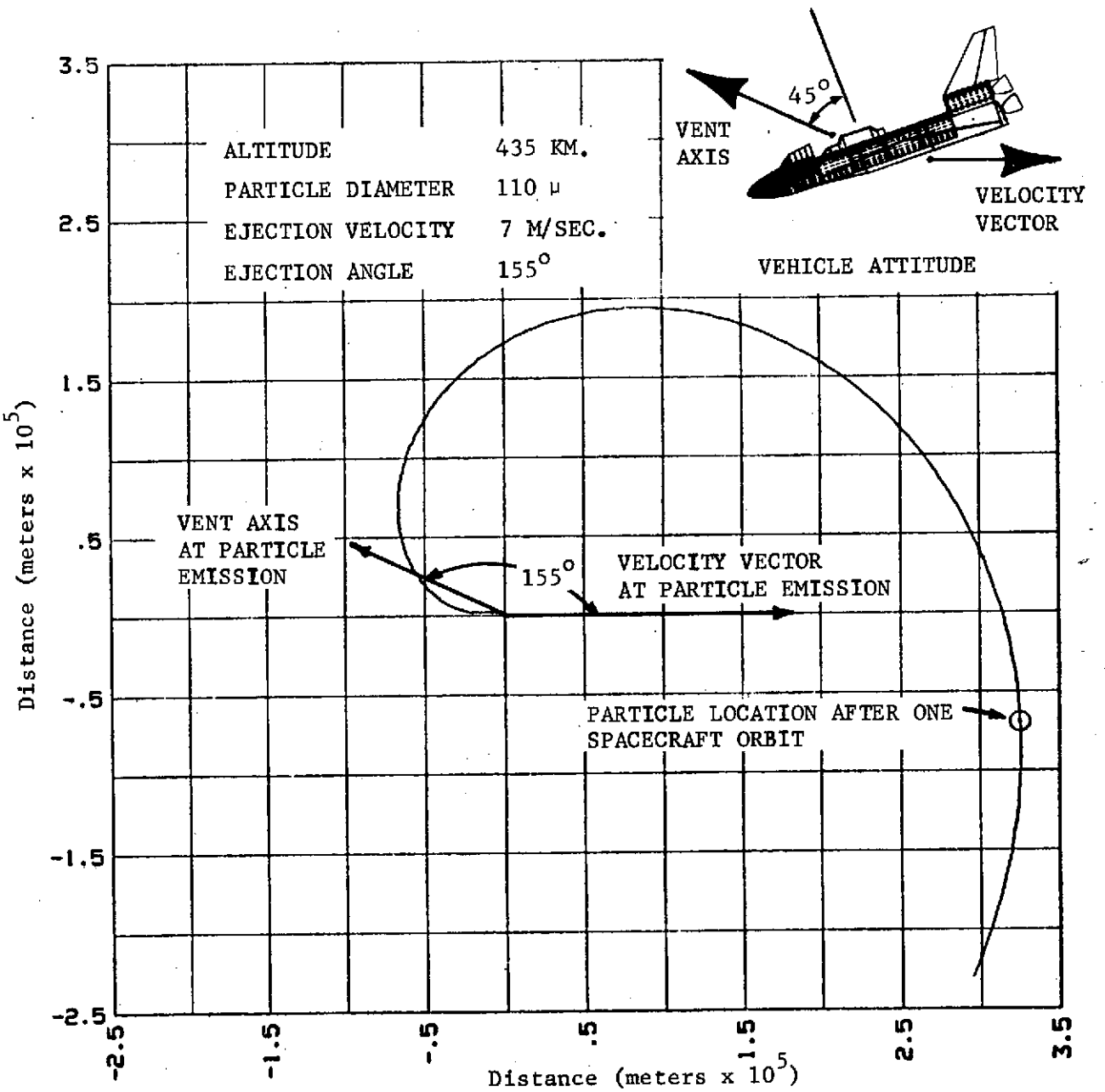

Figure 14. Typical Particle Trajectory for an Inertial Attitude at 435 km Altitude

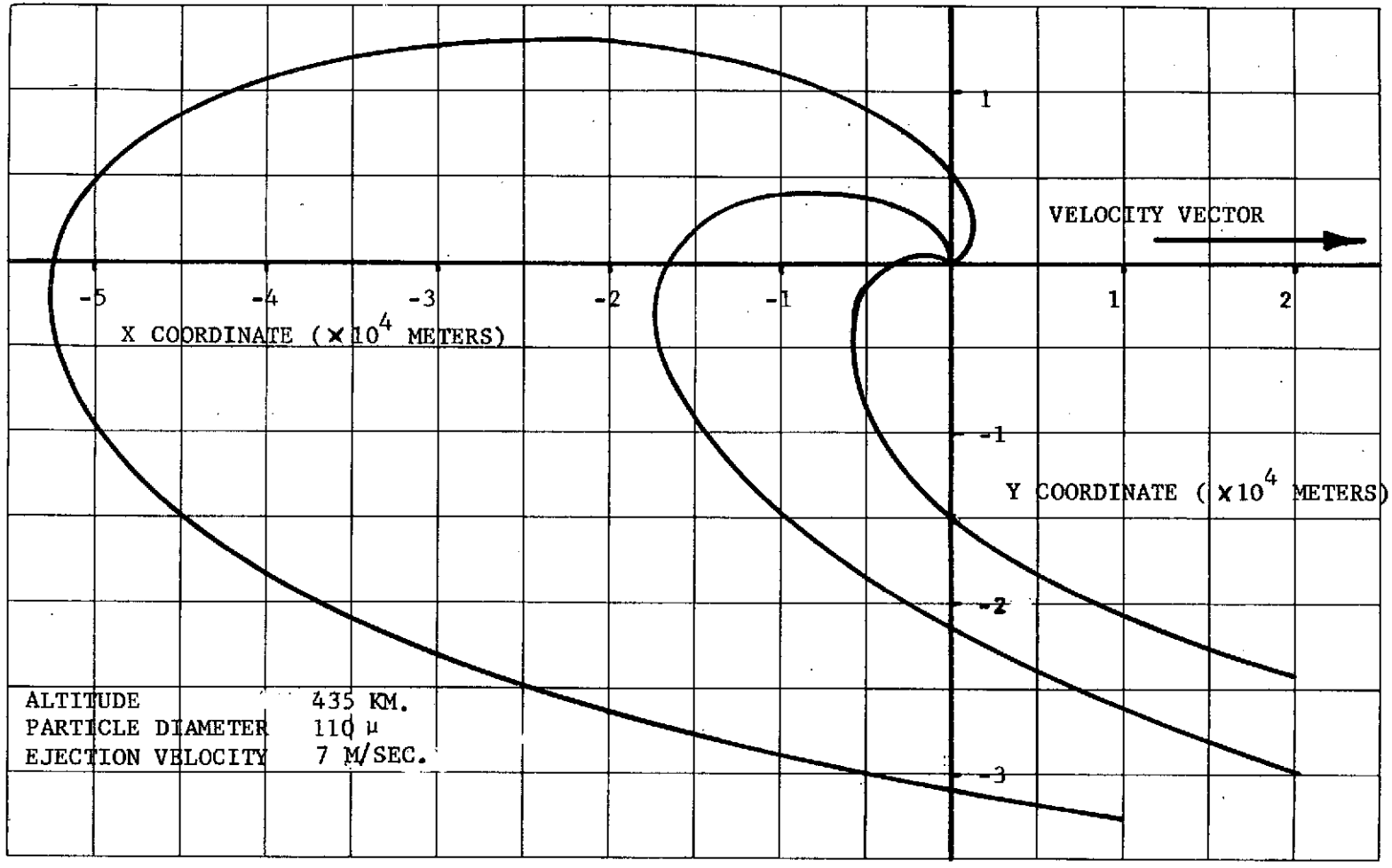

Figure 15. Typical Particle Plume Geometry for a ZLV Attitude at 435 km Altitude

Figure 16 shows the envelopes of clearing times for individual particle trajectories as a function of ejection angle with respect to the velocity vector. The plots encompass the trajectories for 10, 110, and 1800 micron particles for orbital altitudes of 200 Km, 435 Km, and 700 Km. The clearing times shown are for those trajectories which intersect the line-of-sight within the first orbital period only. Trajectory intersections with the line-of-sight after one orbital period is considered reencounter. Reencounter occurs when the atmospheric drag effect on the particle becomes negligible compared to the orbital mechanics effect. This occurs for all particles considered at 700 Km and for the 1800 micron particles at 435 Km.

Figure 17 shows the plume clearing times for a 130 degree full angle plume and a 28 minute vent duration (56 lbs/2 lbs/minute). The plume clearing time is defined as the longest particle clearing time for any trajectory within the plume. The clearing times are plotted as a function of the angle between the vent axis and the Shuttle Orbiter velocity vector at the time of vent initiation. Minimum clearing times and corresponding vent axis orientations for the baseline configuration are summarized below and graphically shown in Figure 18.

Altitude (km)	Minimum Clearing Time (Minutes)	Vent Axis Orientation with the Velocity Vector (Degrees)
200	0	100 to 210
435	17	22
700	16	25

The problem of reencounter was addressed on a very preliminary level. For negligible atmospheric drag, computer trajectory plots showed that particles emitted in the forward direction (along the velocity vector) tend to remain in an orbit above the Shuttle Orbiter orbit but particles emitted aft (against the velocity vector) tend to remain in an orbit below that of the Shuttle Orbiter. It was assumed that an experiment or Payload operating in an inertial mode will not operate with its line-of-sight intersecting the orbit (i.e., view through a higher density atmosphere than the orbital density). Therefore, the allowable particle ejection angles were

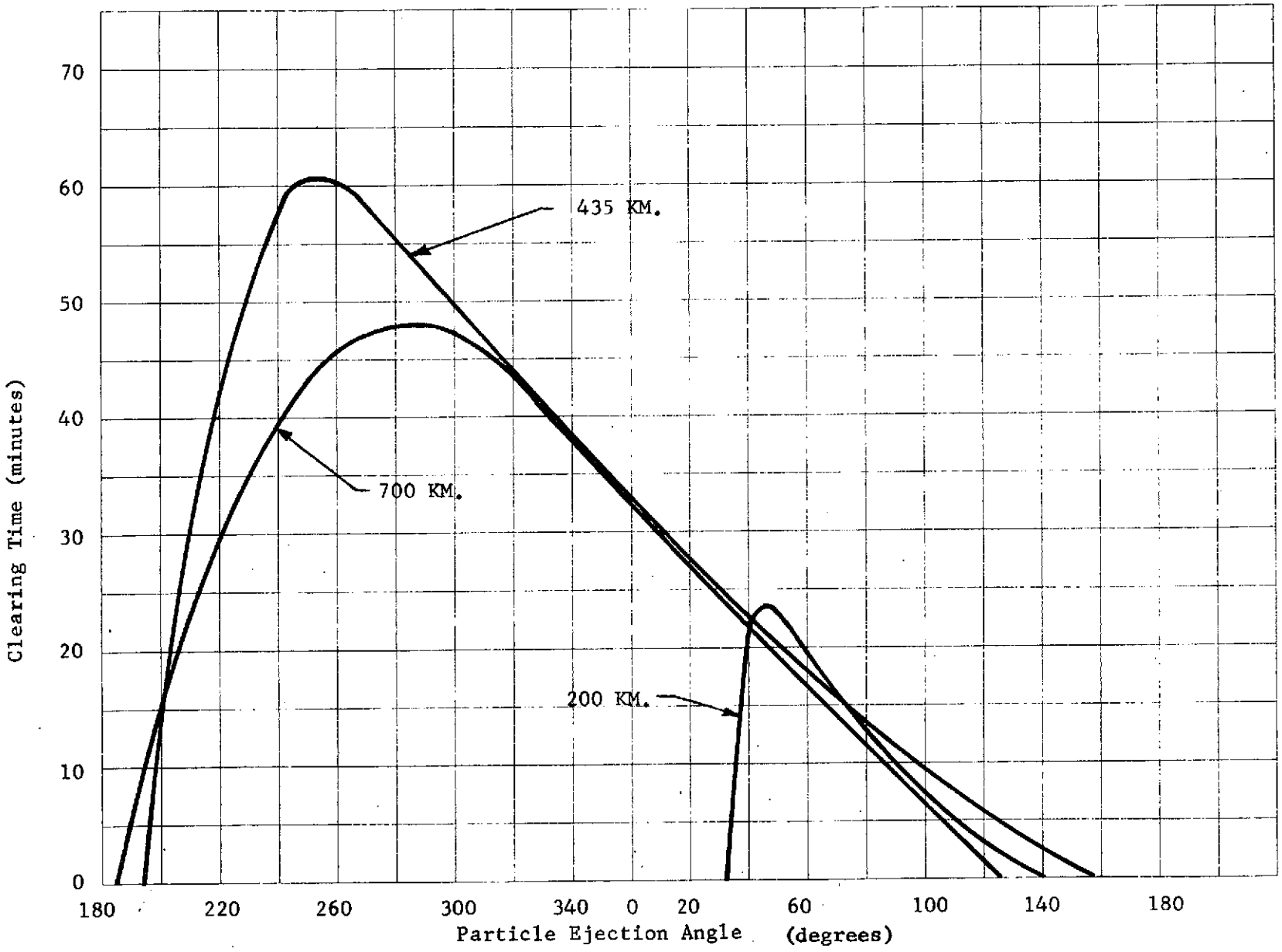

Figure 16. Spacelab Overboard Condensate Vent Particle Clearing Time as a Function of Particle Ejection Angle

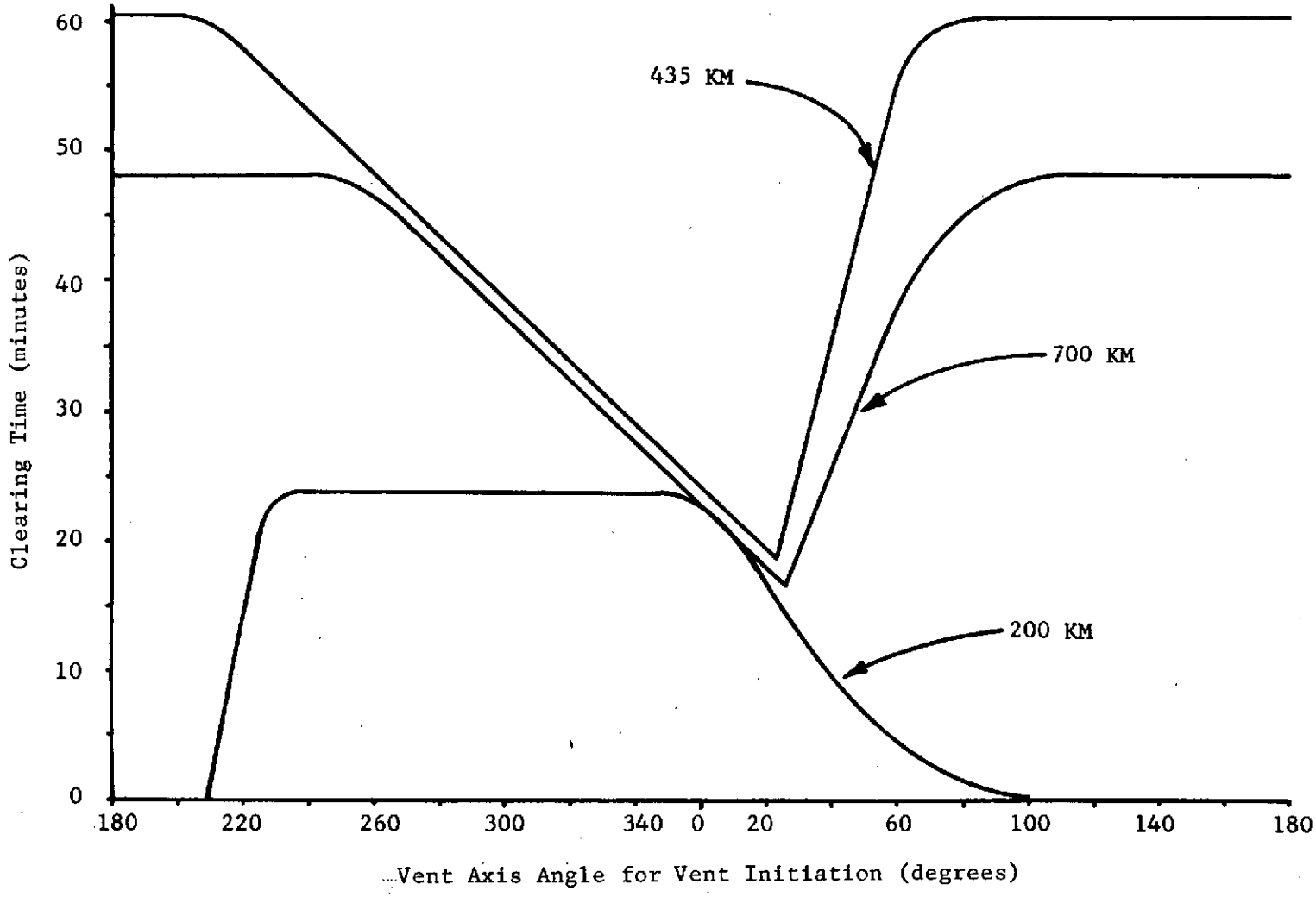

Figure 17. Spacelab Overboard Condensate Vent Plume Clearing Time as a Function of Vent Axis Angle for Vent Initiation

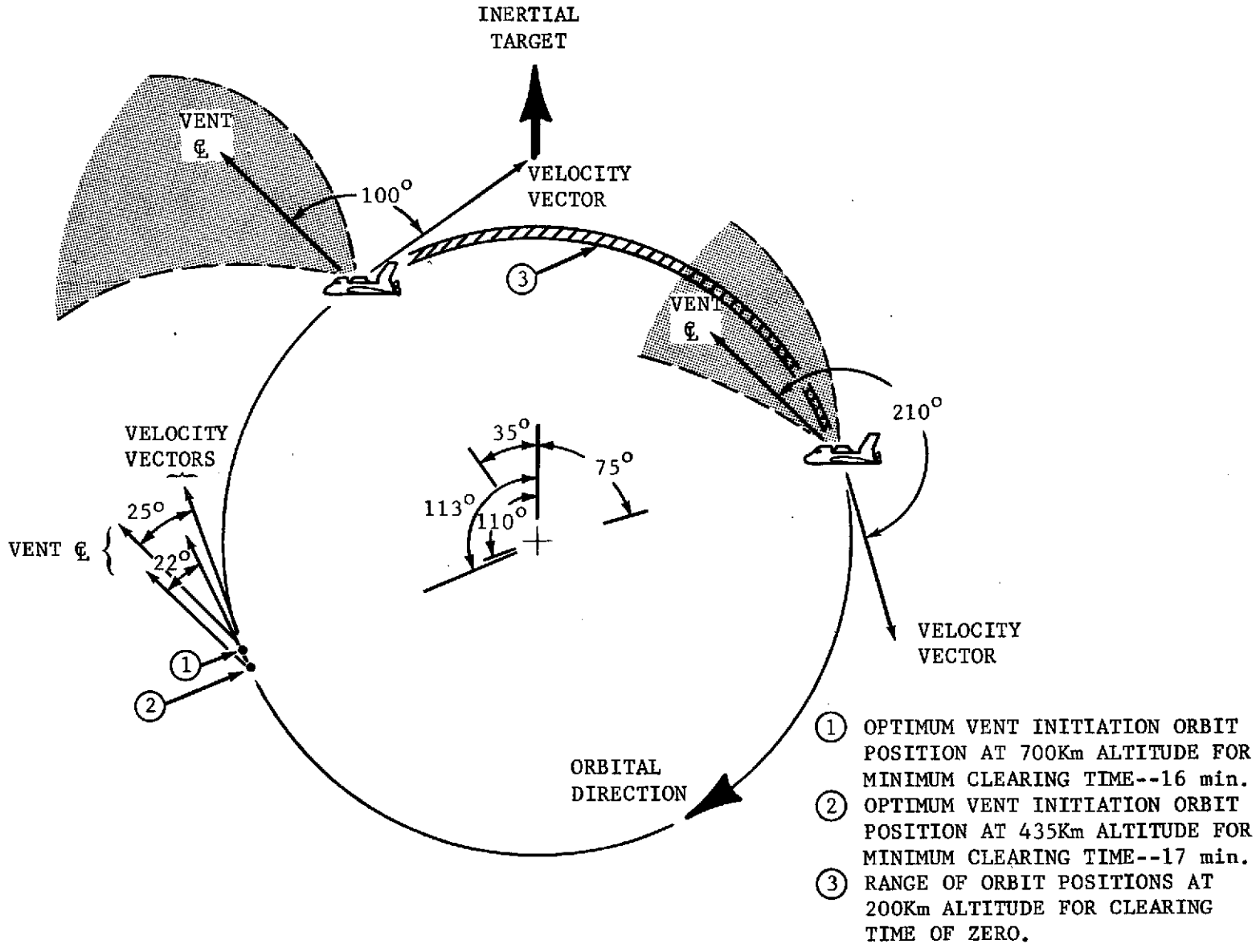

Figure 18. Spacelab Overboard Condensate Vent Initiation Position for Minimum Clearing Time as a Function of Orbital Altitude

restricted to between 90 degrees and 270 degrees to place the particles into orbits with maximum altitudes less than the altitude of the Shuttle Orbiter. The trajectory plots (for negligible drag) also indicated that particles ejected in the immediate vicinity of 90 degrees and 270 degrees tended to remain in the near vicinity of the spacecraft for many successive orbits. Therefore, the allowable particle trajectory region was further restricted to between 100 degrees and 260 degrees. The results of the analysis indicated that a 130 degrees full plume angle vented for 28 minutes could not be accommodated within the constrained region. Therefore, either the full plume angle dimensions would have to be reduced, or the flow rate increased (or a combination) if reencounter is to be minimized. A detailed analysis of these effects was not performed.

The above clearing times indicate that operationally a reasonable minimum clearing time similar to Skylab can be established if required for the Spacelab ECV. Relocation of the current baseline ECV or redesign of the vent should be given consideration to insure that any vented material from the ECV will not impinge upon Shuttle Orbiter/Spacelab surfaces and impede the clearing of particles.

3.3 Payload Contamination Impact Assessment - The preceding subsections presented a series of tables which identified for a number of given conditions the contaminant induced environment predictions for those configurations and sources considered. Although these induced environment predictions can be compared as stated to existing criteria for acceptability, it is important to make a limited assessment of the impact of the induced environment upon the various Spacelab/Payload configurations to be flown. In order to develop a total and an accurate assessment, certain basic additional information must be known. At this point in time and in the evolution of these Spacelab/Payload configurations, limited data is available and basic assumptions must be made.

The Summarized NASA Payload Descriptions - Sortie Payloads (Automated Payloads) Level A and B Data was used to baseline the following contamination impact analysis. Where

data was not available, representative configurations or data were assumed. In many cases, the variables involved are many and complex. Nominal conditions (e.g. orbital altitudes, viewing out of the orbital plane, average mission profile, etc.) were selected to be representative so that a basic assessment could be indicated. The following contamination impact assessment must be considered preliminary and is presented to provide an insight into those areas where contamination may have an impact upon potential Spacelab/Payload configurations.

A contamination impact assessment was made for the following Spacelab/Payload configurations:

a) AS-01-S, Pallet/1.5 Meter Cryogenically Cooled Infrared Telescope;

b) AS-03-S, Pallet/Deep Sky Ultraviolet Survey Telescope;

c) AS-04-S, Pallet/1 Meter Diffraction Limited Ultraviolet Optical Telescope;

d) AS-20-S, Pallet/2.5 Meter Cryogenically Cooled Infrared Telescope;

e) SO-12-S, Pallet/Apollo Telescope Mount (ATM) Spacelab;

f) SO-01-S, Pallet/Dedicated Solar Sortie Mission (DSSM);

g) EO-06-S, Module and Pallet/Scanning Spectroradiometer (Earth Observation);

h) AP-06-S, Module and Pallet/Atmospheric, Magnetospheric, and Plasmas in Space (AMPS).

Particle absorption, emission, and scattering and molecular absorption, scattering, and deposition were considered. The detailed assessment results for each Spacelab/Payload combination are presented in the following subsections along with the assumptions used. No significant contamination susceptibility has been identified for the EO-06-S payload and therefore it is not discussed further.

3.3.1 Infrared Telescope Payloads - The two infrared telescope Payloads were assumed to be 1.5 meter f/16 and 2.5 meter f/12 diffraction limited systems. The impact of particle scattering and black body emission and molecular scattering, absorption, and deposition was assessed.

Figure 19 shows the scattering noise power at the detector for 10, 100, and 1000 micron radius particles as a function of wavelength. The curves were developed for spherical ice particles in the near field for a scattering angle of 45 degrees and a 0.3 mm square solid state detector. The near field is defined as the region where the particle blur circle completely covers the detector. For the 1.5 meter and 2.5 meter telescopes, the near field extends to particle distances of $d_{1.5}$ = 90 Km and $d_{2.5}$ = 190 Km respectively at 10 micrometer wavelength. The noise power is constant for constant particle size at all distances within the near field. Beyond the near field boundary, the noise power falls off as $1/r^2$. The 45 degree scattering angle was selected as a worst case angle while remaining consistent within allowable earth/sun viewing angle constraints.

Figure 19 shows that for wavelengths greater than 3 micrometers particles with radii greater than approximately 300 microns will scatter a noise power in excess of 10^{-17} watts/micrometer at the detector. For λ = 20 micrometers and a $\Delta\lambda/\lambda$ = 0.5, this produces a noise background of 10^{-16} watts which reaches the maximum stated background noise criteria. Larger detectors will increase the noise power assuming all other parameters equal.

Figure 20 shows the noise background at the detector due to black body radiation for 10, 100, and 1000 micron radius ice particles as a function of wavelength. The curves were developed for a 0.3 mm square detector and particles in the near field at T = 200°K and ϵ = 1.0. The curves show that for particles larger than approximately 100 micron radius the blackbody irradiance at the telescope focal plane will exceed the stated limits. Particles other than ice particles will present higher noise backgrounds at the detector for the same conditions

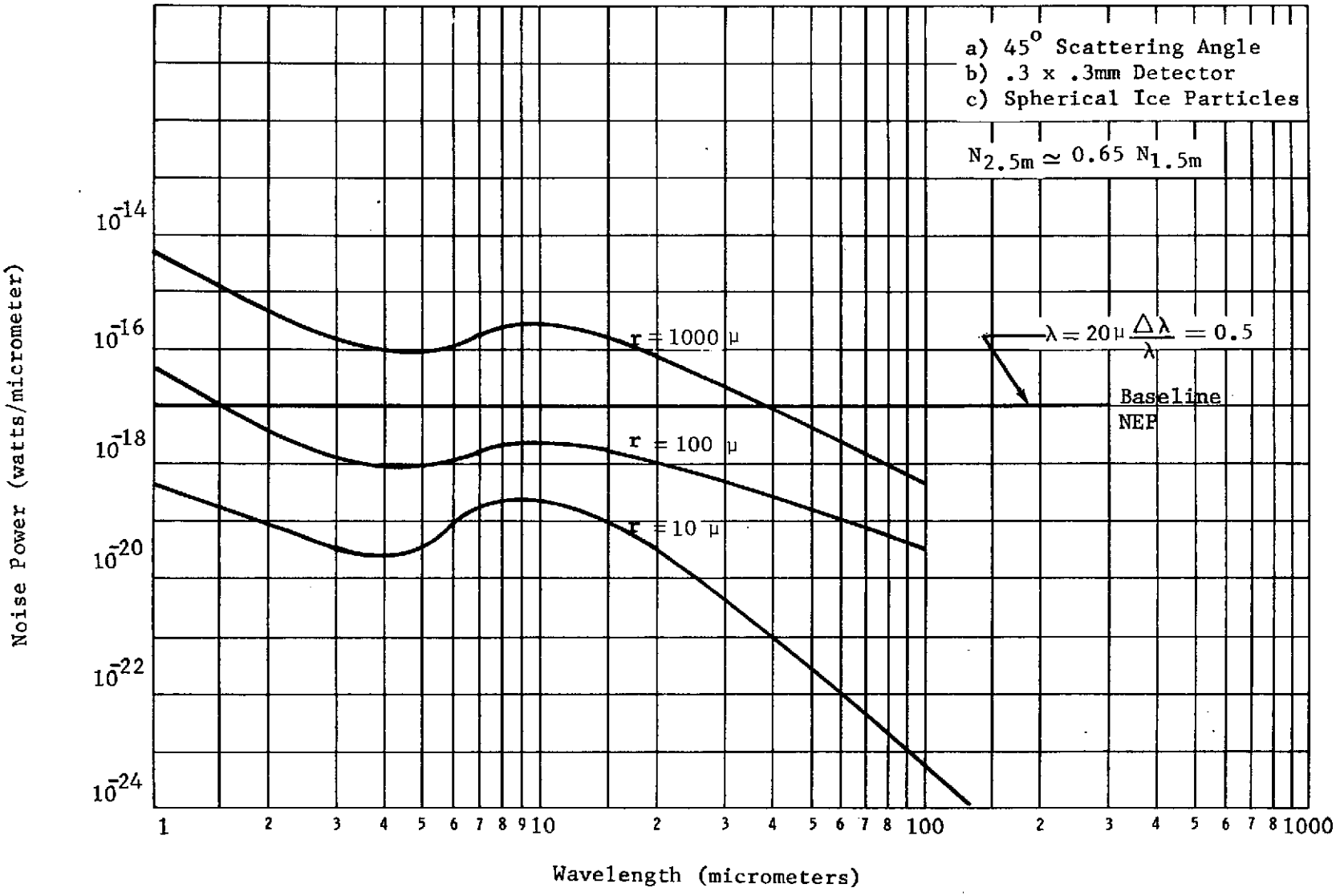

Figure 19. 1.5 Meter Infrared Telescope Particle Scattered Noise as a Function of Wavelength

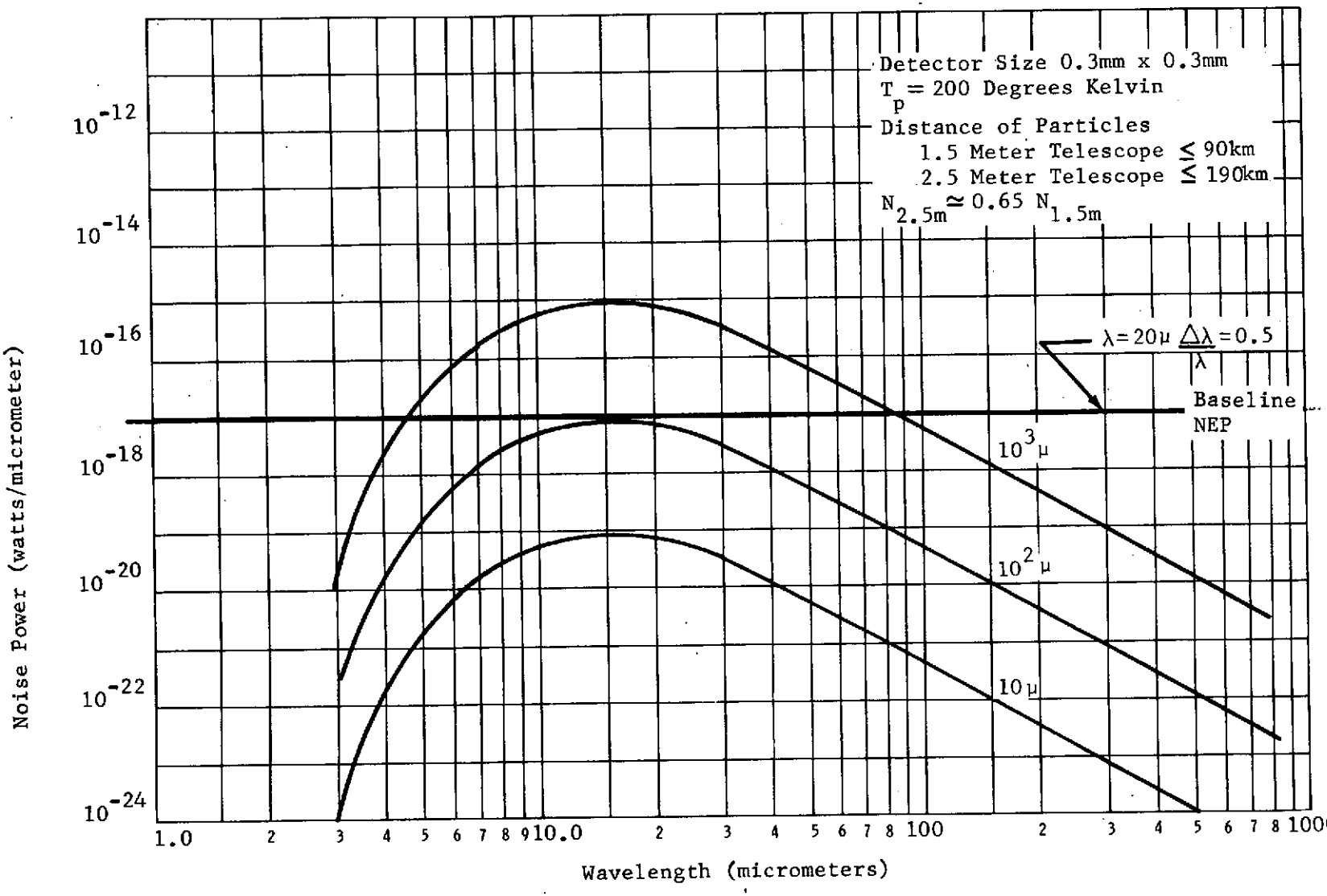

Figure 20. 1.5 Meter Infrared Telescopes Noise Equivalent Power (NEP) versus Wavelength for Particle Emission (Black Body)

since their net thermal temperatures are higher. Paint flakes from the surface of a spacecraft can be expected to be at approximately the temperature of the spacecraft surface which could be as high as 395°K or warmed by the radiation of the earth at approximately 300°K. For the given conditions, particles an order of magnitude smaller than the calculated sizes of ice particles could be seen with temperatures of 395°K. Again, larger detectors will result in greater noise powers.

The induced noise background due to molecular scattering is summarized in Table XV. The values shown are for worst case total column densities for all contaminant sources. Since the infrared telescopes are primarily interested in wavelengths greater than 3 micrometers, no significant noise contribution is anticipated from molecular cloud scattering. However, molecular emission from the hot gases could be a problem. This was not addressed since what might constitute hot gases in the induced environment is unknown at present.

Molecular cloud absorption was calculated for both H_2O and CO_2 for worst case column densities. For H_2O at $\lambda = 63$ micrometers and CO_2 at $\lambda = 4.3$ micrometers (typical worst case absorption bands),[2] the cloud absorption was determined to be less than 0.01%.

The return flux deposition on the infrared telescopes' primary mirrors is summarized in Table XVI. The return flux was calculated for large molecules (M=100), H_2O and CO_2 for the zero line-of-sight at 435 Km. Maximum and minimum outgassing and offgassing column densities were averaged over a full orbit. The telescope line-of-sight was assumed to be oriented 45 degrees to the orbital plane which was considered to be representative of an average orientation. Both telescopes were assumed to have mechanical or physical acceptance angles of 0.2 steradians ($L/D = 2$). The primary mirror temperatures were assumed to be 20°K.

Table XV. Infrared Telescope Molecular Scattering Noise Background Summary

WAVELENGTH micrometers	1.5 METER TELESCOPE Noise Power watts/micrometer		2.5 METER TELESCOPE Noise Power watts/micrometer	
	M = 18	M = 100	M = 18	M = 100
1	8.3×10^{-20}	1.2×10^{-16}	1.5×10^{-19}	2.1×10^{-16}
3	3.3×10^{-22}	4.5×10^{-19}	5.8×10^{-22}	8.3×10^{-19}
10	4.8×10^{-23}	6.8×10^{-22}	8.7×10^{-25}	1.2×10^{-21}
100	7.3×10^{-32}	1.1×10^{-28}	1.3×10^{-31}	1.9×10^{-28}

Table XVI. Infrared Telescopes' Return Flux Deposition Summary

SOURCE	SPECIE	DEPOSITION FROM RETURN FLUX AT 435 Km g/cm^2/orbit	g/cm^2/7 days	Å/7 days
Outgassing	M = 100	1.6×10^{-8}	1.8×10^{-6}	180
Engines	M = 100	3.6×10^{-11}	4.0×10^{-9}	0.4
	H_2O	2.2×10^{-9}	2.5×10^{-7}	25
	CO_2	1.6×10^{-11}	1.8×10^{-9}	0.2
Offgassing	H_2O	1.0×10^{-8}	1.2×10^{-6}	120
	CO_2	7.2×10^{-10}	8.6×10^{-9}	0.9
Evaporator	H_2O	1.8×10^{-7}	2.0×10^{-5}	2000
Leakage	H_2O	4.1×10^{-10}	4.6×10^{-8}	4.6
	CO_2	3.8×10^{-10}	4.2×10^{-8}	4.2

7 Day Totals		30 Day Totals	
M = 100	180Å	M = 100	770Å
H_2O	2150Å	H_2O	9200Å
CO_2	5.3Å	CO_2	23Å

The total deposition for 7 days and 30 days, as shown in Table XVI, is not expected to significantly effect the primary mirrors' reflectance characteristics. Extrapolated Gemini XII absorption data [1] shows that 180Å of M = 100 deposition will cause less than ~ 0.2% absorption at λ = 1 micrometer and above. The absorption due to CO_2 deposition will be negligible. Absorption due to approximately 2200Å deposition of H_2O will be approximately 2%[2] at λ = 1 micrometer for the seven day mission and could increase up to 10% for a 30 day mission. The increase in surface scattering for these deposition levels is expected to be negligible. However, measurements have shown that deposition of H_2O on cryogenically cooled reflective surfaces can significantly effect the surface emissivity[3]. For example, for polished stainless steel at 77°K, a 2000Å thick H_2O film will increase the emissivity from ~ 0.09 to ~ 0.11. This emissivity change could cause a significant change in mirror temperature and consequently overall telescope system performance. The detailed impact of this effect is unknown at this time but should be further evaluated.

The major contributor to deposition for the cryogenically cooled telescopes is shown in Table XVI to be the Evaporator. However, the final Evaporator location has yet to be selected and the current baseline position used for this study results in essentially a worst case condition. Final selection of the position of the Evaporator should reduce the H_2O contribution to the infrared telescopes considerably. Tests currently being defined at JSC will evaluate the Evaporator effluent

(1) Muscari, J. A., and Cunningham, A. C.: "Gemini 12 Contamination Study," Martin Marietta Aerospace Report R-67-2, January 1967.

(2) Witteborn, F. C.: "Preliminary Draft - Infrared Telescopes for a Space Observatory," NASA-Ames Research Center, July 31, 1973.

(3) Viehmann, W. and Eubanks, A. G.: "Effects of Surface Contamination on the Infrared Emissivity and Visible-Light Scattering of Highly Reflective Surfaces at Cryogenic Temperatures," Goddard Space Flight Center, NASA TND-6585, February 1972.

characteristics under simulated geometries to support the final position selection. This should provide basic test data for future analysis of the impact of the final position of the Evaporator upon cryogenically cooled telescopes. In addition, the option may exist that the infrared gelescope could store the Evaporator effluents and then this source would not be an impact under any considerations. If mission durations were sufficiently long and orbital venting of the stowed liquid was a requirement, then possible operational constraints might be required during the venting period similar to those discussed in subsection 3.2.9 for the Spacelab ECV.

The return flux can be significantly reduced by flying these Payloads at higher than 435 Km orbital altitudes since the return flux is directly related to ambient molecular density. The allowable altitude range for these two instruments has been identified to range from 300-630 Km. Conversely, flying these Payloads at lower orbital altitudes than 435 Km will significantly increase the return flux impact upon infrared telescopes.

3.3.2 Ultraviolet Telescope Payloads - The two ultraviolet telescope Payloads were assumed to be 0.75 meter f/2 and 1 meter f/16 systems. The system resolutions were assumed to be one arc second and 0.2 arc seconds respectively. The impact of particle scattering and molecular scattering, absorption, and deposition was assessed.

Table XVII summarizes the particle scattering analyses results. The table shows the equivalent ultraviolet stellar focal plane irradiance as a function of wavelength and particle size. The assumptions used were spherical ice particles in the near field, 45 degree scattering angle (consistent with viewing constraints), and a type AO reference star. The results show that the 1 meter telescope will not see particles with radii up to 1000 microns. Particles with larger radii may be detected. The 0.75 meter telescope will not see particles with radii up through 100 microns but may detect particles with larger radii.

Table XVII. Ultraviolet Particle Scattering Summary

WAVELENGTH micrometers	PARTICLE RADII microns	0.75 METER TELESCOPE STAR BRIGHTNESS MAGNITUDE M_{uv}	1 METER TELESCOPE STAR BRIGHTNESS MAGNITUDE M_{uv}
0.1	10	39	42
0.3		29	33
0.5		27	32
0.1	100	35	38
0.3		25	28
0.5		23	27
0.1	1000	29	33
0.3		18	22
0.5		17	21

The impact of these particles upon these systems will depend upon their mode of operation and upon the particle size and dwell time in the field-of-view of the telescope. For photographic surveys and imaging modes of operation, particles will appear as stars or as bright point sources and should not impact the resulting data. However, if the mode of operation is based upon long integration times for faint sources, then a particle of sufficient brightness and dwell time could influence the data being obtained.

A concern arises from the deposition of large particles on critical optical mirrors and surfaces. Dust and other particulates on the mirror surfaces can scatter radiation from off axis stars and could greatly increase the noise background. This effect would probably not be an effect of the induced environment as developed on orbit unless the telescope was subjected directly to a source of particulate matter. It probably would be an effect as the result of ground handling or an unfavorable prelaunch and launch condition. This particulate effect is hard to assess since the quantity of particulates and the accumulative effect is hard to ascertain prior to a given mission.

Table XVIII summarizes the ultraviolet molecular scattering analysis results. The equivalent M_{uv}'s shown are for worst case total column densities for all contaminant sources. The table shows that no performance degradation is expected for either telescope due to molecular scattering.

Molecular cloud absorption calculations for worst case column densities show that the transmission losses will also be negligible for both systems.

The return flux deposition on the primary mirrors of the two ultraviolet telescopes is summarized in Table XIX. The return flux was calculated for large molecules (M = 100) only since the light molecular species will not deposit at the ultraviolet telescope mirror temperatures. Maximum and minimum outgassing column densities were averaged over a full orbit for the zero line-of-sight at 435 Km altitude. The telescope line-of-sight was assumed to be oriented at 45 degrees to the orbital plane as in the case of the infrared telescopes. The 0.75 meter and the 1 meter telescopes were identified from previous mentioned data books to have acceptance angles of 0.1 and 0.09 steradians respectively. Both primary mirror temperatures were assumed to be at $T = 293^{o}K$.

Table XVIII. Ultraviolet Molecular Scattering Summary

WAVELENGTH micrometers	0.75 METER TELESCOPE STAR BRIGHTNESS MAGNITUDE M_{uv}		1 METER TELESCOPE STAR BRIGHTNESS MAGNITUDE M_{uv}	
	M = 18	M = 100	M = 18	M = 100
0.1	42	34	40	32
0.3	37	29	35	27
0.5	37	30	36	28

Table XIX. Ultraviolet Telescopes' Return Flux Deposition Summary

ULTRAVIOLET PAYLOAD	SOURCE	DEPOSITION FROM RETURNED FLUX AT 435 Km			
		g/cm^2/orbit	g/cm^2/7 days	Å/7 days	Percent Reflectance Loss/7 days @ λ = 0.25 micrometers
0.75 Meter Telescope	Outgassing	2.3×10^{-9}	2.6×10^{-7}	26	2.6
	Engines	2.2×10^{-11}	2.5×10^{-9}	0.3	0
Total				$\sum$ = 26	$\sum$ 2.6
1.0 Meter Telescope	Outgassing	1.8×10^{-9}	2.0×10^{-7}	20	1.9
	Engines	1.7×10^{-11}	1.9×10^{-9}	0.2	0
Total				$\sum$ = 20	$\sum$ 1.9

The reflectance loss was calculated using Gemini XII absorption data at 2500Å. The results show that the reflectance loss for the 0.75 meter and 1 meter systems will reach the 1% maximum allowable criteria in 2.5 and 3.5 days respectively. As previously stated, this analysis was performed for an altitude of 435 Km. Reducing the orbital altitude below a certain altitude can significantly reduce the return flux of the heavy molecules such as outgassing by reducing the mean free paths of these larger molecules. Both ultraviolet telescopes specify an allowable altitude range of 250-400 Km.

As the orbital altitude is lowered, the return flux for all molecules will increase except for the heavier molecules such as the outgassants which will reach a condition much quicker than the light molecules where the mean free path will be very small and will essentially never enter the line-of-sight of a telescope viewing into the velocity vector of the spacecraft. Under these conditions, an optimum orbital altitude could be determined if necessary.

The outgassant contribution to the return flux contributed the most to the predicted values. As noted previously, the values of outgassing rates assumed for this study were based upon available data and the configuration considerations used. Tests currently under way at MSFC for simulated Orbiter tile configurations will present more specific data for evaluation and the above results must be weighed with this in mind.

3.3.3 Solar Payloads - The two solar Payloads are comprised of 23 separate instruments. It was felt that a detailed analysis of all 23 instruments was not justified at this time. Therefore, five instruments were selected as typical of the two Payloads and the contamination impact on these instruments was assessed. The five instruments are:

a) S052 White Light Coronagraph;
b) S055 Scanning Spectrometer;
c) S056 X-Ray Telescope;
d) Photoheliograph; and
e) High Energy Systems (X-Ray/ γ -Ray)

All of these instruments will be susceptible to deposition from an absorption and/or scattering standpoint. The only instrument that will be significantly susceptible to molecular and particulate cloud scattering will be the coronagraph since it will be sensitive to the low light levels in the solar corona. The Photoheliograph and the S055 instruments are potentially susceptible to particulate scattering but their fields-of-view are so small that the probability of a particle entering the field-of-view is negligible.

The return flux deposition on the primary optic of each experiment was calculated and is summarized in Table XX. The deposition was calculated for large molecules only since as in the previous case the light species will not deposit at the primary optic temperatures (assumed 293°K). Maximum column densities were assumed for the zero line-of-sight and 435 Km altitude. The instrument lines-of-sight were assumed to be oriented at 73 degrees to the orbital plane with a full sun orbit. The analysis results show that no significant instrument degradation will occur due to return flux deposition.

The high energy X-ray/γ-ray instruments will probably receive deposition on the order of the maximum levels shown in the table. Although no detailed experiment parameters are available, no performance degradation is expected for deposition levels on this order.

The molecular scattering $B/B_\odot$ was calculated for the S052 coronagraph. The worst case number column density was assumed. The $B/B_\odot$ was determined to be 7.2×10^{-14}. This is several orders of magnitude below the S052 sensitivity.

Particulate scattering for the S052 instrument was assessed from the viewpoint of determining the minimum particle size required to produce a $B/B_\odot = 7 \times 10^{-11}$ (the Skylab S052 sensitivity criteria). The analysis showed that particles in the near field ($d < 800$ m) with radii greater than one micron will produce this equivalent scattering level. The Skylab S052 experiment observed particles in approximately 3% of its total data frames. If the Shuttle Orbiter/Spacelab

Table XX. Solar Experiments' Return Flux Deposition Summary

PAYLOAD INSTRUMENTS	DEPOSITION FROM RETURN FLUX AT 435 Km			
	g/cm^2/orbit	g/cm^2/7 days	Å/7 days	Percent Reflection Loss/7 days
S052				
Outgassing	5.9×10^{-11}	6.6×10^{-9}	0.7	
Engines	6.1×10^{-13}	6.9×10^{-11}	0.007	
Total			$\sum$ = 0.7	0
S055A				
Outgassing	3.6×10^{-11}	4.0×10^{-9}	0.4	
Engines	3.7×10^{-13}	4.1×10^{-11}	0.004	
Total			$\sum$ = 0.4	0.2 @ λ = 1500Å
S056				
Outgassing	9.4×10^{-15}	1.0×10^{-12}	0	
Engines	9.7×10^{-17}	1.1×10^{-14}	0	
Total			$\sum$ = 0	0
Photoheliograph				
Outgassing	3.2×10^{-10}	3.6×10^{-8}	3.6	
Engines	3.3×10^{-12}	3.7×10^{-10}	0.004	
Total			$\sum$ = 3.6	0.2 @ λ = 3000Å

configurations produce the same number of particles as Skylab, no significant data degradation is expected. However, if the Shuttle Orbiter/Spacelab particle production rate is greater than Skylab, then further potential influence on the coronagraph data can be expected.

3.3.4 AMPS Payload - The AMPS Payload is comprised of numerous experiments and instruments designed to observe and artificially perturb the space environment and the earth's upper atmosphere. The major instrument assemblies include a remote sensing platform housing optical instrumentation and field and particle sensors; a laser radar; long booms for remote measurements of the ambient environment and wake studies; transmitters and accelerators for stimulation of the ionosphere and magnetosphere; subsatellites; and a variety of deployable devices.

A detailed assessment of the contamination impact on each Payload instrument is not practical at this time due primarily to the lack of the detailed instrument configuration and operational information required to determine individual instrument susceptibilities. However, it is felt that the instruments attempting to study the ambient environment in the immediate vicinity of the spacecraft will receive the greatest contamination impact. It is felt that the impact will occur from the modification of the ambient environment due to the introduction of contaminant species. The instruments most likely to be effected are the ion probes and the mass spectrometers. To illustrate the potential impact, a hypothetical experiment configuration was selected in order to perform a detailed analysis.

A cylindrical probe was assumed to be located on a boom one meter above the Shuttle Orbiter skinline, parallel to the Orbiter X-axis, at station number 1158. The computer math model was used to calculate the column density along the probe axis. This column density was then used to determine the contaminant return flux flowing through the probe assuming a velocity vector parallel to the Shuttle Orbiter X-axis at a 435 Km orbital altitude. Only the light gases were considered. The results of the analysis are summarized

in Table XXI. The molecular column densities as a function of specie are listed in columns 2 through 4 for the three major sources. The contaminant molecular flux at the probe aperture is listed in column 6. The expected fluxes of the major constituents of the ambient are listed in column 7. Comparison of columns 6 and 7 shows that in some cases the expected contaminant flux from the Shuttle Orbiter and Spacelab module leakage approaches the ambient N_2 and exceeds the O_2. H flux from the VCS exceeds the ambient as does A from off-gassing. In addition, significant fluxes of other species will be introduced.

The relative magnitudes of the contaminant and ambient fluxes will vary significantly as a function of orbital altitude, line-of-sight, and distance from the Orbiter.

Deposition absorption effects were assessed on a preliminary level for a typical ultraviolet telescope system. The return flux deposition on the primary mirror was determined for a reflecting telescope with an acceptance angle of 0.183 steradians. It was assumed that the instrument line-of-sight was in the orbital plane pointed into the velocity vector (worst case). The deposition rate at 435 Km with a sticking coefficient of 0.25 (T_{mirror} = 293°K) was determined to be 1.7×10^{-8} g/cm^2/orbit. For λ = 2500 Å, and continuous operation, a 1% reflectance loss would occur in 0.5 days. A 10% reflectance loss would occur in 6.3 days. Other lines-of-sight orientations could reduce these worst case values significantly. When additional detailed instrument configuration, operational mode information, and data from outgassing tests become available; these values can be refined.

Table XXI. AMPS Probe Flux Summary

SPECIE	NUMBER COLUMN DENSITY (mol/cm^2)			CONTAMINANT RETURN FLUX mol/cm^2/second	AMBIENT FLUX (1) mol/cm^2/second
	OFFGASSING	VCS ENGINES	LEAKAGE		
CO		2.9×10^{12}		8.1×10^{11}	
CO_2	4.4×10^{12}	5.7×10^{11}	1.5×10^{11}	1.4×10^{12}	
H		7.5×10^{12}		2.1×10^{12}	1.7×10^{10}
H_2		5.0×10^{13}		1.4×10^{13}	
H_2O	2.2×10^{13}	1.2×10^{13}	1.7×10^{11}	9.6×10^{12}	
NO		1.3×10^{10}		3.6×10^{9}	
N_2	8.5×10^{12}	6.9×10^{12}	1.1×10^{13}	7.4×10^{12}	1.5×10^{13}
O		1.2×10^{10}		3.4×10^{9}	1.1×10^{14}
OH		2.2×10^{11}		6.2×10^{10}	
O_2	2.7×10^{12}	3.9×10^{9}	3.5×10^{12}	1.7×10^{12}	7.7×10^{11}
A	2.6×10^{11}			7.5×10^{10}	1.9×10^{9}
He				0	7.7×10^{11}

(1) Johnson, F. S.: "Satellite Environment Handbook," Stanford University Press, Stanford, California, 1965.

3.3.5 Random Particle Dwell Times - In order to assess the total impact of the particle induced noise background on integrating systems, the dwell time of the particle noise on the detector must be considered. For example, for a film system, a minimum energy density is required on the film in order to record an image. This energy density, or exposure, is the product of focal plane irradiance and time. The time duration that the background noise is incident on the detector is a function of the particle distance and velocity and the telescope focal ratio, aperture, and the detector size. The computer program NOMAD was used to simulate the trajectories of particles sloughed from the Orbiter. The program accounts for both orbital mechanics and atmospheric drag effects. It was assumed that the Orbiter was at an altitude of 435 Km in an inertial attitude with the telescope oriented along a zero line-of-sight. The particles were assumed to have a 50 micron radius, emitted 10 meters from the payload bay at various angles with the velocity vector. For simplicity both the line-of-sight and the particle trajectory were assumed to be contained in the orbital plane. Particles were assumed to be emitted with velocities of 0.01, 0.1, and 1.0 m/second velocities. The results of the analysis are summarized below for those instruments susceptible to particles.

Instrument	Dwell Time Range (seconds)
1.5 Meter Infrared Telescope	3.8 - 5.0
2.5 Meter Infrared Telescope	6.3 - 8.4
0.75 Meter Ultraviolet Telescope	1.9 - 12
1.0 Meter Ultraviolet Telescope	2.5 - 3.5
S052 White Light Coronagraph	0.2 - 5.9

The dwell times shown when combined with particle appearance rates and predicted focal plane irradiance can be used to assess the overall particle impact on an instrument's performance.

As the orbital altitude decreases the dwell times will decrease because of the predominant drag influence for the lower altitudes. This is also true for smaller particles

which can interact more efficiently with the ambient atmosphere. At higher orbital altitudes where the drag influence is much less, orbital mechanics will play a larger role and particles of all size ranges will tend to remain within the fields-of-view of the instruments considerably longer.

3.4 Contamination Potential of Free Flying Payloads - The deployment, retrieval,and stationkeeping aspects of a Free Flying payload may subject it to sources of contamination from these activities. It is the intent of this subsection to delineate those potential contamination sources that can exist and qualitatively outline the contamination potentials. Where possible, predicted values or rates of contaminant buildup will be presented.

The analysis will be baselined to a 3A type mission for Payload Placement and a 3B Payload Retrieval type mission (pages 26 and 29 in the Applicable Document SD 72-SH-0071B). Because of the many variations possible, an orbital rate of contamination buildup prediction is also identified for deployment/retrieval schemes that have time schedules different from 3A or 3B.

The timeline schedules for 3A and 3B are summarized in Table XXII.

Cabin leakage and Evaporator vents were reviewed and have been assessed as having no potential for contamination during these phases since they are comprised of simple gases that should not deposit at anticipated Payload temperatures. Hydraulic leaks could deposit on external surfaces of the Payload but should not pose a problem since the Payload will be sealed and the allowable leak rates from these sources are small in comparison to the other sources considered.

The major sources that will be predominate during the deployment, retrieval, and stationkeeping phases capable of contaminating are presented in the following subsections with an assessment of their contamination potential.

C-2

Table XXII. Typical Payload Placement (3A) and Payload Retrieval (3B) Mission Timelines

3A - TYPICAL PAYLOAD PLACEMENT MISSION	GET	DURATION
o Launch	00:00:00	
o Initial Orbital Insertion	00:12:01	
o Orbit Adjust Maneuvers	TBD	
o Open Cargo Bay Doors, Activate and Checkout Payload	00:15:45 to 00:24:45	10 minutes
o Extend Manipulator Deploy Appendages, Initialize Payload Attitude Control	00:24:45 to 00:36:00	~8 minutes
o Release Payload, Translate Orbiter (RCS) to Approx. 200 feet, Retract Manipulators, Complete Checkout and Activation of Payload	00:36:10 to 00:42:00	~6 minutes
o Perform Orbiter Separation Maneuver (RCS)	00:42:00	
3B - TYPICAL PAYLOAD RETRIEVAL MISSION		
o Launch	00:00:00	
o Initial Orbital Insertion	00:12:04	
o Perform Rendezvous, Maneuver to Retrieval Attitude, and Close Formation (25 ft. from Payload)	00:16:14 to 00:38:15	12 minutes
o Extend Manipulator Arm and Engage Payload. Deactivate Payload, Retrieve Payload and Secure in Bay	00:38:15 to 00:48:31	10 minutes
o Stow Manipulators and Close Cargo Bay Doors. Deactivate Manipulator and Payload Stations, Commence Deorbit Checkout List, Resolve De-Orbit Burn, Maneuvers For De-Orbit Attitude	00:49:01 to 00:57:50	9 minutes

3.4.1 Orbital Insertion - OMS Engines - Depending on the orbital requirements of a Payload, the 6000 pound thrust OMS engines will be used to obtain the desired orbital parameters. In general, use of the OMS engines occurs during circularizing the initial orbit, transferring, and recircularizing. During these 3 maneuvers, the payload bay doors must be opened because of the heat rejection requirements for the Orbiter.

The potential exists that these engine effluents could create detrimental contamination effects by:

a) altering thermal control surface characteristics;

b) depositing a film that can resublimate with time after deployment;

c) degrading windows, antenna, or solar cell surfaces; and

d) generating particulates that could remain in the vicinity of the deployed system for short periods of time.

The mechanisms that would allow such effects to occur are:

a) engine backflow of material - this is dependent upon mounting of the engines and the nearby structure and engine characteristics;

b) reflection of engine exhausts from the Orbiter tail surfaces;

c) some return of engine exhausts to payload bay area by interactions with the ambient atmosphere; and

d) generation of particulates at various velocities and ejection angles that would have different clear-times and recontact (field-of-view) capabilities from orbit to orbit. (This would be dependent upon engine characteristics, ejection angle, velocities, and orbit parameters.)

The potential of the cause and effects occurring seem favorable when it is considered that the OMS engines can fire a maximum of approximately 10 minutes during the 3 above mentioned maneuvers for a total exhaust mass flow near 24,000 pounds. A small fraction of this mass flow can deposit which is a function of engine efficiency during the firing sequences. The engine design will also dictate the fraction of mass flow that can flow back behind the engine. Further, vehicle geometry near the engine will dictate the capability of this mass flow reaching the payload bay area. To date, there is not sufficient data available for the OMS engine to do a detailed analysis of the contamination threat it poses. However, since no direct line-of-sight exists between the Payloads and the engines, this mechanism will probably be small in magnitude. The reflection of engine exhaust from the tail structure will also be a small effect because of the tail orientation with respect to the payload bay.

The return flux of engine exhausts after interaction with the ambient could result in a deposition rate of $2.2 \times 10^{-8} g/cm^2$/second on surfaces perpendicular to the Z axis. For a maximum burn time of 10 minutes, this would result in a total deposit of $1.3 \times 10^{-5} g/cm^2$. Testing has shown a deposit of $1.2 \times 10^{-5} g/cm^2$ could change the solar absorptivity, α s, by 100% for a S13G white thermal control paint. Equal problems would also be experienced by the radiator surfaces exposed on the payload bay doors.

An exact analysis of the proposed engine and detailed configuration data are required before the OMS problem can be satisfactorily assessed. The huge quantity of exhaust products makes even the smaller contributing mechanisms significant. The possibility exists such that the particular OMS firings mentioned previously could be timelined on orbit to not correspond with the maximum return flux vehicle orientation. This would minimize this contaminant potential. In addition, consideration could be given to closing the payload bay doors during the OMS engine firings which would eliminate this concern completely.

3.4.2 Return Flux of the Induced Environment - Once the proper orbit is attained the Payload will reside in the payload bay for a period of approximately 10 minutes as in the mission 3A profile. During this time, the mass loss of vacuum exposed non-metallics, insulation layers, etc. will be significant.

The mass column densities of induced materials during this time period are $2.9 \times 10^{-11} g/cm^2$ for outgassing (heavy molecules) and $1.7 \times 10^{-10} g/cm^2$ for offgassing (light, volatile molecules) along the Z axis out of the payload bay.

The return flux of this induced atmosphere will depend primarily on orbital altitude, the acceptance angle of a payload surface, and the orientation of the vehicle velocity vector.

The maximum return flux at an altitude of 435 Km would be $1.4 \times 10^{-11} g/cm^2$/second for outgassed products and $2.9 \times 10^{-12} g/cm^2$/second for the smaller molecular offgassed species. For Payload surfaces near $300^{\circ}K$, the only contaminant capable of depositing would be a fraction of the outgassed material. A deposition rate near $3.5 \times 10^{-12} g/cm^2$/second would result. For an attitude which would allow a maximum rate of return, a total of 2.1×10^{-9} g/cm^2 in 10 minutes would result which should be no problem for external surfaces.

For mission profiles that exceed the 3A timeline, the deposition per orbit would be near 1.4×10^{-8} g/cm^2/orbit. Each day (16 orbits), a total possible deposition would be 2.2×10^{-7} g/cm^2/day or a 22Å layer for a density of unity.

For surfaces at other orientations, for different viewing angles, and vehicle attitudes; these predicted values can change. However, the above predictions indicate the order of magnitude effect.

Applying the same type of analysis to the VCS engines (25 lb thrust), an orbital deposition rate of 1.3×10^{-10} g/cm^2/orbit is predicted for an engine firing once every 4.8 seconds for a 40 millisecond pulse. This yields a daily

deposition rate of 2.1×10^{-9} g/cm^2/day which should also be no problem for Payload surface temperatures near 300°K.

3.4.3 Attitude Control During Deployment - Approximately, a 12 minute period is required for a 3A mission during which the manipulator arm deploys the Payload and attitude control is required. The attitude control would be accomplished by the Vernier Control System (VCS) utilizing 25 lb thrust bi-propellant engines.

For a Payload at 50 feet from the orbiter X axis, the flux on a surface from the forward downward firing engine would be 3.1×10^{-14} g/cm^2/second and 2.9×10^{-13} g/cm^2/second for the aft outward firing engine which is the worst case for this configuration. The engine flux presented here results from the backflow region of the engine plume. For the surface in question, the angle with respect to the engine axis is 132 degrees for the forward engine and 99 degrees for the aft engine.

The deposition rate resulting from these engine fluxes ranges from 6.2×10^{-17} to 5.8×10^{-16} g/cm^2/second and should be no problem. For distances closer than 50 feet, the deposition rate may increase slightly but would still be no problem because of the very low deposition levels. For small distances from the vehicle surface, structural shadowing would block the engine backflow.

The flux impinging on the deployed system resulting from engine exhaust reflections off of the Orbiter wing surfaces will not be capable of significant deposition because the condensible fraction should primarily adhere to the wing.

3.4.4 Stationkeeping - After deployment, the Shuttle Orbiter will remain in the vicinity near 200 feet of the Payload for checkout and activation of the Payload for a period of approximately 6 minutes in the mission 3A profile.

During this time, the Payload will be susceptible to the normal contaminant sources of the vehicle. Of these sources, outgassing because of its continuous nature would

be a major source capable of depositing. The flux of vehicle outgassed materials at 200 feet is 2.3×10^{-11} g/cm^2/second for warm portions of an orbit. The total flux of all sources is several orders of magnitude above the outgassing level but is comprised of simple gases not capable of depositing at anticipated ambient external Payload surface temperatures.

For the anticipated temperatures, approximately 50% of the impinging outgassed flux will deposit resulting in a deposition rate of 1.2×10^{-11} g/cm^2/second. If the vehicle were in an attitude such that the surfaces were warm for the 6 minute period (worst case), the accumulative deposition would be near 4.3×10^{-9} g/cm^2 and is no problem.

For time periods longer than 6 minutes, say one hour, the accumulative deposition would be 4.3×10^{-8} g/cm^2 and should still be no problem. For stationkeeping activities that may extend to periods of days, the potential deposition could accumulate to undesirable levels. Under these conditions, stationkeeping distances should be increased to distances on the order of 1000 feet for maximum protection of external surfaces. If critical optical surfaces are to be exposed during checkout, the distance of separation should be increased depending upon the nature of the optical surface and the possibility of "looking" at the Orbiter and its sources. The position of minimum contamination impact is forward and above the Orbiter excluding the forward 900 lb RCS engines. Operational constraints can be established to inhibit these forward engines during checkout thus presenting a position of minimum contaminant potential. This is also best for visual sighting by the Orbiter crew during this phase of operation.

3.4.5 <u>900 Pound Thrust RCS Engines</u> - During deployment, rendezvous, and retrieval; the 900 pound thrust RCS engines will be used for maneuvering. These engines can deposit on Payload surfaces, and impart delta velocities, and/or angular rotation rates to the Payload. Imparting forces or torques on the Payload may require additional RCS usage in establishing rendezvous which will tend to increase the contaminant potential of this activity. An estimate of the magnitude of these effects is presented in the following subsections. Because of the many variations possible, these values can change significantly for specific cases.

3.4.5.1 Deposition - There are 38 - 900 lb RCS engines on the Orbiter which can essentially fire in all directions. An estimate of their contamination potential can be ascertained by considering a +Z firing aft engine flux level along the +Z direction out of the payload bay at the X_o= 1107 position.

Figure 21 shows the deposition rate as a function of distance along +Z from the Orbiter X axis positioned at X_o= 1107. It is shown for a Payload at 25 to 100 feet, the deposition rate is near 2.5×10^{-7} g/cm^2/second. At this rate, a 10 second firing would result in a change in solar absorptivity of 0.023 (approximately a 10% change) for a thermal control white paint like S13G.

At distances of 500 feet, the deposition level is near 2×10^{-8} g/cm^2/second. A 10 second burn would result in a change in solar absorptivity of .01 (approximately a 5% change) for a white thermal control surface like that of S13G.

3.4.5.2 Forces and Torques - For evaluation, a LST type configuration (weight and dimensions) was investigated to determine the forces exerted on it by the Shuttle Orbiter 900 lb RCS engines during deployment or retrieval operations. The forces were calculated by determining the pressures at various surface locations within the engine plume for different configuration orientations. A single rear +Z firing engine was used for this analysis. However, for rendezvous activities, complimentary RCS engines will be fired to maintain proper attitude resulting in increased forces depending upon specific geometry.

For simplicity, the engine centerline and the LST were assumed to be in the Orbiter (X, Z) plane. Three cases were analyzed for the deployment/retrieval operations. The first case assumes the configuration's X axis parallel to the Orbiter X axis and located directly above the payload bay. The second case assumes the configuration X axis parallel to the Orbiter X axis and located above the engine centerline. The third case assumes the X axis parallel to the Orbiter Z axis and located directly above the payload bay.

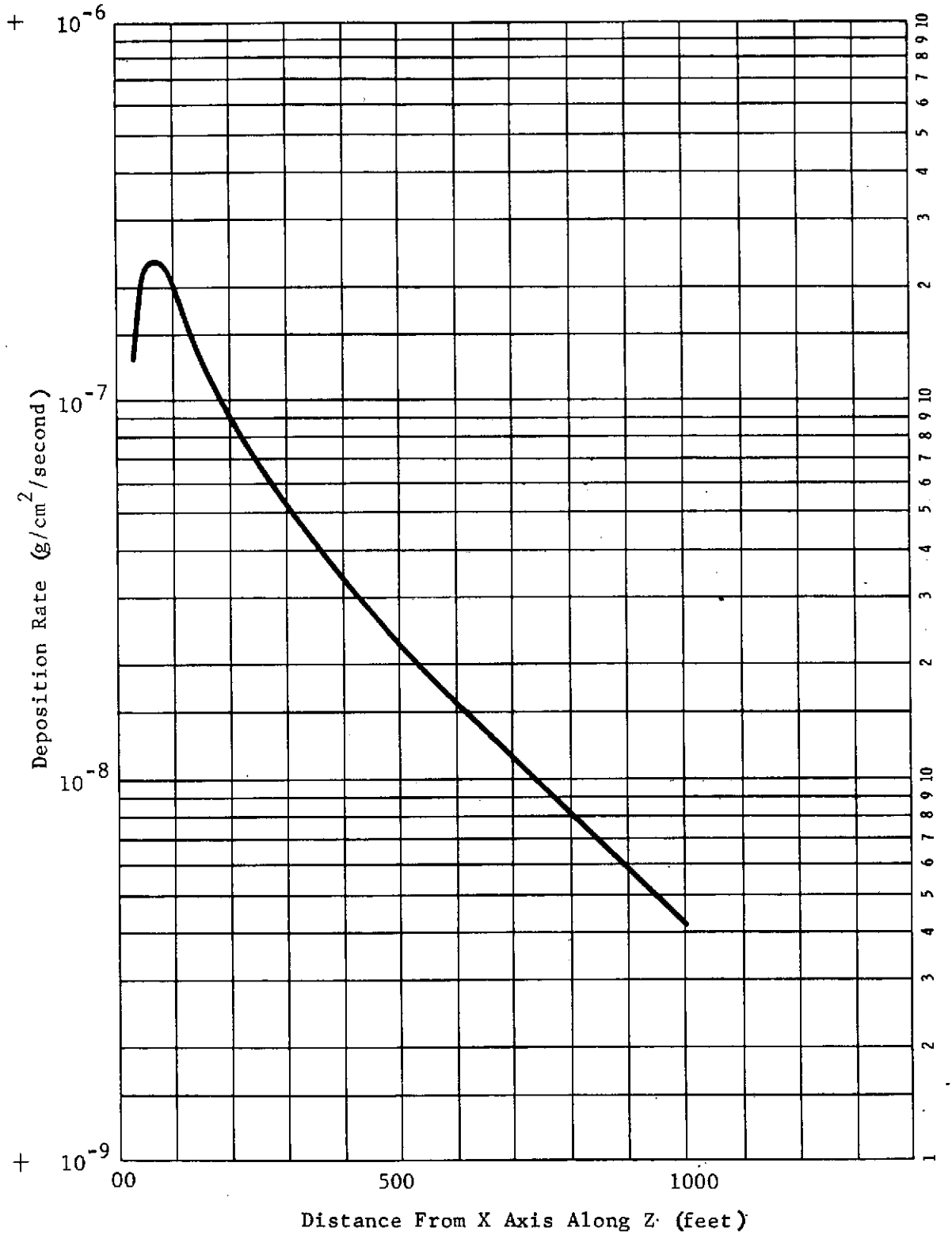

Figure 21. Deposition Rate as a Function of Distance from the Orbiter X Axis Along the Z Axis for a 900 Pound RCS Engine

Calculations were performed for the center of the configuration at distances of 50, 100, and 150 feet from the Shuttle Orbiter X axis for all cases except case II where the 50 foot distance was eliminated because of Shuttle Orbiter tail interference.

The resulting velocities and angular rotation rates per second of initial engine firing for the configuration are presented in Table XXIII.

Table XXIII. Velocities and Angular Rotation Rates per Second of Initial Engine Firing

Configuration \ Distance in Feet from the Orbiter X axis	50 (Feet)	100 (Feet)	150 (Feet)
Case I (X axis parallel to Orbiter X axis above bay)			
V_z (cm/sec)	1.28	1.14	0.8
V_x (cm/sec)	0.42	~ 0	~ 0
ω (degree/sec)	0.08	0.04	0.012
Case II (X axis parallel to Orbiter X axis above engine)			
V_z (cm/sec)	-	2.64	1.18
V_x (cm/sec)	-	0	0
ω (degree/sec)	-	0	0
Case III (X axis parallel to Orbiter Z axis above the payload bay)			
V_z (cm/sec)	0.06	0.22	0.2
V_x (cm/sec)	1.10	0.88	0.44
ω (degree/sec)	0.008	0.010	0.006

3.5 Contamination Detection Instrumentation Considerations - The following subsections discuss on orbit contamination specifications, contamination measurement requirements, instrumentation requirements, and location and pointing considerations for contamination detection instrumentation.

3.5.1 On Orbit Contamination Specifications - The selection of instrument types and sensitivities necessary for monitoring the on orbit, external, contamination characteristics of a space vehicle is somewhat dependent upon the limits established by specifications for the vehicle. The on orbit contaminant environment limits for the Space Shuttle have been established by the Astronomy Working Group Report ASD-PD-18743 and Volume X of JSC 07700. The portion of the JSC specification pertinent to instrumentation selection states: "As a design and operational goal, venting of gases and liquids from the Orbiter will be limited for sensitive Payloads to control in an instrument field-of-view particles of 5 microns in size to one event per orbit, to control induced water vapor column density to 10^{12} molecules/cm^2, or less, to control return flux to 10^{12} molecules/cm^2/sec, to control continuous emissions or scattering to not exceed 20th magnitude/sec^2 in the UV range, and to control to 1% the absorption of UV, visible, and IR radiation by condensibles on optical surfaces."

Contaminant environment limits for some of the Payloads to be carried by the Orbiter have also been established. Some of the specific experiment or other equipment limits established are less stringent than, or not covered by, the two documents mentioned above. The portion of the JSC specification having to do with 5 micron particles has no distance limit specified. Presumably, the specification would not permit more than one 5 micron size particle to come within any instrument's field-of-view at any distance during each orbit. The Astronomy Working Group Report of May, 1973 (ASD-PD-18743) ties particle restrictions down a little more firmly by stating: "Less than one Artificial Star (i.e. 10 sigma event above 10^{-16} W/$\sqrt{Hz}$ as seen by the detector for $\Delta\lambda/\lambda = 0.5$ bandwidth, 10 arc sec circle, and 1M telescope from 10 to a few hundred micrometers wavelength in the

IR) per orbit." Under these conditions, the size of the particle can vary with distance, wavelength, and infrared reflectivity or emissivity. Only effects in the infrared are considered by this specification. R. Naumann in his Contamination Monitoring Plan of September 19, 1974 noted in the Applicable Documents restates the limitation as: "Fewer than 1 particle larger than 10 microns in a 4 arc minute half angle field-of-view per orbit within 1 km." This is a much more definitive specification and establishes bounds that can be related more practicably.

JSC 07700 places a single brightness limit on atmospheric scatter and emission for the entire ultraviolet band. ASD-PD-18743 includes scatter and emission limits for a portion of the infrared band by the statement, "Continuum emission or scattering shall not exceed 10^{-16} watts noise equivalent power in a 10 arc sec circle (1M Telescope) for $\Delta\lambda/\lambda = 0.5$ bandwidth in the IR at wavelengths from 10 to a few hundred micrometers." R. Naumann states the specification to read, "Background brightness from scattering and emission less than 20th magnitude/arc sec in the near ultraviolet." This specification is more limited and simplifies measurement requirements. However, there is no specific limit placed on scatter and emission in the band between 0.35 and 10 microns by any of the specifications. Limitations for this band may be specified at some later time by investigators using instruments operating therein. Undoubtedly, experimenters will place other restrictions on contamination as new instruments are developed.

3.5.2 Contamination Measurement Requirements - The basic contamination characteristics of interest are the amount and effect of contaminants deposited on various surfaces critical to operations and the amount of radiation emitted, scattered, and absorbed by the spacecraft generated contaminant atmosphere. However, contamination limit specifications are not always presented directly in the terms of these basic characteristics. Some of the terms in which specifications are presented are as follows:

a) total mass column density within an instrument's line-of-sight;

b) total molecular number column density within an instrument's line-of-sight;

c) number column density of particular molecular species;

d) percent signal loss permitted as a result of contaminants on surfaces or in the induced atmosphere;

e) permissible return flux rate of emitted contaminants;

f) permissible emission rate of particles within specific size ranges;

g) permissible number of particles above a particular size within a particular field-of-view within a given time;

h) permissible contaminant deposit thickness on particular surfaces;

i) permissible scatter brightness of the contaminant atmosphere;

j) limitations on particular types of emissions (e.g. no waste dumps or no engine exhausts);

k) limitations on contaminant induced pressures during operation of specific equipment; and

l) permissible variations in thermal control surface absorptivity characteristics as a result of contaminant deposits.

Obviously, all the preceding characteristics cannot be measured directly or discretely without extraordinary instrumentation or unnecessarily complicating the experiments or other instruments and surfaces involved. However, some characteristics can be measured directly with relatively uncomplicated instrumentation and the other characteristics can possibly be inferred or deduced from measurements made by simpler apparatus or Payload instrumentation making related measurements.

In order to determine the Shuttle Orbiter contamination environment and effects, it will be necessary to measure or deduce the following basic data or information:

a) contaminant column densities within various possible optical experiment lines-of-sight;

b) return flux rate of emitted contaminants;

c) contaminant deposition rates on surfaces facing various directions and at various locations and the spectral absorption characteristics of the deposits;

d) emission rate of 5 micron or larger particles within optical experiment lines-of-sight;

e) composition of emitted contaminants (molecular species);

f) spectral scatter intensity of the induced environment relative to the solar angle in experiment lines-of-sight; and

g) reflectivity of thermal control surfaces.

Many on orbit contamination processes vary rapidly and radically with time or may be only sporadic. For this reason, instrumentation providing time correlation should be used wherever practicable. Where it is not possible to relay data in real or near-real time, it may be possible to expose instruments cyclically or only during specific operational phases. Time correlation of data is either beneficial or essential in determining:

a) the manner in which the induced atmosphere and contaminant deposition varies with time, direction, and orbit conditions;

b) the contaminant contributions of various operations and conditions;

c) the identity of specific contaminant sources;

d) minimum and maximum contamination conditions; and

e) best conditions for exposure of experiments that are especially sensitive to contamination.

Time correlation is also essential for prediction of future contamination conditions and the approach of contamination limits for the more sensitive Payloads.

3.5.3 Instrumentation Requirements - The following instrumentation requirements are discussed to establish the physical nature of the required measurement.

3.5.3.1 Column Density - This category includes total mass column density, total molecular number column density, and the number column density of particular molecular species. There is no presently known, simple, direct process for measuring total mass or total number column density. In order to make such measurements, it would be necessary to identify each specific molecular and atomic species and measure its radiant emission or absorption characteristics to determine the amount of mass or number of molecules within any particular columnar

line-of-sight. The contaminant molecular distribution about a spacecraft varies continuously with time, direction, and spacecraft orientation relative to the velocity vector. Presumably such measurements could be made with spectroradiometers and absorption spectrometers or spectrographs but it would take an array of complicated instruments to cover all requirements. Ultra sensitive instruments would be required to measure the characteristics of some of the rarer species and the characteristics of some species may be below the threshold of any instrument. The absorption spectrometers or spectrographs would have very limited directional capability because of their requirement for a bright radiation source of known spectral intensity in the direction of measurement.

The instrumentation problem is greatly simplified if it is required only to measure the column density of specific species or only the column density effect on a specific experiment or within a specific narrow radiation band. For these conditions, fewer, less complicated instruments would be required. However, they would be required to scan in all directions that will be covered by the experiments for which they are making the measurements and their sensitivity thresholds should be at least an order of magnitude below those of the experiments.

The above mentioned instrumentation capabilities would require the development of new, ultra-sensitive instruments. Another process for obtaining column density values would be to derive them by inference from measurements of related characteristics. One process that has been used is the development of computer programs to trace the motion of spacecraft contaminant emissions and integrate the mass to be expected in any given direction under various orbit conditions. The difficulty with this process is that it presupposes that all emission source characteristics and how they vary with time, temperature, orbit altitude, etc. are known discretely. The process is effective for sizing particular, possible, worst case conditions and for predicting column densities prior to on orbit operations so that controls can be

established for particularly objectionable contaminant sources. All emission characteristics are not known precisely nor can the complete dynamics of contaminant motion and interactions on orbit be accounted for. This process can become a valuable tool though when many more measurements have been obtained during orbit operations and used in modified computer programs.

Another indirect process involves deducing column density from measurement of the contaminant flux returned to the spacecraft by collision with the ambient atmosphere. Specifications require the measurement of return flux and, with limitations, column density can be inferred from the measurements obtained using a mass spectrometer. The process is discussed in R. Naumann's "Contamination Monitoring Plan" of September 19, 1974 and will not be repeated herein. The process is limited to measurement of the column density within a fairly narrow cone around the velocity vector. For a space vehicle whose orientation is fixed in space, the velocity vector will rotate in a plane around the vehicle and reasonably accurate column densities can be derived within that plane. However, the measurement in any direction around the plane is limited to the particular orbit position, time that the velocity vector was pointed in that direction, and emission source rate changes with time and orbital position. The spacecraft can be rotated so that the velocity vector faces any relative direction at any time so that all directions can be mapped. However, this process would be unrealistic as it would change the emission plume patterns and outgassing rates. Normally, the Shuttle Orbiter will operate at a fixed orientation for complete orbits. For experiments that can view in all directions, it is then important to know the column density in all directions for that particular orientation and how it changes as the velocity vector changes. There is little reason to expect that any flux will be returned from the hemisphere opposite the velocity vector and every reason to suspect that the column density will be greatest in that hemisphere. Some extrapolation may be possible outside the cone of return flux measurement but confidence will decrease as the angle away from the cone increases.

The final and perhaps the best method of deducing column density from related measurements involves measuring the emission density pattern of the Shuttle Orbiter with a mass spectrometer mounted on the Shuttle Orbiter's manipulator arm. This process is also discussed in R. Naumann's Contamination Monitoring Plan. The spectrometer would be directed toward the Orbiter and moved around it to map the emission density profiles spatially at various distances from the Orbiter. The spacial coverage of this process is somewhat limited by the short extent of the manipulator arm (approximately 50 feet) and its fixed location. Contributions from some effluent sources will not intersect particular lines-of-sight until some distance farther than the arm can extend. This distance will vary with the direction of the velocity vector. Other source contributions will fall off at indeterminant rates at distances past the manipulator arm extent. These actions are the result of Orbiter surface shielding effects, emission directional effects, and interaction with the ambient atmosphere. Ideally, measurement should extend out to 200 feet or more along all lines-of-sight of interest (presumably the entire +Z hemisphere). Use of the Wake Shield Boom, if available for such purposes, would make extended measurements possible. In the near field, because of the changing viewfactor with increasing distance, the effluent density cannot be expected to decrease proportional to $1/r^2$. The density at any point is a product of the contribution of effluents from all directions from which they can be expected to arrive. Along some lines-of-sight, the density may decrease only slightly over a considerable distance dependent upon the size and configuration of the spacecraft. If the operation of all possible or probable effluent sources are considered, densities at some locations near the spacecraft can be lower than more distant locations along the same line-of-sight and the density profile plot along this line-of-sight can exhibit a multi-lobed appearance. In any event, the effluent density versus distance will vary continuously with time and position and a considerable number of measurements will be required to determine its dynamic characteristics. However, regardless of its limitations, measurements should be obtained using the manipulator arm if no longer device is available. It will certainly map

the near-field densities and provide a considerable measure of confidence in extrapolations to greater distances. It is the best scheme mentioned so far for the purpose and has side benefits such as the detection and identification of unexpected sources.

The sensitivity required of the mass spectrometer to be used for the column density measurements will be dependent upon the distance from the Shuttle Orbiter, the measurements that are to be made, and the percentage of contribution to pressure of the least important effluent species of interest. Normally, if the partial pressure of a species is more than two orders of magnitude below that of the combined species, its contribution to total density can be considered insignificant. The spectrometer should have the capability of switching between two acceptance angles; a narrow 10 degree angle for isolation and localization of discrete contamination sources at close range (10 feet or less) and a wide ($\sim$180 degrees) angle for measurement of total flux at long range (40 to 50 feet). The flux at 50 ft from approximately 8000 ft^2 (Shuttle upper, single surface area) with an outgassing rate of 10^{-11} gm/cm^2/second and a cosine distribution is approximately 9.6×10^{-12} gm/cm^2/second. The flux using a 10^{o} acceptance angle with the same emission rate source filling the field-of-view is approximately 7.6×10^{-14} gm/cm^2/second. Molecules having a mass of 100 emitted from a surface at approximately $395^{o}K$ would have a most probable velocity of 2.49×10^{4} cm/second. This velocity and the two flux rates above would be equivalent to pressures of 1.76×10^{-10} Torr and 1.42×10^{-12} Torr for the wide angle and 10 degree acceptance angle cases respectively. If pressures, of minor species, two orders of magnitude lower are to be registered, then the mass spectrometer must have detection thresholds of at least 1.7×10^{-12} Torr and 1.4×10^{-14} Torr respectively for the two cases. Flux rates from contaminant sources other than outgassing, if large enough to be of concern, will most likely be greater than those considered in the example above. Therefore, a mass spectrometer having the sensitivity indicated should suffice for all conditions. For small area or point sources, the instrument can be moved closer to the source.

3.5.3.2 Return Flux - The process for measuring return flux has already been discussed to some extent in the preceding section. Return flux, in most cases being two orders of magnitude or more less than the emitted flux, does not contribute appreciably to scatter or absorption but will deposit upon most surfaces which have appreciable exposure times. It is important to determine its directional characteristics and some of the interactions and reactions that may occur in the immediate space surrounding the spacecraft. Also, if the individual species are identified, it is possible to predict which might deposit to surfaces at specific temperatures.

The ideal instrument for measuring return flux would be a mass spectrometer with a variable acceptance angle. With this instrument, it would be possible to determine the amount of return flux to be expected on experiments in its vicinity having various acceptance angles and how return flux varies with angle at various times and velocity vector directions.

Contamination specifications require that return flux be less than 10^{12} molecules/cm^2/second. The pressure represented by this flux rate is extremely variable, dependent upon the relative velocity, and mass of the molecules. Velocity can range from almost infinitesimal to greater than the spacecraft orbital velocity. Mass could vary from a few to hundreds of AMUs. However, to determine a reasonable threshold sensitivity for the mass spectrometer, velocities herein will be considered as ranging between 300 and 8000 meters/second and mass values between 18 and 200 AMU. Table XXIV indicates the pressures represented by these outside conditions. Any other conditions can be extrapolated easily because pressure is directly proportional to molecular mass, velocity, and flux rate.

Table XXIV. Pressures Represented by Various Molecular Velocities and Masses for a Return Flux Rate of 10^{12} molecules/cm^2/second

MASS AMU	VELOCITY m/second	PRESSURE Torr
18	300	6.84×10^{-10}
18	8000	1.82×10^{-8}
200	300	7.6×10^{-9}
200	8000	2.03×10^{-7}

In order to measure lower flux rates, the partial pressure of minor species, and those returning at much lower velocities; an instrument having a threshold sensitivity at least as low as $1x10^{-13}$ Torr should be used. Acceptance angle should vary from a few degrees to ~ 90 degrees.

3.5.3.2 Contaminant Deposition Rates - Contaminant deposition rates are dependent upon impingement rates, molecular species, and surface temperatures. Contamination specifications for the Shuttle Orbiter limits absorption by contaminants deposited on optical surfaces to 1% across the entire optical spectrum. (Surface scattering characteristics should also be considered.) However, knowledge of the deposition mass or thickness provides no direct indication of absorption spectral characteristics other than bulk absorption characteristics. The particular species or combination of species must be known as well as the manner in which it has been deposited (e.g. smoothly or in separate islands). Even knowing these factors, though, in most cases will not indicate the total absorption characteristics. However, measuring deposition rates is the first step toward determining absorption and, if deposition is heavy there is a good probability that absorption is high. Absorption can be measured directly under specific conditions but equipment to measure effects over the entire spectrum and a wide range of temperature conditions can become quite complex.

The ideal instrument for measuring contaminant deposition rates is a temperature controlled quartz crystal microbalance (QCM) such as the device developed at the Faraday Laboratories La Jolla, California. The sensor crystal can be either heated or cooled by a series of junctions operating on the Peltier effect. This capability permits operating the sensor crystal at the same temperature as the optical elements of experiments it is desired to monitor. Alternatively, the crystal can be operated at a much lower temperature to capture all contaminants of interest. By reversing the Peltier effect, the crystal can be heated in steps to drive off contaminants one species at a time for sampling or contaminants can be boiled off to prevent saturation or

to maintain operations in the most sensitive range. The device is capable of controlling crystal temperatures between -59°C and 100°C. The mass sensitivity of this kind of instrument is 3.5×10^{-9} gm/cm^2/Hz. A monolayer of H_2O molecules would weigh approximately 3.1×10^{-8} gm/cm^2 and is approximately 3.1Å thick so that the instrument is theoretically capable of measuring deposited masses and contaminant layer thicknesses much less than those of a monolayer of H_2O molecules. QCM deposited mass readings can be transmitted in real-time so that it is possible to determine how contaminant deposition varies with time, location, orbit conditions, and operational procedures. If the sensor crystal is coated with the same materials as those used on experiment mirrors, then in-situ reflectivity measurements can be obtained to determine the effect of the contaminant deposits on mirror optics operating in the same environment. However, there is no direct method yet devised to determine in-situ absorptivity characteristics of contaminant deposits on the crystal.

Ideally, QCMs should be placed at several locations on the Shuttle Orbiter to determine how deposition varies with location. Also, a series of QCMs with small acceptance angles should be placed in one central location and each QCM's acceptance cone pointed in a different direction so that the direction of arrival of various contaminants can be determined. This will also aid in determining the source of some contaminants, possibly in real-time. Acceptance cones can also be baffled to eliminate the error producing effect of high velocity molecular impingement when the acceptance angle is facing in the direction of the velocity vector.

The value of passive samples for determining deposition characteristics should not be overlooked. They can supplement the QCMs so that a large number of QCMs will not be required. Also they can represent surface conditions and materials that the QCMs cannot and can be used to measure characteristics such as absorption that the QCMs cannot. They cannot provide data in real time unless analyzed periodically by the crew during EVA using a hand operational spectroreflectometer, but their many advantages outweigh this shortcoming.

3.5.3.3 Particulate Detection - Shuttle specifications (Volume X of JSC 07700) require that only one particle of 5 micron size or larger be permitted to enter the field-of-view of sensitive experiments per orbit. No particular instrument sensitivities or particle distance limits are given. The radiant intensity of the image of a particle, located within the near field of a telescope, at the focal plane of the telescope is:

$$H_f = \frac{H_o \lambda^2}{f^2 8 \pi^2} (i_1 + i_2)$$

Where; H_o = the radiant intensity of the radiation source at the particle

f = the focal length of the telescope

λ = wavelength of the source

i_1 & i_2 = the Mie coefficients

The Mie coefficient values of the particle are dependent upon particle size, particle index of refraction, wavelength, and scattering angle. It will be noted that distance to the particle does not enter into the equation, indicating that the image intensity is constant for a given particle anywhere within the near field. As the distance to a particle increases, less radiant energy is received from it but the blur circle decreases proportionately so that the image intensity per unit area remains constant. Outside the near field, the image intensity decreases as $1/r^2$. The distance the near field extends, for a diffraction limited telescope, can be determined from the equation:

$$d_{NF} = \frac{Df}{2 r_a}$$

Where; D = aperture diameter

f = effective focal length

r_a = radius of the airy disc

The radius of the airy disc is:

$$r_a = \hat{r}_a f$$

Where; $\hat{r}_a = \frac{1.22 \lambda}{D}$

The near field of the 1.5 meter infrared telescope at 10 micrometers wavelength, therefore, extends to 90 kilometers and the near field of the 0.75 meter ultraviolet survey instrument at 2100Å extends to nearly 1100 Km. The near field of a 1 meter telescope operating at the peak intensity wavelength of the visible spectrum (4600Å) extends to 890 Km. These are very great distances and the question naturally arises as to whether a 1 meter aperture telescope can "see" a 5 micron particle at a distance of 890 Km. The answer is dependent upon the sensitivity of the telescope detector and the intensity of the background radiance. The brightness of a 5 micron particle at a distance of 10 meters and a 90 degree sun angle is about equal to that of a star of magnitude 8. The particle's apparent brightness is inversely proportional to the square of its distance from the observer. At 890 Km (the extent of the 1 meter telescope's near field), the brightness relative to that at 10 meters is decreased by a factor of 7.9×10^9. This is equal to a change of 24.7 star magnitudes. At 890 Km then, the particle would have a brightness equal to a star of $M_v = 32.7$. This brightness is far below that of the dark sky background and, therefore, no telescope could detect it. Even near a zero degree sun angle where its brightness could be 10^4 greater, its apparent brightness would only be equal to that of a star of $M_v = 22.7$; still below the background level. At 890 Km, the image of the particle at the 1 meter telescope's focal plane would be the size of the airy circle and of the brightness indicated above. As it moved nearer the telescope, the image would increase in diameter inversely proportional to its distance. At a distance equal to the telescope's effective focal length, the image at the focal plane would have a diameter equal to that of the telescope aperture. However, the brightness of the image would still be the same as that at 890 Km so that the telescope could not detect the particle no matter what

its distance might be.

However, the extent of the near field will decrease as the telescope aperture decreases and as the wavelength of interest increases. Also the intensity of a particle in the infrared spectrum bears no particular relationship to its intensity in the visible because particle temperature and telescope detector size may be the controlling factors. Smaller telescopes will be able to detect a 5 micron particle especially if they are focused at their hyperfocal distance, or less, rather than at infinity. Also, the particle intensity at the focal plane of an optical instrument increases as the focal length of the instrument decreases. But, because of the shorter radiant energy integration time, on any particular portion of detector surface, for high angular velocity particles, a very sensitive system may be required to register all particle characteristics.

Particles sloughing off of surfaces will have initial, relative velocities on the order of 0.3 to one meter/second but particles emitted by reaction control systems or driven off by their exhaust or other processes may have relative velocities above 2000 meters/second. If only slow moving particles are of concern, then the problem is greatly simplified. The slow moving particles will seldom get over 50 meters above the Shuttle Orbiter orbit because of ambient atmosphere drag and orbital mechanics limitations. If instruments are constrained to view in the hemisphere away from the earth's atmosphere, then the greatest distance from the Shuttle Orbiter within this hemisphere, that a particle could attain at a 650 Km orbit altitude would be about 26.5 Km. If instruments are required to view below this hemisphere, the earth and its atmosphere effects would cover up the intensity of 5 micron particles at distances greater than 26.5 Km.

A 5 micron particle at a distance of 26.5 kilometers would have a maximum visual magnitude at 90 degree sun angle of approximately 25. This also is below the "black" sky background level. It appears then, that absolute limit controlling factor is the deep sky background level of $M_v = 21$.

In order to discriminate a particle against this background for reasonable exposure times, it should be at least 10^3 brighter or $M_v = 13.5$. In areas such as the milky way and other bright backgrounds, it still may not be possible to discriminate particles of $M_v = 13.5$ from stars during reasonable exposure periods, because the effective angular rates of slow moving particles at the distance representative of that magnitude, would be too small. A practical limit may be as low as $M_v = 10$.

The best known instrument for detection of particles would be a photographic camera. For practical reasons, one with a 50 to 200 mm focal length should be considered. Two or three cameras should be used. One camera would use long exposure times to help in identifying particles by track length and direction where possible. The others would be separated by a known baseline distance and pointed parallel so that the stereo effect could be used to determine particle distance. Shorter, periodic exposures by the latter cameras would permit positive determination of particle direction of motion and a rough evaluation of particle size. Camera focus should be set at the hyperfocal distance. The cameras should be directed so that the outer extent of their fields-of-view is only a few degrees off the sun in order to take advantage of the brighter forward scatter. From this consideration, a coronographic type camera would be best suited but it would be difficult to maintain pointing unless the camera had automatic pointing capability. Other photographic instruments, when available, can be used to supplement the records obtained by the particle cameras. For real-time evaluation, a vidicon type camera could be used. However, continuous monitoring with a vidicon camera would demand excessive earth relay bandwidth, data storage capability, and data reduction time. Time notation on photographs would permit after the fact association of particle generation with operational events. Data obtained with particle monitoring cameras can be supplemented by data obtained from particle sensitive experiment instruments.

3.5.3.4 Sky Brightness - The JSC 07700 specification limits emission or scattering from the induced atmosphere "not to exceed 20th magnitude/sec^2 in the UV range". The ASD-PD-18743 specification states, "Continuous emission or scattering shall not exceed 10^{-16} watts noise equivalent power in a 10 arc second circle (1 M telescope) for $\Delta\lambda/\lambda = 0.5$ bandwidth in the IR at wavelengths from 10 to a few hundred micrometers." Considering the JSC specification first, a star of $M_{2V} = 20$ would have a peak intensity of 4.8×10^{-20} watts/cm^2/micrometer. Therefore, the JSC specification is interpreted to mean that the energy received by a cm^2 of detection area as a result of radiation in the ultraviolet from one square arc second of viewing angle of the induced atmosphere should not exceed 4.8×10^{-20} watts for each micrometer of bandwidth. Considering the ASD specification, a 1 meter telescope would have an area 7854 cm^2 and a 10 arc-second cone would contain 78.54 square arc-seconds of viewing angle. At 10 micrometers wavelength and a 5 micron bandwidth, the radiant energy limit would be 3.24×10^{-23} watts/cm^2/micrometer. At 300 micrometers and 150 micrometers bandwidth, the radiant energy limit would be 1.08×10^{-24} watts/cm^2/micrometer for each square arc-second of viewing angle.

The energies represented by the specifications are extremely small and are an indication of the sensitivities required of monitoring instruments. However, as indicated by the ASD specification, an instrument with a 10 arc second viewing angle and a 1 meter aperture would only have to detect 10^{-16} watts. A monitoring instrument with a 1 meter aperture would be quite expensive but there is a tradeoff possible between aperture size, bandwidth, and viewing angle. For example, an instrument with a 10 degree viewing angle, a 5 cm aperture, a bandwidth of $\Delta\lambda/\lambda = 0.5$, and a detection sensitivity of 3×10^{-14} watts would meet the infrared requirements. However, the instrument would be required to scan the infrared spectrum between 10 and 300 micrometers or at least cover spots at the ends and center of the band. The instrument should also be capable of directional scanning over the entire Shuttle Orbiter's +Z hemisphere. The tradeoff

between viewing angle and aperture should not be carried too far because too wide a viewing angle would not indicate the effect a narrow angle "hot spot" would have on an instrument with a very small field-of-view. Decreasing bandwidth will require a more sensitive instrument.

The ideal instrument to meet the monitoring requirement would be a photoelectric photometer with real-time data relay so that the operation or conditions causing readings in excess of specifications, if any, can be determined. The specifications refer only to the energy radiated or scattered by the induced atmosphere so that a means is required to discriminate between atmospheric radiance and celestial sources. This requirement could be satisfied partially by means of a camera operating in the visible spectrum and pointing in the same direction as the photoelectric photometer. The camera would indicate evident visual sources such as the sun, moon, bright stars, earth, and spacecraft structures in the field-of-view of the photometer. The camera would also indicate what part of the celestial sphere the photometer was viewing so that known, celestial sources could be eliminated from question. Also, camera records cannot be observed in real-time unless a vidicon camera is used with its consequent demand for wide, data relay bandwidth. One process for rationalizing the source is based on the fact that contaminant sources of high intensity radiation will be transient whereas celestial sources will be more permanently located. If a hot spot appears continuously in the same location, it would be considered as having celestial origin. Telescopes will be constrained not to view within 45 degrees of the sun. The photometer should have this same constraint and should also be constrained not to view the earth, moon, or any part of the Shuttle Orbiter or its payload equipment. These constraints will eliminate much data reduction effort and still permit specification requirements to be fulfilled.

3.5.3.5 Changes in Thermal Control Surface Characteristics - Changes in the solar absorptivity and emissivity of various thermal control surface materials at various locations about the Shuttle Orbiter can best be determined by laboratory tests of sample materials attached to the Orbiter in areas of interest. Also, the changes could be determined directly from the Orbiter surfaces after return to earth. However, changes in the two characteristics are not necessarily indicative of contaminant deposit effects. Radiation can also cause changes in these characteristics of many materials. It will, therefore, be necessary to determine the reason for any changes and this can only be accomplished by removing and analyzing surface materials on affected areas. One process for this purpose uses ion sputtering to remove surface material and Auger spectrometry to determine its constituency. It is doubtful that the Shuttle Orbiter's surfaces could be used for this purpose, unless they were going to be changed. Therefore, the sample materials are the best candidates.

One drawback of this process is that it is not possible to determine just when or at what rate the changes occurred. If contaminant deposition is the source of change, it could have occurred during one or more particular operational sequences and it is important to know these conditions if a remedy is to be found. A spectroreflectometer carried with the Shuttle Orbiter can be used to determine the rates of change by a series of periodic measurements of surface reflectivity. The measurements obtained during orbit operations can then be used to supplement the ground tests discussed above to obtain the complete history and cause of the changes.

3.5.3.6 Contaminant Induced Pressure - A time history of the pressure variations about a spacecraft is essential to a more complete understanding of contamination dynamics. At the beginning of orbit operations, the outgassing/offgassing rates will be relatively high. The effect of the high emission rates is to maintain pressures in the vicinity of the spacecraft well above that of the normal ambient pressure at the orbit altitude. This is especially true of unpressurized volumes having restrictive venting apertures

such as equipment enclosures. If the enclosures contain high voltage circuitry, the equipment may be damaged by arcing or corona or data circuits may exhibit noisy characteristics if energized while pressures are within a critical range. This range may extend from 10 Torr to 10^{-5} Torr for some sensitive equipment. High power (above 10 watts) transmitting antennas may also be affected adversely by corona or multipacting effects when pressures at their locations are above ambient. For antennas, the adverse pressures are somewhat frequency dependent but still fall within the range indicated above. Leaks from pressurized systems may suddenly increase the pressures in localized critical areas as may vent and rocket motor operations.

To determine when pressures are within safe operating limits, to determine outgassing/offgassing decay characteristics, and to detect inadvertent leaks; staged pressure gauges capable of indicating a wide range of very low pressures will be required. Locations of particular interest are those containing high voltage equipment. It is also of interest to determine the effects external pressures have on pressure decay within unpressurized enclosures. Therefore, pressures outside the enclosures should also be monitored.

Types of instruments capable of measuring the desired range of pressures are the Knudsen or Pirani Gauge for covering the range from 30 to 10^{-4} Torr, the Cold Cathode Ionization Gauge covering the range from 10^{-4} to 10^{-6} Torr, and the Bayard Alpert Ionization Gauge covering the range from 10^{-4} to 10^{-11} Torr. Mass spectrometers, where available, will indicate pressure variations and, through molecular species identification, indicate the probable source.

3.5.4 Location and Pointing Considerations of Contamination Monitors - Table XIV lists the predicted maximum and minimum induced atmosphere characteristics such as molecular column densities, number column densities, return flux rates, and polar molecule densities produced by all sources combined. The contribution of particular basic sources such as outgassing, offgassing, leakage, etc., are listed in Tables V, VIII, IX, X, and XI. The tables also indicate how the densities are expected to vary with direction of line-of-sight relative to the Shuttle Orbiter axes. The numbers listed are for a wide range of outgassing/offgassing variations including the peak effect of VCS firing. The values listed are indicative of the sensitivities, ranges and pointing directions required of instruments used to monitor the induced atmosphere effects. In particular, Table XIV presents a maximum and minimum range for instrument considerations.

The conditions that influence outgassing/offgassing most strongly are temperature and the direction major surfaces are facing. Outgassing/offgassing, as a general rule, can be expected to be greatest on the solar illuminated side, especially when the Shuttle Orbiter presents the greatest amount of surface area toward the sun. Maximum leakage directions are influenced by the location and size of pressurized compartments, the location and facing direction of the compartment seams and junctions, and the location and directive characteristics of nearby surfaces that can reflect leaked effluence. Induced atmosphere density as a result of leakage and outgassing/offgassing can be expected to be greatest in the Shuttle Orbiter +Z hemisphere because the greatest surface area will be exposed in that hemisphere and the majority of leakage from the cabin, Spacelabs and connecting tunnels will be directed into that hemisphere either directly or by reflection off payload bay and bay door surfaces.

Two possible locations are under consideration for the water Evaporator vents; one, the current baseline position, is aft of the bay and the other is slightly forward of the center of the bay. Both locations would be above the wings and below the bay door hinge lines. The vent axes will be parallel to the Shuttle Y axis. Table XI lists the densities predicted for the aft baseline location. Reflections off the wings cause most of the effluence to be directed into the aft and lateral portions of the +Z hemisphere. If the more central locations should be selected, the majority of effluence is expected to be directed into the forward and lateral portions of the Shuttle -Z hemisphere by reflection off the open payload bay doors and wing leading edges. Some small percentage may be expected to squeeze through the bay door hinge lines into the +Z hemisphere.

The great majority of exhaust from the VCS engines will be directed into the -Z hemisphere but a part of the aft VCS exhaust will reflect off the wings to be widely spread across the +Z hemisphere and ducted between the payload bay doors and wings.

If monitoring instruments are to be located and directed so as to measure the effluents and effects of specific sources, then the source locations and directions indicated in the preceding discussion should be considered. However, the majority of concern with contamination has to do with its effect on optical instruments. The possible exception is the effect of contamination deposited on thermal control surfaces which would effectively extend over the entire payload bay area. On the Shuttle Orbiter, nearly all optical instruments will be located in the +Z hemisphere and make nearly all observations in that hemisphere. Some navigational instruments may be required to point into the -Z hemisphere occasionally. It therefore appears that the location of greatest concern is in the area of the payload bay and the directions of greatest concern cover the entire +Z hemisphere.

Monitoring equipment required to measure the effects of contamination on specific scientific instruments should be located as near to the sensitive elements of those instruments as possible. This requirement suggests that the monitoring equipment be housed within the instrument in most cases. However, this location is impracticable in nearly all cases (except for optical instrument in-situ calibration systems which can serve as contamination monitors to some extent). The next best location for monitors of this type would be mounted externally on the optical instrument so that it would be pointed continuously in the same direction as the instrument it is monitoring. Under this consideration, the monitors should have the same field-of-view and baffling; its detector should have similar or relative physical characteristics as the instrument elements it is monitoring. If this mounting condition is impracticable, then the monitor should be positioned as near the optical instrument's platform as possible and the conditions of pointing, baffling, and temperature mentioned above should be met. A monitor used in this manner can supply data in real-time indicating the optical quality of the instrument it is monitoring. The more the monitor location, geometry, and operation differs from the ideal conditions listed above, the less realistic will be the data obtained from it. If real-time is not desired, then no monitor will be required because the optical instrument itself can probably be tested after return to earth.

For general contamination monitoring, not directed toward determining the effect on any specific instrument or experiment, monitoring equipment should be located near the center of the payload bay but up out of the bay near the plane where the optical instrument entrance apertures would be located. Ideally, such monitors should be pointed in all directions in the +Z hemisphere. If monitors are small and relatively inexpensive, they can be mounted in clusters of five or more instruments pointed in the hemispherical cardinal directions and having contiguous fields-of-view. If monitors are too large or expensive to use in clusters, then some consideration should be given to scanning all

directions with a fixed or variable field-of-view. The value of the cluster lies in its ability to investigate the effects of contamination in all directions simultaneously and continuously so that rapidly varying flux characteristics can be evaluated quickly at any time from any orbit location. The cluster's undesirable characteristic is that too many instruments will be required if fine, directive detail is required. The undesirable characteristic of the scanning instrument is the long time required to cover a complete hemispherical field-of-view, especially if it must scan spectrally as well as directionally. In a rapidly changing flux field, the conditions measured at the end of a scanning period would bear no direct relationship to those measured at the beginning. Transient conditions such as the firing of a thruster, a venting operation, or sporadic emissions of particles might be missed entirely or only partly covered. Both types of instruments are of definite value and should be considered to supplement each other.

For measuring contaminant deposition effects on surfaces, monitoring equipment should be placed on all representative surfaces of interest. Monitoring instrument surface materials, temperatures, and fields-of-view should be the same as those of the surfaces being investigated. Where active, real-time monitors cannot be used to simulate the necessary conditions, periodic readings can be taken with a spectroreflectometer from passive samples or actual surfaces to obtain time histories of deposit effects. It is often important to know from what direction depositing species arrive so that their source can be determined and possible corrective measures taken. In this case, protuberances on passive samples will cause shadowing effect indicating direction of arrival. Alternatively, passive samples or QCMs arranged in directional clusters or a directionally scanning mass spectrometer can be located at major points of interest.

Ideally, from the standpoint of contamination investigation, multiple instruments of all the previous discussed categories should be considered and located within the payload bay and door areas. The one possible exception to this is the location of the mass spectrometer. The mass spectrometer should be located on an extendable boom such as the manipulator assembly to take advantage of spatial considerations. From economical and other practical considerations a much smaller or select number probably will be considered including utilization of data from Payload instruments which can infer the contaminant environment.

At least one of all types should be used and two or more QCMs and cameras. Pressure gages should be located in each unpressurized enclosure containing high voltage (over 250 volts) circuitry and two more should be located in separated external, open areas such as the extremities of the payload bay. This will provide measurements in areas where either cabin leakages or OMS kit and main engine propulsion leakages could be monitored. Surface samples are small and inexpensive and should be used in reasonable numbers in several locations about the payload bay and equipment within the bay. If only a single package of instruments can be carried, then it should be located as near the center and top of the payload bay as the particular mission Payload will permit. It is essential that coverage of the +Z hemisphere be possible with at least QCMs, photometer, and mass spectrometer.

4. OTHER CONSIDERATIONS

4.1 General Discussion - There are two phases other than the on orbit phase which can lead to on orbit contamination problems. These two phases are ground handling and the boost and reentry. These two phases can present basically both condensibles and particulates to the on orbit phase. The most probable contaminant from these phases in comparison to the on orbit induced environment predictions discussed and evaluated previously is the particulate contaminants. The following subsections address both of the phases qualitatively with respect to the mentioned contaminants.

4.2 Contaminant Ground Control Measures - A review of various aspects of ground control contamination activities was made in an attempt to relate ground contaminant control measures to minimize the potential particulate environment on orbit for Spacelab systems/Payloads. The many projected flights for the Shuttle Orbiter, the use of vehicles such as the Tug, and the multiple flights for a variety of particle sensitive Payloads could present different requirements to be addressed for ground contamination control than that used on many of the previous manned and unmanned spacecraft systems. In addition, the multiple usage of systems/Payloads in the Shuttle Program indicates a requirement to be able to turn these systems around in a reasonably short time with possibly minimum ground control.

All of these considerations will have a tendency to possibly increase the particulate impact to the on orbit environment. That is not to indicate that volatile residues may not be a problem but this type of source will boil off early on orbit and should not be a long term influence such as outgassing from non-metallic materials and/or as particulates will be. During the Skylab Program, the observed particulate rate was observed to be approximately 1.3 particles/steradian/second (16 particles/second). This rate appeared to persist throughout the missions without correlation to any known source indicating a general random sloughing of the particulates. If the general trend of particulate sightings was higher during the early part of the mission, this might indicate that contributions were the

result of ground handling and they were undergoing general clean up through the mission. Conversely, if the particulate rate increased during the mission, it might be attributed to the deterioration of non-metallic materials with space exposure. Anomalous events such as the loss of the meteoroid shield or deployment of the thermal sails should have increased the potential particulate rates during these phases of operations. The general random sloughing of particles observed on Skylab probably was the result of normal spacecraft development such as design, manufacturing, ground control, and operational usage.

In order to attempt to correlate the potential importance of the above mentioned sources to on orbit particulates, a review of ground control activities and requirements established during the Skylab Program for modules/experiments was made. The review comments from this activity are presented in Appendix A. A review was also made of various previous unmanned and manned systems and available aircraft measurement programs. These review findings and comments are presented in Appendices B and C for the previous space programs and the aircraft programs respectively. Particular interest was paid to the level of cleanliness control through final clean room stages of development activities.

Post manufacturing cleanliness or clean room requirements were also reviewed to see if correlation or if a relationship could be developed or established to define possible on orbit particulate environment as a function of clean room levels. The following subsection discusses the influence of clean rooms on the on orbit particulate environment, the relationships derived from the above mentioned reviews, and the relationships with current on orbit particulate criteria for Spacelab systems and Payloads.

4.2.1 Influence of Clean Rooms on the On Orbit Particulate Environment - As indicated in the Appendices where a series of reviews were conducted to ascertain the impact of ground handling upon these systems, the general theme that appeared was that condensible outgassants played an important role in the observed contaminant. However, for most of these systems; the experiments, instruments, and systems were relatively insensitive to particulate contamination except that of the Mariner series. This is not to say that particulates were not part of the overall induced environment but indicates that if they were they were not detectable. The majority of unmanned systems reviewed were small systems in comparison to that of Skylab and those envisioned for the Shuttle Program. Because of this, many of the processes involved in the development, manufacturing, assembly and testing, transportation, and storage could be controlled rather closely.

It is evident from the Skylab ground control review that with the many different modules, involved agencies, and varying requirements, the systematic monitoring throughout the various phases was a very large and difficult activity. The ultimate impact of clean room control during these phases can be considered somewhat unknown. The Mariner series was controlled to Class 10K clean rooms or better during ground handling and the various Skylab modules were controlled from Class 10K to Class 100K to minimal control. Yet both of these systems can point to observed particulate environments during their operational phases. The ultimate importance of the induced particulate environment is highly dependent upon the mission objectives and the sensitivities of the involved instruments and systems. Operationally, systems such as Star Trackers can be modified to accommodate a particulate environment and perform satisfactorily. However, as more sensitive instruments such as cryogenic infrared telescopes and large ultraviolet telescopes are flown, the particulate environment concern becomes more important.

The role clean rooms play in the induced particulate environment was assessed to some degree not only to establish if there could be a related function but to operationally indicate how necessary they may be. There are many specifications, standards, and procedures which have been written in the clean room field. Probably the most well known standard and/or the most widely used reference to clean rooms is the classification with respect to particulate density control. There are basically six major classifications of clean rooms and they are:

a) Class 100: 100 particles/ft^3 0.5 microns;
b) Class 1000: 1000 particles/ft^3 0.5 microns;
c) Class 10,000: 10,000 particles/ft^3 0.5 microns;
d) Class 30,000: 30,000 particles/ft^3 0.5 microns;
e) Class 70,000: 70,000 particles/ft^3 0.5 microns; and
f) Class 100,000: 100,000 particles/ft^3 0.5 microns.

Of these, there are three classes of clean rooms which are considered as preferred and most widely utilized. These are the Class 100, Class 10,000 (or 10K), and Class 100,000 (or 100K) clean rooms. There are other considerations in clean room standardizations and these deal with temperature, humidity, construction, filters, maintainability, etc.. With these conditions considered fixed for a given clean room, the main concern and that of this study is the particulate characteristics of these rooms.

Presented in Figure 22 is a plot of particle count per cubic foot greater than the stated particle size as a function of particle size for the three above preferred clean rooms. Also presented in Figure 22 is a plot of settling rates of airborne particulates having the shape of spheres with a specific gravity of 1.0 settling in relative still air at a temperature of 70°F. The settling rate relationship can be defined by Stokes law (When a particle falls under the attraction of gravity through a viscous medium, it ultimately acquires a constant velocity.) and as noted is essentially a linear function. It is recognized that the particle settling curve in Figure 22 is but one of many potential curves that may be drawn representing the

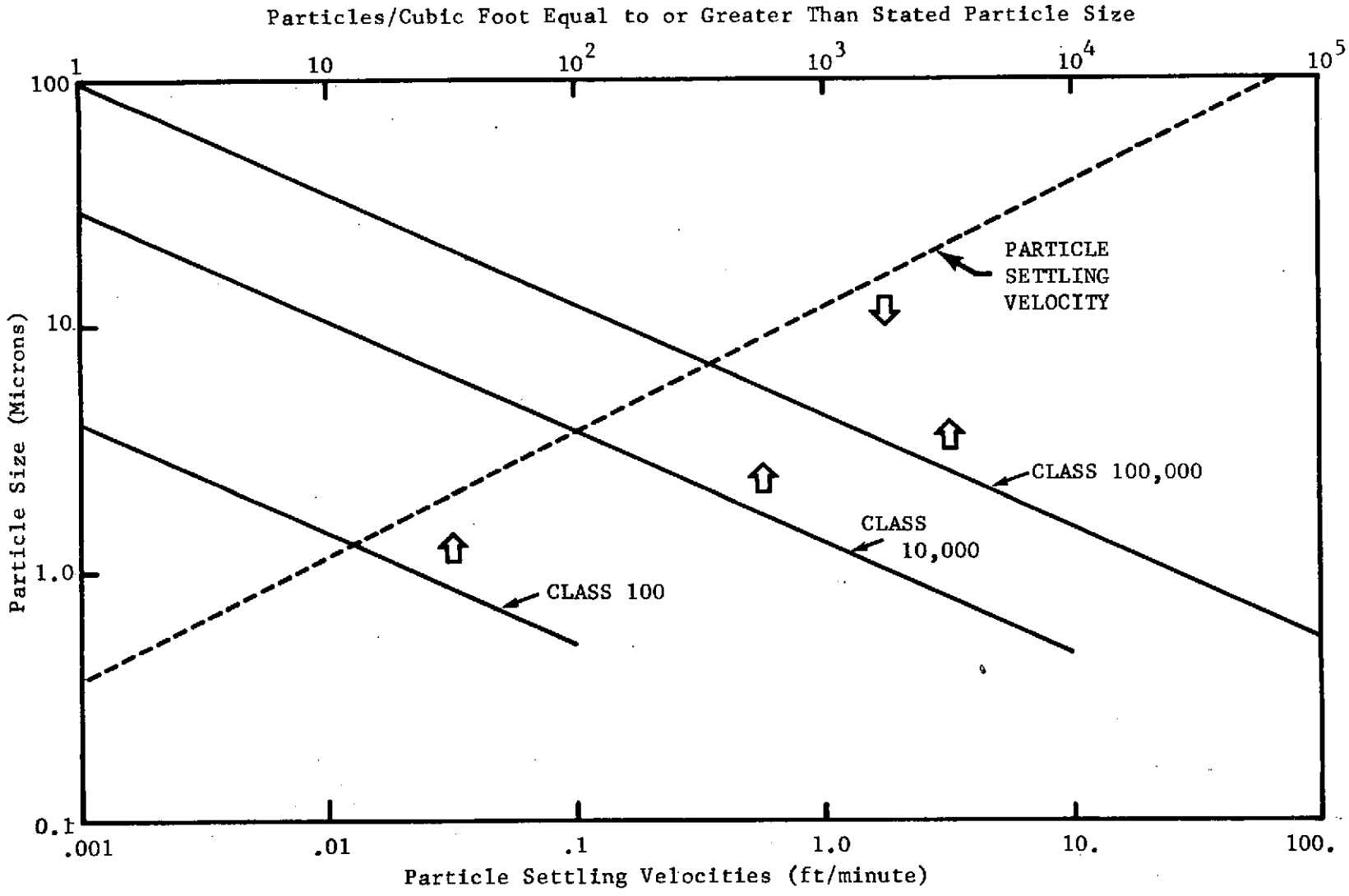

Figure 22. Clean Room Particle Size Distribution and Settling Rate Curves as a Function of Particle Size

settling time for particulate matter in air. If the particulate is of such a shape and configuration that it has a greater projected drag area than the sphere shape that was used to calculate the presented curve, a shift of the curve will take place but the relationship of particles of one size to those of another will remain essentially the same. This is also true for moderate changes in the temperature of the air and is also true for different densities of the particulates.

Of additional interest is the fact that the magnitude of the slope of the curves of particulate density, for all clean room classes, is very nearly the same as that of the curve for settling velocity. The product of particle density and settling velocity indicates the resulting flux rate of particles depositing per unit area of surface. For any particular clean room, therefore, the deposition rate for all particle sizes would be the same if particle size distribution matches the specification curve.

Present particulate criteria of "Fewer than 1 particle larger than 10 microns in a 4 arc minute half angle field-of-view per orbit within 1 km" (Applicable Documents - memo from R. Naumann to W. Emanuel) translates to an allowable particle rate of approximately 530 particles per second of the stated particle size or larger leaving the Shuttle Orbiter/Payload. This compares to the 16 particles/second observed during the Skylab program of similar particle sizes. The 16 particles/second observed during the Skylab Program is based upon measurements made by S052 (White Light Coronagraph) and the Star Tracker. Data from the T027 Photometer has yet to be fully analyzed to provide additional supportive data to the observed particulate rate. Of more importance, the completed analysis of the T027 Photometer data may provide an indication of the distribution and the particle sizes which may make up the submicron range. Although no experiment on Skylab gave any indication of being effected by scattered brightness levels from submicron particles, this may yet be an important concern during the Shuttle Program. If cleanliness requirements were to be relaxed, the number density of available submicron particulates

could increase significantly and possibly could contribute to overall scattered light background as opposed to that of individual particles and molecules.

Appendix A which was concerned with the review of Skylab ground control activities indicates that essentially the majority of modules were controlled prior to launch through assembly at about a Class 100K level clean room. Assuming that particulates of 10 microns or larger are undesirable as based upon Skylab experience and the current Shuttle particulate criteria, the number density of particulates in a Class 100K clean room 10 microns or larger would be approximately 150 particles/ft^3. Based upon the given settling velocity in Figure 22, the resulting flux of particles greater than 10 microns would be 90 particles/ft^2/minute. The total surface area of Skylab was approximately 12,000 ft^2 which is similar to the Shuttle Orbiter. Assuming that approximately 1/2 (the top half) of this total surface area would be exposed to particulate settling in a Class 100K clean room, the total number of particles settling under these conditions would be 5.4×10^5 particles/minute or 7.8×10^8 particles/day. It is not unreasonable to assume that any one of the Skylab modules may have spent weeks to months in a clean room environment which would tend to increase the exposure potential to particles by orders of magnitude.

This calculation tends to demonstrate that under even a very simple clean room environment the available particulate rate is orders of magnitude above what one would want to try to correlate to on orbit observations. Further, the standard of measurement of particulate number density in a clean room is between the inlet vent system and the object in question. This particulate number density is then the lowest possible for the local environment since any activities with respect to the immediate vicinity of the object in question could produce many times this particulate count. A wide range of clean room activities are possible as long as the clean room filtering system can effectively scrub or control the total particulate count in the returned flow. It also points out that analytically or quantitatively there

are too many unknown variables (which include prior manufacturing, assembly, test, and handling history) to ascertain the impact of clean room procedures to on orbit observations of particulates. Empirical information from two programs which employed basically two different classes of clean room control indicated that particulates were observed at sufficient rates to be of some concern. Possibly empirical information from early Shuttle flights may help establish long range ground controls other than those currently envisioned.

This discussion is not intended to imply that clean rooms serve no useful purpose. They do provide the necessary control to insure that through final stages of assembly, testing, and stowage the integrity of the system is kept at a high standard. It does imply that from a particulate point-of-view that a very high standard of control may not be necessary. This could be very important for the Shuttle Program since the carrier vehicle is a reusable system and inherently cannot be kept at a high quality cleanliness level as one would expect from a one-of-a-kind payload or system such as unmanned satellites. This is also true for the many Payloads and Tug systems which will be flown over and over throughout the duration of the Shuttle Program. The additional consideration of quick turnaround time for refurbishment to meet the high launch rate tends to diminish the utility of total clean room control of Payloads and systems.

The total importance of clean room control for particulate deposition is tied to a number of physical processes which influence the deposition rate in a clean room environment. The relative energy level or gradients between a particle and a probable point of deposition controls the rate at which the particles are collected and retained. The types of energy gradients of the most importance for particle deposition are electric, kinetic, and thermal. Electric gradients which cause electrostatic deposition are capable of effecting the collection of particles in a wide range of sizes. Once the particles have been charged (which can occur in movement through ducts and surrounding airflow), they will be strongly attracted to grounded or oppositely charged surfaces.

The term kinetic energy gradient is used to summarize inertia forces depending upon velocity differences between the contaminant particle and the component surface. Direct gravitational effects and impaction effects as they arise from motion of the particle when carried in a flow field of air are considered as kinetic energy deposition. The gravitational influence becomes of greater concern for large particles since the small particles can be suspended for a long period of time with the exception of being blown onto a surface or component. The controlling factors in kinetic deposition are the surface or component shape, particle size, and the air flow. These factors will generally establish whether the particle will deposit on the surface or will follow in the air streamlines around the surface.

Thermal energy gradients cause thermal precipitation to take place when the surface in question is at a lower temperature than the surrounding air. Generally submicron particles will deposit which may under some circumstances combine to make particles large enough to be of concern. This is also true for particles which undergo temperature gradients as the result of the absorption of radiation from strong light sources. If the particle absorbs radiation energy and is a thermal insulator, it becomes heated on the side which receives the radiation. Under this condition, the adjacent gas warms and moves away from the source of the radiation thus transporting the particle in a gas diffusion process. Another way in which gas diffusion can induce motion of particles is in the presence of a gradient of molecular weight. At least two gases must be present and a concentration gradient is necessary. Gas diffusion proceeds in the direction of molecular gradient and small particles are impelled in the direction of the diffusion flow of the heavier gas by differential molecular bombardment. These latter cases are primarily second order effects when taking into account gravitational, electrostatic, and air flow forces which principally are the major factors in clean rooms for particle transportation and deposition.

Gravitational deposition is the predominant effect for particles above the micron range where the Stoke's relationship governs the particle settling rate. In the presence of static charges on a surface, electrostatic deposition of particles below 0.1 micron increases rapidly as the size of the particle decreases. Very strong fields would be needed for larger particles. Thermal gradients are very important for sizes below 5 microns and become the main mechanism around 0.1 microns. Radiation gradients could be as important as the thermal gradients over a similar range of particle sizes. Strictly gas diffusion processes or Brownian motion are considered unlikely to be major factors in particle deposition since these processes are negligible for sizes over 0.01 microns.

All of the above processes play a role in particle deposition whether in a clean room or not. Very few of the factors which can influence particle cohesion and adhesion can be quantitatively defined. Some of the factors known to influence the strength of these bonds are particle material, size, shape, and surface roughness. Other considerations are relative humidity of the ambient air, the presence of electrostatic charge, and the nature and physical characteristics of the substrate in the case of adhesive bonds. Adhering particles can be dislodged from surfaces by mechanical, electrical, or air drag forces. There is some experimental evidence for deposited particles less than 80 microns in size that indicates that it is unlikely in the usual clean room environment to develop mechanical, electrical, or velocity forces large enough to disrupt the bond between these particles and the surface.

Although there may be a large number of interrelated and different forces involved in particle deposition both in a clean room or in a semicontrolled environment, the predominant particle deposition force is gravity for the large particles in the tens-of-micron size range and larger. This factor plus the indication the larger particles are the easiest to physically disrupt tends to indicate that surface clean up favors large particles. It is unlikely that particles in the micron and submicron range adhering to surfaces

will be subjected to mechanical, electrical, or velocity force fields on orbit such as those found in normal clean room clean up equipment, procedures, and/or hardware.

Should clean room requirements be relaxed in favor of employing thorough clean up procedures prior to launch and at key interim points, the requirement of designing Payloads and systems for maximum clean up utility becomes paramount and has to be recognized early in the design and manufacturing phases. This consideration has additional benefits in that refurbishment of Payloads and Systems requires certain physical access to all major components which in turn allows access for clean up. This was not considered necessary or acceptable for previous systems which were flown and never anticipated to be retrieved.

4.3 Boost and Reentry Contamination - The following subsections discuss the possible contamination sources during boost and reentry. A typical boost to a 685 Km altitude and subsequent reentry are discussed from a contamination viewpoint. An indepth assessment was made for a typical cryogenically cooled infrared system with respect to condensation of potential ingested material. This assessment is presented in Appendix D and summarized in this subsection.

4.3.1 General Discussion - The sources of possible contamination during boost and reentry are:

a) outgassing products;

b) engine exhaust products;

c) leaks from pressurized systems;

d) migration of particulates collected during ground handling;

e) fine sand, dust, salt, and moisture at low altitudes;

f) thermal protective system erosion products; and

g) landing strip materials and tire erosion products.

The protective devices used for reduction of contamination during boost, reentry, and landing are:

a) sealed payload bay doors;

b) payload bay liner;

c) controllable, filtered, pressurization/depressurization vents for the payload bay;

d) enclosures with controllable covers or vents for sensitive equipment; and

e) payload bay purge.

If these protective devices can be used in an ideal manner, then contamination during boost, reentry, and landing can be held to a low and acceptable level. However, it is not always possible to use all protective devices in an ideal manner. The following subsections discuss the contamination potential from those sources outlined indicating the role the protective devices play.

4.3.2 Launch, Boost, and Orbit Insertion Contamination - Table XXV indicates the boost events and timeline for a typical launch to a 685 Km altitude circular orbit having an inclination angle of 57 degrees. The active vents into the payload bay are opened 10 seconds after liftoff and remain open until just prior to the Solid Rocket Booster (SRB) separation. At the time of active vent opening, the Shuttle Orbiter has risen to 120 meters from the launch pad and the launch pad overpressures have subsided. The payload bay pressure is then approximately 10.7 mm of H_g (approx. 0.2 psi) above the external ambient pressure. This pressure difference is sufficient to prevent entrance of external atmospheric constituents (other than high velocity sand and dust particles) into the payload bay. If the wind velocity were great enough to drive particles to this altitude at a velocity sufficient to enter the bay, a launch would most likely not be permitted. As the launch vehicle gains altitude and velocity, the pressure difference will increase to approximately 25 mm of H_g because

Table XXV. Boost and Orbit Insertion Operations (Typical for Missions at 685 Km circular Orbit)

EVENT	TIME (sec)	ALTITUDE	REMARKS
Liftoff	0	Sea Level	Active vents closed
Open active vents	10	120 meters	Reduces internal pressure
SRM burnout	114	41 km	Active vents closed
SRB separation	120	42.7 km	Active vents open after separation
MECO	468	111 km	20x146 km orbit
Burn RCS for ET Sep	530	-	Coast to ET Sep
OMS ignition	540	-	Burn for 1st orbit injection
OMS shutdown	576	117.4 km	Injection into 55x185 km orbit
Release P/L bay latches	576	-	Coast to apogee
Open bay doors	636	-	Aid in cooling
OMS ignition	1908	185 km	Orbit circularization burn
OMS shutdown	1980	185 km	185 km circular orbit
Coast 1 orbit	-	185 km	Systems checkout
OMS ignition	7080	185 km	Hohman transfer to 685 km apogee
OMS shutdown	7368	185 km +	
OMS ignition	9972	685 km	Burn to circularize orbit @ 685 km
OMS shutdown	10,188	685 km (370 n.m.)	685 km circular orbit

of vent and filter restrictions. As the external dynamic pressure due to boost velocity increases, variable pressure profiles will be developed over the external surfaces. If pitch and yaw angles of attack are developed for purposes of maneuvering during high dynamic pressure conditions, pressure differences across the external surfaces can become great enough to cause air to become ingested at one vent where the pressure is the highest, entrained through the bay and exhausted out another vent. The ambient air at the altitudes where this action can occur is at least as clean as that in a Class 100K clean room. However, the aerodynamic heating that occurs across the maximum dynamic pressure regime can cause release of contaminants deposited on external surfaces and cracks and boost vibration can shake loose external particulates which can become entrained with the air. The period during which this condition can occur though is short and any resulting contamination must be considered of little consequence. The active vent filters will trap any particle over 35 microns diameter, as well as a large percentage of smaller ones. Instruments that are very sensitive to contamination will usually have further protection such as enclosures with vents that operate only when internal pressures are much higher than external pressures.

When the SRBs are expended, they will be separated from the external tanks by smaller solid rockets. These rocket exhausts can develop pressures on the external Shuttle Orbiter surfaces estimated as high as 5 psi. At this time, the active vents to the payload bay will be closed so that no exhaust products may enter. However, the separation rocket exhaust can enter passive vents and also be trapped on outer surfaces and in cracks between the surface tiles.

After main engine cut off, the external tank will be released and the 900 lb thrust RCS engines will be fired to drive the Shuttle Orbiter away from the tank. Shortly thereafter, the OMS will be fired for approximately 36 seconds to inject the Shuttle Orbiter into the first coasting orbit. After the first OMS shutdown, the payload bay doors will be opened exposing the radiators for necessary support of the Shuttle Orbiter cooling system. During the successive three

OMS firings for orbit circularization, Hohman transfer to higher orbit, and circularization at final orbit altitudes; the payload bay doors will be open. OMS exhaust backflow during these periods will be between 1% and 2% as discussed previously in subsection 3.4. Exhaust from the RCS engines, which are used for attitude control and orbit velocity refinement during the injection phase, can be expected to be more contaminating because these engines are used in the pulse mode where combustion is less complete. However, only about 100 lbs of RCS propellant is expected to be used during injection and only backflow can reach the payload bay. These effects are discussed in more detail in subsection 3.4.

Contamination during launch, boost, and orbit insertion therefore will be limited to the following processes:

a) migration of particles trapped within the payload bay during ground operations and shaken loose by boost vibrations;

b) migration of particles and molecular species deposited on external Shuttle Orbiter surfaces during ground operations and by SRB and separation rockets operations;

c) migration of separation rocket exhaust products forced into passive vents;

d) ingestion through active vents of particulates and outgassing products from external surfaces during boost maneuvers that develop pressure differences permitting entrainment of the external atmosphere; and

e) direct deposit of OMS and RCS backflow exhaust products on internal payload bay surfaces if the payload bay doors are open. (If payload instruments are further protected by enclosures, then this contamination will be limited to later migration of contaminants from payload bay surfaces deposited on during the engine operations.)

None of the above processes are particularly severe. However, if sensitive instruments have no other protection than the payload bay liner, consideration should be given to having the payload bay doors closed during operation of the OMS and RCS engines for the major and preliminary early orbital adjustments.

4.3.3 Deorbit, Reentry, and Landing Contamination - Table XXVI indicates the events and timeline for deorbit, reentry, and landing from a 685 Km, circular orbit. Approximately 12 hours prior to the deorbit retro burn of the OMS engines, the RCS engines will be fired to cause the Shuttle Orbiter to rotate continuously at a predetermined, slow rate. This "toasting" operation will tend to equalize temperatures on the Shuttle Orbiter external surfaces and within the payload bay. Some small amount of contamination may result from the RCS operation because the payload bay doors will be open. However, only 60 pounds of propellant is expected to be used and only exhaust backflow can reach equipment in the payload bay through the return flux mechanism so that any resultant contamination should be minor. Combined burning times for all engines fired will be less than 20 seconds and they will be fired in a more continuous rather than pulse mode so that combustion will be more complete and the exhaust products less contaminating.

Approximately two hours prior to retro-thrust, the payload bay doors will be closed and latched. They will remain closed from this time until 17 hours after landing. The active vents into the payload bay may remain open until just prior to the start of reentry at approximately 400,000 feet altitude. Whether or not the vents are closed during the 4.8 minute OMS retroburn will be up to the discretion of those having contamination sensitive equipment aboard. Very little OMS exhaust can enter the relatively small, filtered, vent openings into the bay.

The active vents will be closed during the reentry blackout period. During the descent from 400,000 to 70,000 feet, the dynamic pressures on surfaces facing in the direction of the velocity vector will rise to very high values although the ambient pressure will only rise to 42 Torr at

Table XXVI. Deorbit, Reentry, and Landing Operations from a 685 km Circular Orbit

EVENT	TIME	ALTITUDE	REMARKS
Fire RCS engines	T-12 hr,7.2 min	685 km	Rotates Shuttle to reduce thermal gradients
Close payload bay doors	T-1 hr, 51.6 min	685 km	Three minutes to close, 1 minute to latch
Start reentry preparations	T-1 hr, 49.2 min	685 km	1 hr, 24 min to complete
Fire OMS engines	0	685 km	Retro-thrust for deorbit, 4.8 min burn duration
Dump OMS excess propellant	5 min	685 km	Reduces reentry weight
Close active vents	39.6 min	123 km	Start of high heating phase
Open active vents, initiate transition	1 hr, 6.6 min	21.3 km	Mach 6, blackout period over
Touchdown	1 hr, 20.4 min	0	Start cooldown period
Start Bay purge	1 hr, 50.4 min	-	50% Rh Clean gas or air
Deactivation complete, crew removed	2 hr, 20.4 min	-	Shuttle towed to processing facility
Payload bay doors opened	18 hr, 20 min	-	Start payload removal

70,000 feet. Aerodynamic and plasma sheath radiant heating will raise temperatures on the external payload bay door surfaces to above 800°F in some areas. The outer bottom surfaces of the bay will reach temperatures of over 2000°F. However, because of the payload bay and payload bay liner insulations, the temperature of the liner inner surface will remain below 120°F until touchdown. Aerodynamic heating and erosion of the hotter surfaces will cause a hot molecular and particulate plasma to envelope the Shuttle Orbiter during the blackout period. The active bay vents, being closed during this period, prevent these contaminants from entering the bay and depositing on the much cooler internal surfaces. However, the inner surfaces of the outer skin and the outer layers of insulation will become hot and outgassing products from these materials can condense on the cooler surfaces of Payload equipment. The hot plasma from the outer surfaces can enter passive vents which will be open continuously. The passively vented areas therefore become a possible contamination source for subsequent missions and considerations should be given to monitor and provide the necessary clean up of these areas depending upon the observed contaminant.

When the active payload bay vents are opened at 70,000 ft altitude, the external surfaces are still quite hot and will still be smoking and outgassing although to a much lesser degree than during the blackout period. The payload bay pressure will be approximately 0.8 psi below the external ambient pressure and some of the contaminant products from the external surfaces will be forced into the bay to condense on the much cooler internal surfaces. However, the payload bay doors must be opened at this time to reduce pressure stresses. During the remainder of the time until shortly after touchdown, the payload bay pressure will remain below the external pressure so that any contaminants generated externally or already existent in the external atmosphere (such as sand, dust, salt, fog, and smog) will be continuously forced into the open vents. Upon touchdown, erosion products from the landing strip surface and from the Shuttle tires could be forced into the vents, although the Shuttle lower body and wings will provide a good shield against such action.

During the 30 minute cooldown period, heat from the external surfaces will continue to soak into the interior so that the inner bay liner surfaces may reach temperatures as high as 200°F with temperatures progressively higher through the insulation toward the outer surface. The actual payload surfaces will remain cooler so that outgassing products from the interior surfaces will continue to condense on them. When the cool gas purge is started, 30 minutes after touchdown, outgassing condensation will be greatly reduced and eventually stopped. The purge over-pressure will force most of the outgassing products out through the vents and, by cooling the hot materials, reduce the outgassing to a very low level.

Contamination during the deorbit, renetry, landing, and cooldown period therefore will be limited to the following processes:

a) deposition of RCS exhaust backflow products on bay equipment surfaces during RCS firings for "toasting" rotation with the payload bay door open;

b) possible entry of OMS exhaust backflow products through open payload bay vents during retro thrust;

c) condensation of outgassing products from hot internal bay surfaces on to cooler Payload surfaces during reentry blackout period;

d) ingestion into the payload bay of outgassing, burnt, and erosion molecular and particulate products from extremely hot exterior surfaces from the time vents are opened at 70,000 feet altitude until shortly after touchdown;

e) ingestion of atmospheric and landing strip contaminants from the lower altitudes during the landing process; and

f) condensation on cooler Payload surfaces of outgassing products from the Payload bay inner surfaces

and liners, which continue to increase in temperature as a result of heat soak from outer surfaces, after landing and until after purge is started.

Of the above listed processes, all are considered relatively minor except for d) and f). Little can be done about process d) unless the payload bay can tolerate greater pressure differences. The later the vents are opened the better. Process f) can be alleviated by starting the purge sooner and, in this case, the sooner the better. Ingestion of atmospheric contaminants (process d)) during landing can be reduced by closing the active vents during the last 150 meters of landing altitude and leaving them closed until purging is started.

It may be argued that contamination occurring during the reentry, landing, and post landing period is of no consequence because the instruments have completed their mission and can be cleaned before reuse. However, investigators may be interested in maintaining orbit condition cleanliness of their experiments as a calibration check condition and contamination occurring after the orbit period would invalidate such a check. This would certainly be true for non real time contamination monitoring instruments. Also, contaminants can get into locations where they may not be noticed or from which they cannot be removed. They could then migrate to more sensitive areas during later missions. It is quite possible that contaminating some instruments in inaccessible locations during reentry would require complete refurbishing for the next mission.

Too much emphasis cannot be placed on separate protective enclosures for instruments that are very contamination sensitive. Sometimes only a cover over one end of an instrument is required. Other enclosures may be such that they can be sealed under space vacuum conditions and not opened until they are returned to the investigator's laboratory. Others may require pressurization with a clean gas in orbit prior to sealing.

The instruments most susceptible to boost and reentry contamination would be the cryogenically cooled infrared telescopes if special precautions are not taken to protect

them during these periods. In order to save time and weight on orbit, it is planned to cool these instruments prior to launch. Cryogen supply to the instruments will be sufficient to last throughout the orbital mission and reentry phases. Optical elements and other internal surfaces will therefore be cold enough to condense and freeze most of the gases and vapors encountered in the various environments to which the instruments will be subjected. A review of planned contamination control and operational procedures for a 1 meter class infrared telescope was made. This assessment is presented in Appendix D.

This review indicated that for a 1 meter class infrared telescope the planned use of a Vacuum End Cap Assembly (VECA) and the use of a vacuum external jacket should minimize any contaminant potential discussed previously for the boost and reentry phases of this type Payloads. The VECA will seal the sensitive internal surfaces of the telescope from any condensibles or particulate contaminants. In addition, the vacuum jacket will provide the necessary thermal relationships with the payload bay to minimize condensing of gases or vapors present during these phases. Only upon contingency modes would the infrared type Payloads be compromised. Two possible modes could occur. In case of complete failure of the VECA to close, the telescope would start pressurizing with the payload bay during reentry. Because of the extremely low telescope inner surface temperatures, nearly all gases ingested will start to condense. This will continue until the telescope cryogen is totally exhausted and the temperatures of the telescope rises above the condensation temperatures of the contaminants. The amount of condensed buildup cannot be calculated accurately under these conditions as it is dependent upon the cooling capacity and characteristics of the telescope, the insulation characteristics, and the nature of the condensibles. However it is felt that under this condition considerable contaminants would condense and compromise the system.

In the case where the VECA can be closed but a leak in the seal developes, condensation will occur at a much slower rate. Under these conditions, the condensing of the ambient environment would keep the pressure in the telescope tube below the external pressure until a sufficient volume of the

ambient air had entered to raise the telescope inner surface temperatures slightly above the temperature of liquid air. The condensed air would boil off and raise the pressure in the tube to or slightly above the external pressure thus excluding any entry of additional air. This stalemate could last for a long time depending upon the rate at which heat could be conducted through the telescope. Under these conditions only a very small amount of water vapor would be ingested. At a maximum, this would amount to approximately 528 grams (1.16 lbs) at 25°C, 100% relative humidity air for two telescope volumes.

These contingency conditions are cited to indicate that this possibility exists for these type telescopes and that possible preventive measures could be implemented to preclude additional degradation of the system. Total failure of the VECA generally precludes any preventive measures while in the small leak case (which probably would most likely happen) internal telescope pressure gages and a dry gas support system for purging could detect and minimize this anomalous contaminant potential.

5. CONCLUSIONS AND RECOMMENDATIONS

5.1 General Discussion - The conclusions and recommendations presented in this study are based upon identified Shuttle Orbiter and Spacelab/Payload physical and operational characteristics consistent to the time frame within which this study was conducted, to the relevant supportive data gained from technical literature and the Skylab Program, and assumed mission profiles used to assess the specific effects of contamination. The results presented in Section 3 were established against those considerations where weighted worst case conditions would exist (e.g. during evaporator operation, maximum leakage rate, RCS 25 lb thrust engine firings, and the 10 hour offgassing rate point) for the sources evaluated. Depending upon actual mission profiles, attitude and pointing requirements, and specific Payload configurations and sources, subsequent evaluations may produce conditions in excess of or less than those indicated for this study.

The results presented are felt to be indicative of actual contamination concerns for those conditions modeled and the conclusions and recommendations presented below are weighed with this in mind along with anticipated program requirements and changes.

The closed form analytical model approach used for this study was shown on Skylab to be an effective tool in contamination evaluation and assessment. The effectiveness of this approach, as is the case with any analytical approach to a problem, is highly dependent upon the quality of input data such as material characteristics, mission profiles and surface temperatures, vent characteristics, and the development of the physics involved in establishing how the induced molecular and particulate environment will interact with critical surfaces or lines-of-sight in question.

These types of limitations are inherent in all forms of modeling. However, they do not detract from the overall utility of such an approach. An assessment of this nature allows basic parameters to be identified, geometric considerations to be established, and formulates in a systematic

perspective the trends that evolve from variations of important physical parameters. As test data concerning many of the complex functions becomes available along with improved definitions of mission requirements, the inherent model limitations can be minimized.

5.2 Study Conclusions and Recommendations - The following conclusions and recommendations are made with respect to identifying study results which may indicate program concerns for contamination control on the identified Spacelab/Payload configurations and/or the Shuttle Orbiter/Spacelab interfaces.

5.2.1 Conclusions

a) Spacelab Sources - Since the non-metallic thermal control material has not been specifically identified for the three Spacelab configurations modeled, an assumed outgassing and offgassing characteristic was established to assess this contribution to the predicted induced environment. The outgassing and offgassing characteristics were based upon those felt representative of a S13G type white thermal control paint. Although this type of paint may not be the final paint used, it does present a basis for evaluation of these two Spacelab sources.

The calculated mass and number column densities for these sources slightly exceeded the stated number column density from the previous given criteria. Although assumed values were used for the outgassing and offgassing rates, the analysis does indicate that in order to keep the number column density from these sources below the stated criteria they should be on the order of 1×10^{-9} g/cm^2/second at 100°C. This value is one order of magnitude below that used for outgassing and two orders of magnitude below that used for offgassing at the 10 hr. mission point. This provides an indication of the needed characteristics for the selected non-metallic thermal control material used for Spacelab. It also provides an indication of the adequacy of current materials selection criteria. The maximum acceptable mass loss rate stated for non-metallic materials in Applicable Documents MSFC 50M02442 (0.04%/cm^2/hour) and JSC SP-R-0022 (total weight loss 1%) is approximately a factor of 6 greater than the recommended value for Spacelab. Specific surface thermal profiles, temperature dependence of rates of the selected material, and external area of coverage will influence this final recommended value.

Based upon the modeled Spacelab module leakage rates, leakage should be no problem to the induced environment. The total number column density exceeds the stated criteria but the dipole content of the leakages never exceeds the 10^{12} molecules/cm^2 stated criteria and should be no problem.

Analysis of the Environmental Condensate Vent indicated that for the planned nozzle position and orifice design the vented plume would impinge upon the forward Orbiter payload bay bulkhead (see Figure 12). This situation is undesirable because impingement of the vented material upon the bulkhead will tend to retain ice particles in and around the payload bay area. Optimum venting of the condensate overboard will be when the condensate can clear the vicinity of the Orbiter as quickly as possible. A preliminary analysis was made to establish what clearing times might be expected for this vent. The clearing time analysis indicated that clearing times comparable to Skylab clearing times (approximately 15 minutes) could be established for Spacelab providing vent initiation would occur under the proper orbital conditions. One consideration must be looked into further and that is the potential for reencounter of particles on subsequent orbits. This potential could be eliminated depending upon the final design of the ECV system (e.g. increase flow rates, decrease plume extent, and increase-decrease plume extent vent velocities). Proper selection of Payload/system operations with this vent would minimize its impact. Specific constraints will depend upon final position selection and characteristics of this vent.

b) Infrared Payloads - The two infrared Payloads were assessed to be the most susceptible of the Payloads analyzed. These Payloads were assumed to be 1.5 meter f/16 and 2.5 meter f/12 diffraction limited systems. The impact of particle scattering and black body emission and molecular scattering, absorption, and deposition was assessed. The levels of contamination identified by this study from the major contaminant sources will present various problems to these types of Payloads.

For wavelengths greater than 3 micrometers, particles with radii greater than approximately 300 microns will scatter a noise power in excess of 10^{-17} watts/micrometer at the detector. At 20 micrometers wavelength and a bandpass of $\Delta\lambda/\lambda = 0.5$, this would produce a noise background of 10^{-16} watts. This background noise level approaches that of the previous stated criteria. For ice particles larger than approximately 100 microns radius, the black body irradiance at the telescope focal plane will exceed the allowable limit. Based upon observed Skylab particulate rates, these infrared Payloads could potentially have undesirable signal interference approximately every two or three orbits which should be no problem. The very nature of the Shuttle Orbiter surface tiles and seams, the gimballed nature of these large telescopes, and the large movable payload bay doors on the Orbiter (which are not characteristic of a fixed system such as Skylab) could increase the potential particulate production by an order of magnitude or two. In addition, potential particulates arising from the RCS engine firings[1] for attitude and pointing control could significantly add to the particulate environment and subsequently the observation of particulates.

Molecular cloud absorption was calculated for both H_2O and CO_2 for the worst case column densities of these molecules. For H_2O at a wavelength of 63 micrometers and CO_2 at a wavelength at 4.3 micrometers (typical worst case absorption bands), the induced environment absorption was determined to be less than 0.01 percent. The induced noise background due to molecular scattering for worst case total number column densities for all contaminant sources for wavelengths greater than 3 micrometers will present no significant noise contribution to the infrared Payloads.

(1) Hoffman, R. J., et al: "Plume Contamination Effects Predictions," the CONTAM Computer Program Version II, AFRPL-TR-73-46 MDC G4733, August 1973.

The cryogenic nature of these systems inherently make them susceptible to condensing practically every contaminant source effluent capable of impinging upon the cooled surfaces. Deposition as it results from the contaminant cloud interaction with the ambient environment is the primary influence in changing thermal backgrounds in cryogenically cooled telescopes. Thermal background changes occur in two basic areas. These are in the active thermal control of the telescope as a whole and in the specific properties of the critical optical and detector surfaces. As a result, a change in emittance properties of these surfaces from deposited contaminants will increase the thermal background from the surfaces. The resultant changes in the telescope's thermal background will increase the usage rate of cryogens and could severely limit some aspects of its dynamic performance.

Internal mirror surfaces of an infrared telescope are generally highly reflective specular surfaces with low emittance and absorptance characteristics for both infrared and solar radiation. Doubling the emissivity of these surfaces from values of approximately 0.02 to 0.04 (typical of evaporated aluminum or gold) can cause a temperature change at the detector stage of 5 to 10 degrees Kelvin (depending upon the telescope design) on passively cooled detectors operating in the 80 to 120 degree Kelvin range.[1] Roughly 1 micron of ice buildup can raise the emissivity of these surfaces by 0.1 which can represent an order of magnitude change in the background signal for infrared telescopes. On actively cooled systems, temperatures will be only slightly affected and a slight emissivity change alone will not significantly change the thermal background from the telescope surfaces. However, this condition will significantly increase cryogenic cooling requirements.

The return flux deposition on the infrared telescope primary mirrors was calculated for large molecules (outgassing M = 100), H_2O, and CO_2. The total deposition for seven days was approximately 0.23 microns resulting in less than a 2% absorption loss. The total deposition for thirty days was approximately 0.98 microns resulting in less than 10% absorption loss. The increase in surface scattering for the above

(1) See footnote (2) on page 77.

deposition levels is expected to be negligible. Measurements have shown that deposition of H_2O on cryogenically cooled reflective surfaces can significantly affect the surface emissivity as mentioned previously. An additional example is that polished stainless steel at 77 degrees Kelvin will increase its emissivity from approximately 0.09 to approximately 0.11 for a 0.2 micron thick film of H_2O. This is comparable to that of a typical mission profile of seven days.

The major contributor to the predicted deposition is the Evaporator. The final Evaporator location has yet to be selected and the current baseline position used for this study results in what may be considered as worst case. Final selection of the position of the Evaporator should reduce the H_2O contributions to the telescope significantly. Tests currently being defined at JSC will evaluate the Evaporator effluent characteristics under simulated geometries to support this position selection. The option may exist that the infrared Payloads could store the Evaporator effluents and then this particular source would not be an impact.

c) Ultraviolet Payloads - The two ultraviolet telescope Payloads were assumed to be 0.75 meter f/2 and 1 meter f/16 systems. The system resolutions were assumed to be one arc second and 0.2 arc second respectively. The impact of particle scattering and molecular scattering, absorption, and deposition were assessed.

For particle scattering, the 1 meter telescope will see particles with radii greater than 1000 microns and the 0.75 meter telescope will see particles with radii greater than 100 microns. The impact of these particles upon these systems will depend upon their mode of operation and upon the particle size and dwell time of the particle in the field-of-view of the telescope. For photographic surveys and imaging modes of operation, particles will appear as stars or as bright point sources and should not impact the resulting data. If the mode of operation is based upon long integration times for faint

sources, then a particle of sufficient brightness and dwell time could influence the data being obtained. Particulate rates on the order of 1 per orbit or less will not effect the majority of these systems except for the measurements which may require successive long integration times.

A concern arises from the deposition of large particles on critical optical mirrors and surfaces. Dust and other particulates on the mirror surfaces can scatter radiation from off axis stars and could greatly increase the noise background. This effect would probably not be an effect of the induced environment as developed on orbit unless the telescope was subjected directly to a source of particulate matter. It probably would be an effect as the result of ground handling or an unfavorable prelaunch and launch condition. This particulate effect is hard to assess since the quantity of particulates and the accumulative effect is hard to ascertain prior to a given mission.

For those molecular number column densities predicted in this study, both the scattering and the absorption appears to be of no concern for the two ultraviolet Payloads.

The ultraviolet Payloads, as is the case with the infrared Payloads, will be susceptible to deposition from the returned flux. These systems will degrade rapidly in the ultraviolet from the deposition of thin films. The reflectance loss for 100% exposure was calculated to reach the 1% maximum allowable at 2500Å for the 0.75 meter and 1 meter systems in 2.5 and 3.5 days respectively. The outgassant contributions to the return flux contributed the most to the predicted values. As discussed previously, the values of outgassing rates assumed for this study were based upon available data and the configuration considerations used. Tests currently under way at MSFC for simulated Orbiter tile configurations will present more specific data for evaluation along with a final selection for the Spacelab thermal control material. The above results must be weighed with this in mind.

Although the potential loss of signal due to deposition on the ultraviolet Payloads is marginal for the conditions stated, the impact could become significant if one takes into account the number of potential missions to be flown and the duration of any one mission increasing to 30 days. There is also an implied probable impact on similar Free Flying Payloads such as the LST where the self induced environment of the Payload is very small but with mission life times of 15 years could be of some concern.

d) Solar Payloads - The only instrumentation that will be significantly susceptible to molecular and particulate cloud scattering will be the coronagraph type instrumentation since it will be sensitive to the low light levels in the solar corona. The molecular scattering was calculated for the worst case predicted number column density and was determined to be three orders of magnitude below the sensitivity of the coronagraph type instrumentation. The Photoheliograph and the S055 scanning spectrometer type instruments are potentially susceptible to particle scattering but their fields-of-view are so small that the probability of a particle entering the field-of-view is negligible. Particle scattering for the S052 instrument was assessed from the viewpoint of determining the minimum particle size required to produce a scattered light level of $B/B_{\odot} = 7x10^{-11}$ (the Skylab S052 sensitivity criteria). The analysis showed that particles in the near field ($d < 800$ meters) with radii greater than 1 micron will produce this equivalent scattering level. The Skylab S052 experiment observed particles approximately 3% of its total data frames. If the Shuttle Orbiter/Spacelab configuration produces the same number of particles as Skylab, no significant data degradation is expected. However, if the Shuttle Orbiter/Spacelab particle production rate is greater than Skylab, then a potential influencing of the coronagraph data can be expected.

The return flux deposition was calculated for the primary optic of each of the analyzed solar physics class instruments. The analysis indicated that no significant instrument degradation will occur due to the return flux. Although these instruments are as susceptible as the ultraviolet telescopes, they

have very limited physical acceptance angles for the contaminant as opposed to the rather large physical apertures of the ultraviolet telescopes. Little detailed information is available for the high energy X-ray/γ-ray instruments. They are expected not to be impacted by the contaminant induced environment.

e) AMPS Payload - The AMPS Payload is comprised of numerous experiments and instruments designed to observe and artificially perturb the space environment and the upper earth's atmosphere. The major impact of contamination for the AMPS Payload is the modification of the ambient environment due to the introduction of various similar contaminant species. The instruments most likely to be effected are the ion probes and the mass spectrometers. Comparison of similar anticipated contaminant species with those of the ambient shows that in some cases the expected contaminant flux from the Shuttle Orbiter and Spacelab module leakage approaches the ambient N_2 and exceeds the O_2. H flux from the VCS exceeds the ambient as does A from offgassing. Under these conditions, it may be difficult for the ion probes and the mass spectrometers to obtain representative data concerning the levels of ambient flux. The atmospheric science instruments on AMPS, in particular, the ultraviolet measuring instruments will see reflectance losses similar to those previously discussed for the ultraviolet Payloads. The induced environment is not anticipated to impact the subsatellite systems or those experiments which are designed to perturb the ambient environment.

f) Free Flying Payloads - The contamination potential of Free Flying Payloads was assessed based upon OMS engine burns for orbital considerations, the return flux of the induced environment, attitude control during deployment, stationkeeping, retrieval, and the potential impact of the 900 lb RCS engines to impart forces and torques upon a typical Free Flying Payload. Depending upon the orbital requirements of any Free Flying Payload and in fact for any Sortie Payload, the OMS engines could be fired for approximately 10 minutes during 3 potential maneuvers expelling approximately 24,000 lbs of propellant. Characteristically 2% of this can be expected in the backflow from these engines. This amounts to some 480 lbs of engine exhaust

products capable of being directed towards the payload bay area. Geometric considerations indicate no direct line-of-sight exists between the Payloads and the engines. The potential exists that the Orbiter tail structure may reflect some material into the payload bay. Although there is no line-of-sight, the extensive flow fields of an engine the size of the OMS must be closely evaluated for effects which may impact a Payload during these maneuvers. As these engines are developed and the final geometries become established, this potential problem should be reassessed. A possible solution to this problem would be to close the payload bay doors during these firings.

The return flux deposition from the OMS engines for a 10 minute total burn could impact any thermal control surface in the payload bay. Changes in solar absorptivity of a 100% could occur for thermal control paints like S13G. To eliminate this contaminant potential, the payload doors could be closed during the engine burn times as mentioned previously or these burns could be timelined to the proper velocity vector orientation to allow minimum return flux deposition.

Once the proper orbit has been attained, the Free Flying Payload will reside in the payload bay and be subjected to the return flux of the Shuttle Orbiter/Payload induced environment. The maximum return flux at an altitude at 435 Km would be 1.4×10^{-11} g/cm^2/second for the outgassed products. For Payload surfaces near 300^{o}K, the only contaminant capable of depositing would be a fraction of the outgassed material. A deposition rate near 3.5×10^{-12} g/cm^2/second would result. Based upon an orbital altitude where the maximum allowed rate of return could happen, a total of 2.1×10^{-9} g/cm^2/second would result. For deployment times similar to that defined for a 3A type mission (10 minutes), the return flux would present no problem. Mission profiles that exceed the 3A timeline, the deposition per orbit would be near 1.4×10^{-8} g/cm^2/orbit or 2.2×10^{-7} g/cm^2/day. For up to a seven day mission, return fluxes of this level should not impact operational surfaces of any Payload.

Applying the same type of analysis to the VCS engine (25 lb thrust) return flux, an orbital deposition rate of 1.3×10^{-10} g/cm^2/orbit is predicted for an engine firing once every 4.8 seconds for a 40 millisecond pulse. This is worst case condition since the attitude and pointing requirements to fire the VCS at the above rate would not be required for Payload deployment periods. This yields a worst case return flux of 2.1×10^{-9} g/cm^2/day which should also be no problem for Payload surface temperatures near 300°K.

Approximately a 12 minute period is required for a 3A type mission deployment of a Payload during which the manipulator arm deploys the Payload and attitude control is required. During this period, the Payload is susceptible to direct backflow contributions from the VCS engines. For a Payload at 50 feet from the Orbiter X axis during deployment, the flux on a surface from the forward downward firing engines would be 3.1×10^{-14} g/cm^2/second and 2.9×10^{-13} g/cm^2/second for the aft outward firing engines (worst case for this configuration). The deposition rate may increase slightly but still would be no problem because of the very low deposition levels. For small distances from the Orbiter, surface shadowing would block the engine backflow.

After deployment, the Shuttle Orbiter will remain in the vicinity (near 200 feet as stated for the 3A mission) of the Payload for checkout and activation. During this time, the Payload will be susceptible to the normal contaminant sources of the Orbiter. Of these sources, outgassing will be the major source capable of depositing. The flux of the Orbiter outgassed materials at 200 feet is 2.3×10^{-11} g/cm^2/second for warm portions of the orbit. The total flux of all the sources is several orders of magnitude above the outgassing level but these are comprised of simple gases and will not deposit at the anticipated ambient Payload temperatures. For these temperatures, the anticipated outgassant deposition rate would be 1.2×10^{-11} g/cm^2/second. For short periods of checkout and activation on the order of hours, this rate should be no problem. However, for stationkeeping activities that may extend to periods of days, the potential deposition could accumulate

to undesirable levels. Under these conditions, stationkeeping distances should be increased to distances on the order of a 1000 feet for maximum protection. The position of minimum contamination impact is forward and above the Orbiter providing the forward RCS engines are inhibited. This is also the best position for visual sighting by the Orbiter crew during this period.

During rendezvous with a Payload for retrieval, the 900 lb RCS engines on the Orbiter will be used for maneuvering and braking. In this case, there is the potential that the +Z firing 900 lb engines may be required for final rendezvous maneuvers. In this event, these engines could directly impinge upon the Payload. For closing distances of 500 feet to 25 to 100 feet, a 10 second total firing from these engines could result in a change in solar absorptivity of a white thermal control paint such as S13G from 0.01 (5%) to 0.023 (10%) respectively. Depending upon the number of engine firings required to rendezvous, this could become a significant factor. A secondary factor is that under these conditions, these engines could impart a force or torque to the Payload which would result in increased attitude control requirements plus additional rendezvous maneuvers. This factor may tend to increase the total potential degradation to exterior Payload surfaces more than necessary. For a case where a Payload (typical in weight and dimensions of a LST) were impinged upon by one of the aft +Z firing 900 lb engine while its X axis was parallel to the X axis of the Orbiter at 50 feet distance, a velocity component in the +Z direction of 1.28 cm/second could be imparted. For a 10 second firing this would amount to a 12.8 cm/second drift velocity relative to the Orbiter. This means that depending upon the retrieval procedures and difficulties the Payload may separate far enough to require additional engine firing to reach the Payload.

During deployment and retrieval, those potential problems that may arise from RCS or VCS engine firings may be minimized through establishing operational requirements that inhibit certain engine firing combinations. As deployment and retrieval schemes become better defined, RCS/VCS impingement trade studies can be made to minimize this potential

contaminant source through inhibiting certain engines when within a given closing range.

g) Contamination Detection - The on orbit contamination specifications, the contamination measurement requirements, the instrumentation requirements, and location and positioning considerations of contamination monitors were discussed. These discussions covered a variety of instruments and their possible uses. The resulting recommended contamination monitoring instruments and their uses are summarized below.

a) Mass Spectrometers

1) contaminant flux emission rates
2) mass column densities
3) identification of molecular species
4) number column density
5) return flux rate
6) detection of leaks
7) identification of contaminant source

b) Quartz Crystal Microbalances

1) contaminant deposition mass and rate
2) effect of temperature, location, direction, and acceptance angle on deposition rates
3) effect of deposits on surface reflectivity for limited material types

c) Surface Material and Optical Element Samples

1) deposition characteristics for various surfaces and locations
2) effect of deposits on surface characteristics
3) identification of deposited species and probable source

d) Cameras

1) particle emission rate
2) rough determination of particle size, location, and direction of motion
3) discrimination between atmospheric and celestial radiation sources

e) Spectral Photoelectric Photometers

1) sky brightness as a function of wavelength
2) variations of sky brightness with time, direction, solar angle, event, and orbit location

f) Spectroreflectometer

1) changes in spectral reflectivity of surfaces
2) changes in thermal control surface solar absorptivity

g) Pressure Gauges

1) outgassing/offgassing pressure decay rates
2) pressures within critical enclosures
3) effect of leaks, vents, and reaction motor exhausts on local pressures
4) determination of safe times to energize high voltage circuitry

Ideally, from the standpoint of contamination investigation, multiple instruments of all the above categories should be considered and located within the payload bay and door areas with the exception of the mass spectrometer which should be located on the manipulator assembly to take advantage of spatial considerations. They should be pointed so as to cover all directions in the Shuttle Orbiter +Z hemisphere without the necessity of excessive directional scanning. However, from economical and other practical standpoints only a select number will probably be considered. At least one of all types should be used and two or more QCMs and cameras. Pressure gauges should be located in each unpressurized enclosure containing high voltage (over 250 volts) circuitry and at least two more should be located in separated, external open areas such as the extremities of the payload bay. This will provide measurements in areas where either cabin leakages or possible OMS kit leakages could be monitored. Surface samples are small and inexpensive and should be used in reasonable numbers in several locations about the payload bay and equipment within the bay. If only a single package of instruments

can be carried, then it should be located as near the center and top of the payload bay as the particular mission payload will permit. It is essential that coverage of the +Z hemisphere be possible with at least QCMs, photometer, and mass spectrometer. The mass spectrometer should also be capable of being moved by remote control and pointed directively back toward the Shuttle from the +Z hemisphere.

h) Ground Control - The potential for contamination during on orbit operations (which can be at least semi quantitatively treated) prelaunch contamination impact to on orbit operations presents a much larger variable condition. Because of the enormous number of steps involved in selection of materials, design and manufacturing, fabrication, assembly, test, transportation, and storage of a complex spacecraft or Payload, it is extremely difficult to establish and perform systematic monitoring throughout these phases and consequently treat quantitatively.

Although quality control and protection procedures have been developed, identified, and generally implemented, a large spacecraft system such as Spacelab cannot be given the same degree of protection as a small individual laboratory developed payload. Even in this case as pointed out in Appendices A and B, contamination has been observed which can be related to some of the mentioned phases associated with ground control. In general, even with the best manufacturing control, the presence of a spacecraft in a clean room environment theoretically offers significant probability for particulate contamination of structural surfaces.

In addition to manufacturing conditions, there are potential problems associated with transportation and launch site storage. Although those Shuttle Payload systems protected in the payload bay will not be subjected to prelaunch weather conditions, the Orbiter and its many surface irregularities due to the RSI will possibly be susceptible to prelaunch weather conditions.

Those criteria which presently express an on orbit particle sighting or false star sighting requirements tend to indicate that the Shuttle Orbiter/Spacelab Payload environment can be somewhat higher than that observed on Skylab. Current criteria states that "Fewer than 1 particle larger than 10 microns in a 4 arc minute half-angle field of view per orbit within 1 Km." This translates to approximately 530 particles/second as compared to 16 particles/second for Skylab for particles of the same size class. Of all the criteria, this criteria may be the most difficult to relate to an effective control of on orbit particulate contamination.

An additional consideration is that from the Skylab Program and currently for the Shuttle Program the molecular scattering does not appear to be a significant contamination potential. How much submicron particles may add to the general scattering background is unknown. This may be answered eventually by the results of the T027 Photometer data analysis. Since the bonding strengths of submicron particles are very high in comparison to large particles and the probability of finding mechanical or electric forces on orbit to dislodge these particles is very small, surface clean up techniques may tend to favor the larger particles. This may indicate that special emphasis could be placed upon final clean up as a way to minimize the potential on orbit particulate contamination in the above stated size ranges.

The most effective period for employing clean up procedures of this nature would be as close as possible to final integration into the Shuttle Orbiter payload bay since any open storage of a Payload even in a clean room tends to add to the particulate potential. Where last minute clean up is not practical, bagging and storage become an important consideration. Consideration could be given prior to final closure of the Shuttle Orbiter payload bay to performing a high degree of clean up. This could eliminate the local particulate environment of the payload bay although the environment seen by the Shuttle Orbiter external surfaces just prior to launch and through boost may establish the final observed particulate environment.

An important aspect to considering final clean up techniques over highly controlled and restrictive environments of a clean room is the design for maximum clean up. Inherent in the reusability of the Orbiter, Tug systems, and Payloads is the accessibility of subsystems for refurbishment. This tends to provide access for clean up where it normally would not be available if a system was considered for a one-of-a-kind mission. Concurrent to accessibility, a maximum clean up capability hardware design could be incorporated to assist this potential technique for additional utility in limiting on orbit particulate matter.

This does not imply that the adequate and proper controls employed during other phases of ground development of a system or Payload are not necessary. It does imply that effective clean up at the proper time may provide relief from final over restrictive and potentially timely final phases of Payload integration and still meet the criteria in limiting on orbit particulate contamination.

i) Boost and Reentry - Contamination during launch, boost, and orbit insertion will be limited to the following processes:

a) migration of particles trapped within the payload bay during ground operations and shaken loose by boost vibrations;

b) migration of particles and molecular species deposited on external Shuttle Orbiter surfaces during ground operations and by SRB and separation rockets;

c) migration of separation rocket exhaust products forced into passive vents;

d) ingestion through active vents of particulate and outgassing products from external surfaces during boost maneuvers; and

e) direct deposit of OMS and RCS exhaust products on internal payload bay surfaces while the payload bay doors are open.

None of these processes are considered particularly severe. However, if sensitive instruments have no other protection than the payload bay liner, consideration should be given to having the payload bay doors closed during operations of the OMS and RCS engines for major and preliminary early orbit adjustment. Particulate migration cannot be directly controlled especially that as a result of SRB and separation rocket firings.

Contamination during the deorbit, reentry, and landing will be limited to the following processes:

a) deposition of RCS exhaust backflow products on bay equipment surfaces during RCS firings for "toasting" rotation with the payload bay doors open;

b) possible entry of OMS exhaust backflow through open payload bay vents during retro thrust;

c) condensation of outgassing products from hot internal bay surfaces on to cooler payload bay surfaces during reentry blackout period;

d) ingestion into the payload bay of outgassing, burnt, and erosion molecular and particulate products from extremely hot exterior surfaces from the time vents are opened at 70,000 feet altitude until shortly after touchdown;

e) ingestion of atmospheric and landing strip contaminants from the lower altitudes during the landing process; and

f) condensation on cooler Payload surfaces of outgassing products from the payload bay inner surfaces and liners.

Of the above listed processes, all are considered relatively minor except for d) and f). Little can be done about process d) unless the payload bay can tolerate greater pressure differences. The later the vents are opened the

better. Process f) can be alleviated by starting the purge sooner. Ingestion of atmospheric contaminants (process e)) during landing can be reduced by closing the active vents during the last 150 meters of landing altitudes and leaving them closed until purging is started.

A review of planned contamination control and operational procedures was made for a 1 meter class cryogenically cooled infrared telescope. This review indicated that the planned use of a Vacuum End Cap Assembly (VECA) and the use of a vacuum external jacket should minimize any contaminant potential previously discussed for the boost and reentry phases of these payloads. The VECA will seal the sensitive internal surfaces of the telescope from any condensibles or particulate contaminants. In addition, the external vacuum jacket will provide the necessary thermal relationships with the payload bay to minimize condensing of gaseous vapors present during these phases.

5.2.2 Recommendations - As a result of this study, the following recommendations are made with respect to identifying those program considerations felt important for implementing the necessary contamination control on those Spacelab/Payload configurations studied and the related Shuttle Orbiter/Spacelab interfaces.

a) Selection of external Spacelab non-metallic should be made with characteristic outgassing rates of no more than 1×10^{-9} g/cm^2/second at 100°C. The current maximum mass loss rate stated for non-metallic materials in Applicable Documents MSFC 50M02442 (0.04%/cm^2/hour) and JSC SP-R-0022 (total weight loss 1%) is approximately a factor of 6 greater than the recommended value. Specific surface thermal profiles, temperature dependence of the selected material, and external area of coverage will influence the final recommended outgassing rate.

b) Relocation of the Environmental Condensate Vent should be considered such that the vented plume of material will not impinge upon any Shuttle Orbiter/Spacelab surfaces. It is recommended that consideration be given to venting parallel to the +Z axis.

c) Consideration should be given to establishing a detailed analysis of ground contamination control clean up procedures, equipment, and utility with the emphasis towards utilization of less standard clean room control and maximum prelaunch conditioning to minimize potential on orbit particulate matter.

d) Further detailed analysis should be conducted to establish the impact of the OMS backflow contribution to the payload bay. An alternate recommendation is to close the payload bay doors during individual OMS firings. Timelining OMS firings such that the return flux would be a minimum should also be considered.

e) RCS and VCS engine firing constraints should be established to minimize the external Payload surface degradation during deployment, rendezvous, and retrieval activities. These constraints should be established in conjunction with rendezvous procedures and operations to insure minimum contaminant potential.

f) Stationkeeping for Free Flying Payloads during checkout should be no less than 200 feet for deployment times and checkout times on the order of orbits. Stationkeeping for those periods which may take a day or longer should be on the order of a 1000 feet for minimum contaminant potential. Recommended stationkeeping position for minimum contaminant potential is above and forward of the Shuttle Orbiter providing inhibiting of certain forward firing Orbiter thrusters is feasible.

g) Consideration should be given in the early design and manufacturing stages to provide accessibility, to structural surfaces and proper selection of construction materials which would be conducive to clean up for maximum particulate control.

h) Optical instruments that have contamination concerns should consider in-situ calibration systems which can serve as contamination monitors.

i) The use of a Vacuum End Cap Assembly (as in the case of an infrared type Payload) or the use of aperture covers will be an effective mechanism for contaminant sensitive Payload to minimize contamination during non-operational periods such as boost, reentry, and stowage.

j) For systems employing a VECA, consideration should be given to the use of internal Payload pressure gages and a non-condensing dry gas support system for purging which could detect and minimize the contaminant potential from anomalous conditions such as small leaks.

5.3 Future Study Activity Recommendations - The following future study activities are identified. These study recommendations are based upon those areas felt necessary to support the Spacelab program for contamination control, those areas identified as a result of this study that require further investigation, and those of which their scope was beyond this study or insufficient detailed information was available.

a) Continue the development of a Spacelab Contamination Configuration Model which can be used independently (or complementary with the JSC Space Shuttle Orbiter Contamination Model) to identify Spacelab contamination impacts or to establish Spacelab/Shuttle Orbiter interface requirements. The Spacelab Contamination Configuration Model should include:

   1) modeling the remaining major Spacelab configurations;

   2) assessing and modeling major Spacelab sources;

   3) modeling the most contamination susceptible first two year mission Experiment configurations;

   4) assessing and modeling the major first two year mission Experiment sources; and

   5) identification of the first two year mission Spacelab/Experiments operational timelines.

b) A contamination Mission Requirements and Profile Data Bank should be established to define for each Spacelab/Experiment configuration and the first two year mission profiles the necessary contamination related data. As a mission is defined and the associated Spacelab/Experiment configurations are established, the proper mission requirements and profile can be selected to identify important contamination related data. The Mission Requirements and Profile Data Bank should include:

1) mission durations, orbital altitudes, Spacelab/Experiment definitions, attitude and pointing requirements, and observation/target requirements;

2) critical Experiment/surface usage time;

3) Spacelab/Experiment configuration thermal profiles; and

4) Spacelab/Orbiter interface and special subsystem requirements.

c) Based upon the definition of the Spacelab/Experiment configuration to be flown for a given mission and the resulting mission requirements and profile, integrated contamination predictions and assessments should be established to provide a timely Mission Feasibility Status in support of mission definition. The Mission Feasibility Status should identify the following:

1) a description of the contaminant induced environment;

2) the Spacelab/Experiment configuration sensitivities;

3) the Spacelab/Experiment configuration variances and risk factors;

4) the identification of recommended improvements and studies;

5) the identification of recommended testing (both small and large chamber); and

6) the identification of operational constraints.

d) As a result of this study, the following areas are considered to require additional specific study and/or investigation:

1) the potential impact of the OMS engine firings upon Payloads exposed in the payload bay area;

2) an optimum location and the resulting clearing time constraints for the ECV such that the vented condensate material will not impinge upon any Orbiter or Spacelab surfaces and will clear the vicinity of the spacecraft effectively;

3) the particle production capability of the RCS engines;

4) the rendezvous/retrieval RCS engine constraints to minimize the contaminant potential of externally exposed Payload surfaces during these phases; and

5) the importance of and/or the potential of particle reencounter on successive orbits as a result of ECV, RCS, and general sloughing of material from the Shuttle spacecraft.

e) A Spacelab Contamination Users Guide should be developed to provide a contamination assessment guide for use by groups engaged in the design and development of Spacelab experiments and systems for assessing the impact of contamination on Spacelab experiments and systems. This guide could establish a consistent basis for this assessment at a time when required controls and modifications identified during assessment can be implemented with minimum impact to the Spacelab Program.

6. NOTES

6.1 Abstracts - The following abstracts are presented where applicable in support of technical footnotes contained in this report.

a. Chirivella, J. E. and Simon, E.: "Molecular Flux Measurements in the Back Flow Region of a Nozzle Plume," J.P.L., JANNAF 7th Plume Technology Meeting, April 1973.

Abstract - A series of tests were conducted at JPL to measure the mass flux in the far field of a nozzle plume in a high vacuum with emphasis on the back flow region. Existing theories to predict the far field of a plume are not adequate for large angular departures from the plume axis. The measurements presented in this report provide fairly accurate data for off-axis angles as large as 140° (i.e., in the back flow region). This region, since it is well behind the exit plane, is of particular interest to those concerned with instrument contamination. Usually, sensitive spacecraft surfaces are located in the region affected by the back flow.

The tests, which utilized five different nozzles, were performed at the JPL Molsink facility. Parameters such as expansion ratio, throat diameter, nozzle lip shape, and plenum (chamber) pressure were varied. Carbon dioxide and nitrogen gases were flowed and mass flux measurements were taken using quartz crystal microbalances in as many as nine different locations relative to the test nozzle.

The tests have resulted in a large matrix of data that were correlated and compared to the Hill and Draper flow prediction theory. These tests are a continuation of earlier attempts to provide quantitative data, the results of which were previously published in two JPL reports.

Several conclusions with respect to the effect of nozzle and gas parameters on the amount of back flow mass flux are offered, and it was demonstrated that gaseous mass fluxes, which are not predictable by present theories, are encountered in the region behind the nozzle exit plane. This knowledge is significant if materials incompatible with the gaseous exhaust products are used in this region.

b. Simons, G. A.: "Effect of Nozzle Boundary Layers on Rocket Exhaust Plumes," AIAA Journal, Vol. 10, No. 11, November 1972.

Conclusion - It has been shown that the density in the plume at large angles from the centerline is a sensitive function of the ratio of the nozzle boundary-layer thickness to the exit radius. Analytic expressions have been developed which relate the gas density to the rocket nozzle and boundary-layer properties. However, these relations possess an arbitrary constant (U_{1ave}/U_1), the value of which lies between 0.5 and 1. Further numerical experiments are required to confirm the existence and the value of this constant.

The angular distribution of the boundary-layer streamlines in the rocket plume has been obtained, and it has been demonstrated that only a very small portion of the boundary-layer gas expands beyond the inviscid turning angle θ_x. The primary effect of viscosity at the walls of the rocket nozzle is to raise the density of the expanding boundary-layer gas and reduce its velocity.

These conclusions are valid only if the "exponential" density profile is a universal result. Additional numerical computations are necessary to establish this assumption and confirm the present results for the plume density.

c. Viehmann, W. and Eubanks, A. G.: "Effects of Surface Contamination on the Infrared and Visible-Light

Scattering of Highly Reflective Surfaces at Cryogenic Temperatures," Goddard Space Flight Center, NASA TDN-6585, February 1972.

Summary and Conclusions - Infrared emittance and visible-light scattering of highly reflective substrates are strongly affected by the deposition of contaminant layers. Emissivity increases most noticeably between zero and approximately 2.5 micron thickness of the contaminant film as a result of reflection and absorption losses in the surface coating. In this thickness range, emissivity increase per unit film thickness is highest for water, followed in order by aliphatic hydrocarbons, silicone oil, aromatic hydrocarbons, and carbon dioxide. Scattering of visible light changes very little below about 2 microns thickness but increases rapidly with thickness beyond 2 to 3 microns. Shielded two-stage passive radiation coolers will be significantly degraded by the deposition of infrared absorbing contaminants of between 200 and 500 microns thickness.

d. Muscari, J. A., and Cunningham, A. C.: "Gemini 12 Contamination Study," Martin Marietta Aerospace Report R-67-2, January 1967.

Conclusions - The transmission curves indicate that visible and near infrared radiation are not attenuated significantly by the deposits on the samples. Therefore, this experiment does not support the concern for error in the horizon sensor optics (infrared region) by contamination from the Titan III Stage I/II staging exhaust products.

However, in the ultraviolet region the transmission does decrease significantly as the wavelength of the radiation becomes shorter. The decrease in transmission due to the deposit appears to be the same for the samples which witnessed powered flight to 1st EVA and those from 1st EVA to

2nd EVA. Since both sets of samples experienced about the same time in orbital flight, the similarity in percent transmission indicates that very little if any contamination was deposited during the powered flight. Therefore, this experiment does not support the concern for significant degradation of optical payloads by contamination from the Titan III Stage I/II staging exhaust products.

However, it must be recognized that in future space flights attempts to obtain very precise or absolute optical measurements in the ultraviolet wavelength region must take into account the error introduced by the contamination deposited on the surface of the optical components as found in this experiment.

e. Hittman Associates, Inc.: "Investigation of Materials Contamination on the ATS-F Spacecraft," NAS5-11826 - Modification No. 6 - Report No. HIT-495, May 1971.

Abstract - A preliminary technology survey and an evaluation of materials contamination control on the ATS-F have been conducted. The existing approach to contamination control of the ATS is to minimize outgassing materials on the spacecraft and to correct problems pertaining to contamination as they are recognized by technical personnel. Determination of acceptable materials is principally based on short term total weight loss and condensable (on a 25°C surface) weight loss in a vacuum. There appears to be little consideration of the materials that are given off or how they behave in a long term application. Some of the experimental packages appear to have been constructed with little consideration of the materials that are inside them.

A coordinated contamination control program should be initiated immediately by the appointment of a

contamination control representative who is responsible to the ATS project management or functions as a part of the quality control organization. His first assignment should be to plan a contamination control program for the ATS spacecraft with a full realization of the present status of the spacecraft program. Much of the design and some of the hardware has been completed, and therefore the number of changes that can be made in the spacecraft must be minimized.

There are a number of recognized potential contamination problems. The major ones are outgassed materials from the solar panels that may affect sensors on the Earth Viewing Module, particulate contamination that may perturb the startrackers, effluent from the N_2H_4 thrusters which may be a problem, possible interactions with the ion thrusters, and the spacecraft test facility. Tests and analyses are required to evaluate these and other contamination areas.

Contamination monitors should be flown on the spacecraft. These should be selected so that the location and the sensory techniques are consistent with the desired data and the expected spacecraft characteristics.

f. Hoffman, R. J., et al: "Plume Contamination Effects Predictions," the CONTAM Computer Program Version II, AFRPL-TR-73-46 MDC G4733, August 1973.

Abstract - The effect of rocket exhaust plume impingement on sensitive vehicle surfaces is an area of continuing concern in the design of spacecraft, missiles, and reentry vehicle systems. Specifically, the contamination and subsequent degradation of functional surfaces, such as solar cells, thermal control coatings, optical lenses, optical view ports, and highly reflective surfaces, have resulted in compromises of mission effectiveness. The objective of this study was to develop a single computer code capable of predicting the production, transport, and deposition of engine and plume contaminants, and the

change in absorptivity, emissivity, reflectivity, and transmissivity of a functional spacecraft surface, such as thermal control coatings and optical view ports and lenses, resulting from plume contaminant deposition or mechanical abrasion (sand blasting). Both bipropellants and monopropellants have been treated. Surface chemical reaction with a deposited plume contaminant layer was not treated. Analytical models and computer subprograms have been developed and integrated to form the CONTAM computer program. Complete User's manuals for each of the computer subprograms as well as the CONTAM program are included in this report, along with details of the analysis and numerical methods. A sample case illustrating the CONTAM program's capability is presented.

6.2 Abbreviations - The following abbreviations were used in this report and represent terminology relevant to this study and programs used to obtain supportive data for this study.

AAP	-	Apollo Applications Program
AM	-	Airlock Module
AMPS	-	Atmospheric, Magnetospheric and Plasmas in Space
AMU	-	Atomic Mass Unit
ATM	-	Apollo Telescope Mount
ATM-DA	-	Apollo Telescope Mount Deployment Assembly
CEI	-	Contract End Item
CMG	-	Control Moment Gyro
COFW	-	Certificate of Flight Worthiness
CRS	-	Cluster Requirements Specification
CSM	-	Command and Service Module
DSSM	-	Dedicated Solar Sortie Mission
ECV	-	Environmental Condensate Vent
ESRO	-	European Space Research Organization
ESTEC	-	European Space Research and Technology Centre
EVA	-	Extravehicular Activity
FAS	-	Fixed Airlock Shroud
GET	-	Ground Elapsed Time
GSFC	-	Goddard Space Flight Center
HRIR	-	High Resolution Infrared Radiometer
IBM	-	International Business Machines
IR	-	Infrared
ISIS	-	Ionosphere Test Satellite
IU	-	Instrument Unit
JSC	-	Lyndon B. Johnson Spacecraft Center
KSC	-	Kennedy Space Center
LES	-	Launch Escape System
LOX	-	Liquid Oxygen
LST	-	Large Space Telescope
LTV	-	Low Temperature Vulcanized
MCD	-	Mass Column Density
MDA	-	Multiple Docking Adapter
MDAC-E	-	McDonnell Douglas Astronautics-East
MDAC-W	-	McDonnell Douglas Astronautics-West
MOL	-	Molecules
MSFC	-	Marshall Space Flight Center
NASA	-	National Aeronautics and Space Administration

NCD	-	Number Column Density
NEP	-	Noise Equivalent Power
NOMAD	-	Newtonian Orbital Mechanics and Atmospheric Drag
NVR	-	Non Volatile Residue
OA	-	Office of Applications
O&C	-	Operations and Checkout
OMS	-	Orbital Maneuvering System
OWS	-	Orbital Workshop
PI	-	Principal Investigator
PIB	-	Payload Integration Building
PS	-	Payload Shroud
QCM	-	Quartz Crystal Microbalance
RCS	-	Reaction Control Subsystem
RSI	-	Reusable Surface Insulation
RTV	-	Room Temperature Vulcanized
SAS	-	Solar Array System
SCCV	-	Skylab Contingency Condensate Vent
SL-1	-	Spacelab-1
SL-2	-	Spacelab-2
SL-3	-	Spacelab-3
TRW	-	Thompson Ramo Woolridge
UV	-	Ultraviolet
VAB	-	Vertical Assembly Building
VECA	-	Vacuum End Cap Assembly
VCS	-	Vernier Control Subsystem
Y-POP	-	Y Axis Perpendicular to Orbital Plane
ZLV	-	Z Axis Local Vertical

Å	-	Angstrom
$B/B_{\odot}$	-	Brightness ratio
cm	-	centimeter
$d_{1.5}$	-	Distance from 1.5 m telescope
$D^{1.5}$	-	Diameter aperture
$\Delta \alpha$	-	Change in solar absorptivity
$\Delta\lambda/\lambda$	-	Bandwidth
f	-	Effective focal length
f/	-	Focal ratio
ft	-	Feet
g	-	Gram
H_f	-	Focal Plane Irradiance
H_o	-	Input Irradiance
hr	-	Hour
Hz	-	Hertz
(i_1+i_2)	-	Mie Coefficients
^oK	-	Degrees Kelvin
km	-	Kilometer
λ	-	Wavelength
lb	-	Pound
L/D	-	Length to diameter ratio
M	-	Molecular Weight
Muv	-	Star Magnitude - Ultraviolet
Mv	-	Star Magnitude - Visible
$N_{1.5}$	-	Noise at 1.5 Meter Telescope
r_a	-	Airy disc radius
r	-	Particle Radius
t	-	Time
T	-	Temperature
Vx	-	Velocity-X direction
Vz	-	Velocity-Z direction
W	-	Watts
ω	-	Angular velocity
X_o	-	Station Number - X Axis
Y_o	-	Station Number - Y Axis
Z_o	-	Station Number - Z Axis

6.3 Definitions - The following definitions are presented to clarify terminology used in this report which reflect unique characterization of the principles, procedures, and methods of application that would be generally applicable to utilization of the results of this study.

a. Mass Column Density - The mass contained in a constant unit cross-sectional area extending from an origin to infinity, expressed in units of Mass/Unit Area.

b. Number Column Density - The number of molecules contained in a constant unit cross-sectional area extending from an origin to infinity, expressed in units of Molecules/Unit Area.

c. Flux - Mass flow through a unit area, expressed in units of Mass/Unit Area/Unit Time.

d. Line-of-Sight - The line being sighted from a critical surface and extending along a given direction of interest to infinity. Column densities are calculated along lines-of-sight.

e. View Factor - That fraction of the total mass leaving one surface that is capable of impinging upon another surface of interest in its field-of-view.

f. Interaction Sphere - Geometrically developed spheres along a given line-of-sight which establishes surface-to-surface relationships in its field-of-view such as distance, angular, and view factor.

g. Interaction Plane - Geometrically developed discs along a given line-of-sight which establishes surface-to-surface relationships in their fields-of-view such that for a calculated contaminant density at a given disc location the returned flux to a surface of interest from contaminant interaction with the ambient atmosphere can be calculated.

h. Return Flux - The mass flow of contaminants through a unit area reflected back to a surface of interest as a result of collisions with the ambient atmosphere expressed in Mass/Unit Area/Unit Time.

i. Outgassing - That contribution to contamination which comes from the material bulk characteristics and is long term in nature.

k. Offgassing - That contribution to contamination which is related to the volatiles which are either adsorbed to the material and/or carried in the preparation of a material and boil off very rapidly when exposed to vacuum.

l. Beta Angle - That angle between the orbit plane and the earth-sun line.

APPENDIX A

Skylab Manufacturing to Launch Contamination Control

The Skylab program cleanliness requirements for different ground handling phases were developed for the different module and experiment contractors and were contained in their respective ground contamination control plans. A general summary of these requirements is as follows:

a) Contamination control shall be practiced throughout all phases from manufacturing thru prior to launch.

b) Major elements of hardware which makes up the orbital payload shall be maintained to cleanliness specified in the Cluster Requirement Specification (CRS) and shall be implemented by the Contract End Item (CEI) specification for each hardware item. A certificate of cleanliness will be required for submittal at the time of Certificate of Flight Worthiness (COFW).

c) Exterior surfaces of modules installed within the payload shroud: Airlock Module (AM), Multiple Docking Adapter (MDA), internal Payload Shroud (PS), internal Instrumentation Unit (IU), forward S-IVB dome, Apollo Telescope Mount Deployment Assembly (ATM DA), and Orbital Work Shop (OWS) solar arrays shall be maintained visibly clean. ATM cleanliness requirements shall be in accordance with 50M02412.

Exterior surfaces of the payloads exposed to the normal atmospheric conditions while on launch pad (OWS, IU, Fixed Airlock Shroud (FAS), PS) will be maintained to a visibly clean condition which will not permit gross physical contamination.

d) Interior surfaces of habitable areas shall be maintained to a visibly clean condition.

e) Cleaning shall be accomplished in a clean area Class 100K/MSFC Std-246A. (No more than 700 particles per cubic foot greater than 5 microns.)

f) Portable equipment and supplies brought on-board the habitable crew areas shall be maintained in accordance with MSC-SPEC-C-8.

g) OWS Waste Liquid Oxygen (LOX) Tank interior surfaces shall be maintained at the above specification for interior surfaces of habitable areas.

h) The interiors and exteriors of hardware and all exposed surfaces within the enclosure formed by the PS, FAS, IU and OWS forward dome; and the habitable areas of the OWS, AM and MDA shall be maintained visibly clean during periods of transportation and storage and during all phases of operations at Kennedy Space Center (KSC).

In addition, the enclosure formed by the payload shroud and the forward dome of the OWS and the cluster cabin interior shall be maintained at a Class 100K clean room level in accordance with MSFC-STD-246A. Surfaces shall be visually clean.

i) Plastic covers, used to insure cleanliness for transportation, shall remain in place until after stacking.

j) Internal and external surfaces of the Command Service Module (CSM) shall be controlled in accordance with MSC specification MSC-Spec C-5A Specification for Apollo Spacecraft Cleanliness, and MSC-Spec C-8 Cleanliness Specification for Spacecraft onboard equipment.

k) The Apollo Applications Program (AAP) payloads will be purged while in the stacked position in accordance with the requirements specified in AAP-1 Fluid Requirements 10M30831. Purge gas supply shall be controlled as specified in MSFC-PROC-404 or 10M30831 as applicable.

l) Covers used to facilitate cleanliness during transportation and storage shall remain in place except where essential to accomplishment of checkout and/or stacking operations.

m) Payloads will be purged while in the stacked position in accordance with 65ICD9541, 65ICD9542, 65ICD9793 and 66ICD8042.

n) Cleanliness work shall be maintained in a Class 100K clean room during all servicing and repair operations.

o) Experiments which require installation or removal after stacking shall be controlled within the requirements specified in individual experiment CEIs.

The contamination control phase of the flow of the Skylab-1 module and experiment hardware from post manufacturing to launch are discussed below.

a) Cleanliness requirements for the Airlock Module/Multiple Docking Adapter/Payload Shroud and the Deployment Assembly from the completion of their respective building programs to their movement into the Vertical Assemply Building (VAB) at KSC are discussed below.

1) The AM which included the FAS and the ATM DA assembly and installation were scheduled to be performed under clean room conditions in accordance with process specification PS 20501 in the manufacturing area. When the AM was moved to Building 66 at McDonnell Douglas Aerospace Corporation - East (MDAC-E), it was scheduled to have items packaged to maintain contamination control. Building 66 by specification is a Class 100K clean room facility.

On completion of activities in Building 66, the AM was transferred to Building 103 and prepared for altitude chamber test with the MDA. On completion of the tests in the altitude chamber, the AM/MDA was prepared for shipment to the Operations and Checkout Building (O&C) at KSC. This installation was packaged to maintain contamination control. During shipment, this installation was scheduled to have contamination control. On arrival at the O&C Building at KSC, the AM/MDA was contamination controlled during receiving and inspection. The low and high bay area of this facility are Class 100K clean rooms.

On completion of activities in this Building, the AM was installed to the MDA/FAS/DA & PS and was prepared for shipment to maintain contamination control and was subjected to contamination control during transfer to the Payload Integration Building (PIB). During O_2/N_2 system flight pressure checks in the PIB, the installation was in a Class 10K clean room environment. On completion of activities in the PIB, the installation was packaged to maintain contamination control for transfer to the VAB.

2) The MDA cleanliness requirements specified that the exterior and interior of the MDA would be visually clean when viewing with a white light. The exterior of the MDA equipment truss was subjected to the same requirements. All work on the MDA and MDA Equipment Truss at Denver was accomplished in a Class 100K clean room following all cleanliness requirements for this level of clean room. Both the MDA and the MDA Equipment Truss were packaged for shipment to maintain complete contamination control. The MDA Equipment Truss was subjected to contamination/environmental control during shipment. On arrival at MDAC-E Building 103, the MDA Equipment Truss was under contamination control during receiving inspection. The MDA was delivered to MDAC-E Building 66 and was under contamination control during receiving inspection. The MDA and MDA Equipment Truss were mated with the AM in Building 66. The contamination control condition discussed for the AM in 1) above applied to the MDA and Equipment Truss through the remaining steps of its activities before going to the VAB.

3) Payload Shroud - The contamination control requirements imposed on the PS were equivalent to the program requirements. However, the CEI further required the inspection of the interior surfaces of the PS with ultraviolet light.

During manufacturing and storage at MDAC-W, the PS was scheduled to be under contamination control. Contamination control/environmental control was imposed during shipment from MDAC-W to the O&C Building at KSC. All activities in the O&C Building including receiving inspection, checkout and installation to the payload were conducted in a Class 100K environment. The nose cone of the PS was moved to the PIB and to the VAB under contamination/environmental control. The lower section of the PS was installed to the payload in the O&C Building. As mentioned above, this total assembly was packaged to maintain contamination control and contamination/environmental control imposed during shipment.

4) ATM-Post Manufacturing and Checkout - The vendor and experiment developers including solar wings, thermal shield, and the following experiments including the S052, S054, S055A, S056, S082A & B and the H-Alpha 1 & 2 were packaged for shipment to maintain contamination control. The experiments were shipped to the MSFC ATM fabrication area which has contamination control within the facility. They were scheduled to be under contamination control during receiving inspection. After installation and alignment and assembly of the Rack to the Spar, the instrumentation was packaged and shipped to the Building 4708 clean room under complete contamination control. In Building 4708, the clean room which is contamination controlled to MSFC-STD 256A, both the ATM subsystem containing the experiments and the solar wings were integrated to make up the ATM assembly and were system tested. The ATM assembly was then moved to Building 4755 and 4619 under completely contamination control conditions. On completion of these tests, the solar wings were disassembled, packaged and shipped under completely controlled contamination conditions to the O&C Building at KSC.

The ATM assembly less the solar wings were then packaged and shipped to Johnson Space Center Buildings (JSC) 36 and 32 for thermal vacuum tests under complete contamination control. Contamination control was maintained while in the ATM was in these two facilities.

The ATM was then packaged and shipped under contamination/environmental control conditions to the O&C Building at KSC. After being off loaded in the O&C Building, the ATM including the solar wings was moved into the Class 10K ATM clean room for receiving inspection and system tests. The total assembly was then packaged to maintain contamination control for movement to the VAB.

5) Orbital Workshop (OWS) Post Manufacturing and Checkout - The OWS contamination control requirements at MDAC-W in STP 0350 were that the OWS would appear clean to white light inspection. Additionally, the habitable area surface was required to be inspected with ultraviolet light as a part of final inspection. Contamination Control Plan MDC 60384 defined the ways and means of implementing the CEI requirements and identified the various contractor specifications and procedures which further defined the activities and materials to be used to achieve the CEI requirements. The plan also identified that the OWS would be enclosed in an Environmental Protective Kit 1B84818 for storage and transportation and that the environment within the OWS would be maintained by the operation of a Dynamic Desiccant System.

1B84053 described the monitoring requirements, environmental protection and surveillance that was provided the OWS during transit by barge to KSC. No special contamination control/cleanliness requirements were imposed. This document also specified that certain experiments would be packaged to maintain contamination control until it went through receiving inspection at the low bay

in the VAB at KSC. The VAB low bay maintained a contamination control environment while the OWS was located in it.

6) Instrument Unit (IU) Post Manufacturing and Checkout - The IU was fabricated at the International Business Machine's (IBM) facility in Huntsville under partial contamination controlled conditions. The IU was packaged under completely contamination controlled conditions and shipped to the VAB high bay area at KSC under complete contamination/ environmental conditions specified in 10Z01445.

7) Solar Array System (SAS) Post Manufacturing and Checkout - The SAS was fabricated and tested at Thompson Ramo Woolridge (TRW) in a facility having contamination control. It was packaged for shipment under partially contamination controlled conditions. The SAS went through receiving inspection at the O&C Building at KSC with contamination control in effect. After checkout, it was packed and shipped to the VAB high bay area under contamination/environmental conditions. In the VAB high bay, the OWS was installed onto the launch vehicle with the IU and SAS attached to it and preps were made to move the complete assembly to the pad.

8) Experiment Post Manufacturing and Checkout - The following experiments were shipped from the vendor to the VAB under environmentally controlled conditions: D024A, M512B, S009A, S190, S191, S192A, S193A, S194, PRSP-BU and EREP-SE. While in the VAB, the experiment developers performed the following under facility contamination control conditions:

   a) Returned the D024B protective cover to their facility for disposition.

   b) Added flight emulsion to S009C to make S009B.

   c) Refurbished the PRSP-BU.

Upon completion of these activities above, these were put in bonded storage with contamination control and held there as late as possible before installation to the Skylab assembly. The Proton Spectrometer 479 and M512, S192B and S193B were packaged at the vendor to maintain contamination control during shipment. On receipt at the VAB, the Proton Spectrometer was installed and checked out on the MDA. After receiving inspection under contamination control conditions the M479 and M512 and the S192B and S193B were placed in bonded storage under contamination control where they were held as late as possible before installation to the Skylab assembly.

After closeout of the SWS the completed payload was packaged and transferred to the pad under environment/contamination controlled conditions. The following instruments were shipped to MDAC-W (STP 0350) under complete contamination control conditions:

ESS-OT, M074, M092, M093, M131A,C,D; M133A, M171, M172, M478A, M509A, S019A,B,C; S020A,B; S073A, T020, S149A,C; T002A, T003A&B; T013, T025A and T027B,C,E,F.

The following experiments were installed in the OWS and shipped to the VAB low bay at KSC under the environmental control level that the OWS was subjected to: ESS, M074, M092, M093, M131A,B,C,D; M133A, M171, M172, M487A, M509A, S019B, S020A, S073A, S149A, S182C&D; T002A, T025A. Since these experiments remained with the OTA from then on, they were subject to the same contamination control as the OWS.

Experiments T003A&B, S019A&C, S020B, S149C, S183F, T027B/S073B, T027C and T013 were returned from the STP 0350 to the vendors where they were under contamination control during receiving inspection. They were later packaged to maintain

contamination control and shipped to the VAB low bay area where they were subjected to receiving inspection under contamination control conditions. After undergoing tests in the VAB low bay area, they were moved to the high bay area for final disposition.

b) Central Ground Contamination Control Organization - A central ground contamination control integration organization was chartered in November 1969 and was in effect until January 1973. The bulk of the effort of this organization was terminated in July 1972. This group reviewed the contamination control plans for all major contractor hardware and made recommendations on the adequacy of the plans.

They developed detail plans for monitoring contamination control of experiment fabrication and test for approximately 52 Skylab experiments for which they had contamination control responsibility.

The task of monitoring ground contamination control was accomplished by NASA and the responsible contractor.

Specific on orbit observation of Skylab contamination that could be attributable to ground conditions include the following:

1) Streaks were noted on the outside of the Wardroom Window that possibly could have been the result of rain water getting on it while on the launch stand since this window did not have an external cover.

2) The S052 Principal Investigator (PI) stated that particle streaks showed on about 3% of photographs taken by this experiment which were caused by particulates external to the vehicle. Particles were noted on the S052 occulting disc three different times. Attempts were made by the astronauts

to remove the particles during EVA's on SL-1/2 and SL-3. The particles appeared to "go away" on cleaning but later returned.

3) While retrieving film from the EVA, an astronaut commented that a loose washer floated out of the ATM.

APPENDIX B

Contamination Review of Unmanned and Manned Systems

A review of contamination effects on a series of unmanned satellites and manned space vehicles was made for Goddard Space Flight Center (GSFC)[1] in 1971. The following is a summary of these effects and other independent investigations.

a) Nimbus - The Nimbus II and III spacecraft carried High Resolution Infrared Radiometers (HRIR) which depended, in part, upon a suitable cold temperature surface for good sensitivity. This cold surface was to be provided by a radiant cooler. In both spacecraft, the operation of the cooler was unsatisfactory because of poor temperature control. The probable cause of the behavior has been attributed to contaminant recondensation.

The HRIR contained an infrared detector composed of a lead selenide photoconductor that has an optimum operating temperature of approximately 195°K. The radiant cooler portion of the radiometer was designed to maintain the temperature of the detector at a temperature lower than the optimum. A small electric heater is provided to raise the temperature to the operating point.

Since the reasons for the behavior of Nimbus II and III were not understood, a committee was formed to look into the situation and attempted to find an explanation. Several possible sources of the effects were considered and the most probable cause was stated as contamination. Condensation of contaminants on the cold patch would explain the observed temporary improvement of performance after each of the attitude perturbations during which the sun could have boiled the contaminants off of the cold patch. The gradual degradation of performance following the postulated cleaning could be explained by the recondensation of

(1) Hittman Associates, Inc.: "Investigation of Materials Contamination on the ATS-F Spacecraft," NAS5-11826 - Modification No. 6 - Report No. HIT-495, May 1971.

material that was continuing to outgas from the spacecraft. No contamination control fixes were made to Nimbus IV based on data analysis of Nimbus II and III.

The Nimbus IV was launched about a year after the Nimbus III and immediate problems were encountered with contamination. In this case, the experiment was not identical with the one on Nimbus II and III but the basic reason was the same. In Nimbus IV, the failure was with the filter wedge spectrometer (FWS). The problem was attributed to the presence of ice on the detector with indications that it was compounded by the presence of other impurities.

Upon investigation, it was found that the complete mechanism of ice formation was not clear since one would have expected that the ice would sublime when the partial pressure of water vapor in the vicinity of the detector fell below the vapor pressure of water at the detector temperature. The apparent sublimation rate was not as high as one would expect and the effect may have been due to the effect of combination with other contaminants with low vapor pressures such as outgassing products originating from oils, adhesives, or plasticizers. These could form a barrier or could depress the temperature of the ice and thereby decrease the sublimation rate.

It was deducted that most of the problem was due to the design and construction of the FWS. The detector was in a venting pathway and acted as a cryogenic trap. Large quantities of water vapor flow out of the vent from multifoil insulation in the vicinity and further, the interior of the FWS and the detector serve as a source of contaminants that would vent in the same manner. To complicate the situation, there were large quantities of outgassing materials in the vicinity of the FWS.

b) OAO - A review of a thermal vacuum test of OAO A-2 indicated that the edges of the cryo-panel and aluminized mylar between the cryo-panel and spacecraft had heavy deposits of a single phthalate ester, dimethylsilicone (at least 10 members of a homologous series), and a complex series of hydrocarbons. These compounds also were found on the walls of the gap between the experiment package and the spacecraft. The only organic deposits found in the electronic bays of the spacecraft were some hydrocarbons on the Star Tracker and also silicones and hydrocarbons on the Star Tracker pitch package.

The source of the contaminants was not determined but the dimethylsilicone was thought to be the result of the combined outgassing of the various RTV, LTV, and other silicone resins used in the spacecraft. The hydrocarbon fraction could have come from poor cleaning of the cutting oils, various lubricants, and possibly white oils sometimes used as plasticizers. The phthalate ester was felt to most likely come from some single type of plasticizer polymer.

c) OGO - On OGO II, the concentration of water vapor at launch was observed to be 1×10^{10} particles/cm^3 which decayed to 2×10^8 after 80 days with a leveling in the decay rate after this. A level of $2 \times 10^7/cm^3$ was reached in 180 days. On OGO IV, the level at launch was observed to be $8 \times 10^9/cm^3$ and was about $3 \times 10^8/cm^3$ after 40 days. A $2 \times 10^7/cm^3$ value was reached at the end of 220 days on OGO IV. The difference has been explained as due to the presence of super insulation in the case of the OGO II, whereas it was not present on the OGO IV. A mass spectrometer was located on the end of a boom and could be rotated about an axis perpendicular to the velocity vector of the spacecraft. When this was done, there was no significant change in the detected water vapor indicating that there was no ram effect such as would be expected if the spacecraft were passing through a cloud of water vapor as opposed to being imbedded in a cloud

of the contaminant. Another mass spectrometer on the OGO IV was evacuated and sealed prior to launch and not opened until the second day in orbit. There was no indication of contaminants prior to opening the seal. Then there was an immediate rise in mass No. 18 (supposedly water vapor) with a peak of $4 \times 10^8/cm^3$ reached about 100 minutes after the seal was broken. The mass No. 18 indication reached the noise level of the instrument of $3 \times 10^6/cm^3$ after 90 days. Similar behavior was found with the Explorer XVII. The mass No. 18 measurement was about $10^7/cm^3$ at first, with the noise level of the instrument reached in about 20 days.

It was reported on OGO III that spacecraft outgassing seemed to have been the dominating influence upon the neutral composition observed by the mass spectrometer. There appears to be some correlation between instrument container temperature and the observed concentration of mass No. 18 (water vapor - the most dominant constituent). Generally, there was little variation of neutral concentrations during a single orbit but a decrease in concentrations with increasing time on orbit was noted.

Further, analyses of the OGO III mass spectrometer data showed a molecular flux density in the vicinity of the spacecraft of about three orders of magnitude above the density that one would predict from satellite drag determinations. Consideration of the theory of interaction of outgassed molecules indicated that the molecules at that altitude should have been swept away very rapidly by collisions with the ambient materials. No explanations of this phenomenon was made.

A review of the surface contamination measurements of OGO-VI was made. The measurements utilized a quartz crystal microbalance to define the condition of Al and Au surfaces. The primary source of outgassing on the spacecraft was indicated to be the two solar

panels baking in the sun. A time constant for the exponential decay of the outgassing was ascertained to be 1000 hours. The maximum amount of contamination adsorbed by surfaces exposed to outgassing was reached after five months in orbit (96 mg/m^2 for the Al surface and 52 mg/m^2 for the Au surface). The contamination had a desorption activation energy of 26 kcal/g mol which is in the range of energies expected for epoxies and vacuum oils. The surfaces were stated to be undergoing cleaning by desorption and sputtering by upper atmosphere neutral impacts at rates of $1.2 \times 10^{-9} g/m^2$/second and 2.3×10^{-9} g/m^2/second, respectively.

Studies in which the surfaces were pointed in various directions showed that the contamination flux reached a maximum when pointed toward one of the two solar panels and that the contamination flux dropped to near zero when the surfaces were pointed toward deep space. This is stated to show that the panels appeared to be the major source of the contamination.

The satellite outgassing flux was also stated to consist of two main components; volatile gases such as oxygen, nitrogen, carbon dioxide, and water; and low volatility materials such as oil and paint that require a long time to outgas. The volatiles are stated to boil off very rapidly and to reach very low levels in the first few days after launch. The cloud that enveloped the satellite apparently shielded it from direct atmospheric impacts for many hours and the incoming atmospheric molecules lost a significant portion of their kinetic energy by particle-particle interactions before impacting on surfaces.

Since the low volatility materials do stick to the surfaces, these can be determined. The outgassing flux in the yicinity of the experiment was 2.7×10^{11} particles/cm^2/second. This decreased exponentially

with time and the time constant which fits the data was 1000 hours as mentioned previously. The maximum amount of material absorbed by the Al surface was calculated to be 9.6 $\mu g/cm^2$. The front surfaces of the solar panels were solar cells and the back was coated with Zn_2O pigmented potassium silicate inorganic paint, both of which have low vapor pressures. It was therefore concluded that the source of the outgassed material must be the epoxies used in the panels and from contamination absorbed in vacuum tests.

d) ISIS (Ionosphere Test Satellite) - Testing was conducted in thermal vacuum and solar vacuum test chambers to determine outgassing characteristics for ISIS. Gas chromatographic analysis of post-test cold plate witness samples revealed that they had no less than 20 separate compounds which were identified by infrared analysis. These were methyl siloxamer, aliphatic hydrocarbons, and esters.

Thermal vacuum retest scans showed a comparatively low level of outgassing material as compared to the levels found during the initial thermal vacuum tests. Analysis of this post-test cold plate sample showed about the same compounds as found in the initial thermal vacuum tests but the amounts were smaller.

The only general conclusions that were drawn were that the methyl siloxamer were fragments of larger silicone molecules such as RTVs. The pthalate esters are typical of epoxy adhesives such as FM 1000.

During solar vacuum test, methyl phenyl siloxanes and aliphatic hydrocarbons predominated and were determined also by infrared analysis.

A part of the ISIS outer surface was composed of solar panels. Some of the panels appeared to be bleeding. Two of these panels were analyzed to determine the source of this bleeding. One of the

panels had undergone a thermal vacuum treatment and the other was identical (apparently) but had not been subjected to this treatment. The solar cells were adhered to the module substrate with GE RTV 511 methyl phenyl silicone. Since this silicone rubber is white, it was coated with RTV colored black with silicone color V-1747. The total amount of polymer on each panel was reported as about 100 gms. Washing of the panels with chloroform followed by evaporation yielded a white residue with an infrared spectrum identical to that of a low molecular weight silicone oil. Evaluation of the available literature concerning the RTV 511 led the authors to conclude that they could expect about 3.2 gms of the low molecular weight silicone oil for each 100 gms of the polymer. Under conditions of space, the material would coat most of the outer surface of the satellite.

e) RAE - An analysis was made of the outgassants of materials during thermal vacuum testing on the RAE-A Satellite. A complex mixture of outgassing products was found on the condensor plate of chamber 237. Analysis showed it to have the composition 20% complex mixture of aliphatic and/or alecyclic hydrocarbons (probably a lubricating oil of a high boiling petroleum fraction); 45% a mixture of silicone fluids consisting of about 30 percent dimethylsilicones and 15% phenyl-methylsilicones; and other minor compounds (dimethylsilicones most likely come from outgassing of RTV or other silicone resins); 30% a mixture of phthalate esters and aliphatic ketones (most likely a result of plasticizer outgassing from polymers); and 5% of a complex residue that was not further characterized.

In reviewing the potential contaminant sources, the material did not contain any residue from oil from the diffusion pumps or from the mechanical pumps used with the vacuum chamber. However, during the latter portion of the time the satellite was in the

test chamber, there was a spill of Dow Corning 200 (10 centistokes fluid) and it was not possible to conclude whether this was the reason for the dimethylsilicone or whether this came from some other source. The records appear to indicate, however, that the sample may have been taken prior to the spill. If this were the case, then the contaminant could not have come from the spilled oil.

One possible source of outgassed material is the considerable volume of honeycomb core structure on the satellite. This uses FM-100 adhesive, a proven high outgasser. It has a total weight loss of five to eight percent, of which about four and one-half percent is volatile condensables.

f) Mariner - A consistent problem that plagued the Mariner IV spacecraft during the early portion of its mission was that roll error signal transients would occur frequently and on occasion would cause loss of the Canopus star lock. The first attempt at a midcourse maneuver was aborted by a loss of lock shortly after the gyros began spinup. Canopus lock was lost six times within a period of less than three weeks after launch and each time a sequence of radio commands would be required to reacquire the star. After a study of the problem, the investigators concluded that the behavior was due to small dust particles that were being released from the spacecraft by some means and were drifting through the star sensor field-of-view. Sunlight scattered from the particles then appeared as illumination equivalent to that from a bright star. This would cause a roll error transient as the object passed through the field-of-view while the sensor was locked onto Canopus. When the object was bright enough that it exceeded the high gate limits at eight times the Canopus intensity, the spacecraft would automatically disacquire Canopus and initiate a roll search for a new star. Finally, a radio command was reset that removed the high gate limit. There was no further loss of Canopus lock, although roll transients occurred 38 more times before planetary encounter.

The problem was handled similarly with the Mariner V by effectively removing the high gate limit through setting it to infinity.

Dust particles caused roll transients on Mariner VI and VII. Violent responses were observed on the roll error channel during the mid-course motor burn and after explosive valve firings on both of the spacecraft. Apparently, large numbers of dust particles were released from the spacecraft during these events. As a result of this behavior, the spacecraft was programmed to operate on gyro roll control for the planet flyby period.

On the recent Mariner X mission, considerable attitude control gas was lost as a result of the Star Tracker locking on to what was considered to be a bright particle.

g) AIMP-E - A study was made of the launch phase contaminant environment of the AIMP-E satellite which was launched on July 19, 1967. No contamination was found at the experiment location during the initial launch phases but contamination was found about three and one-half minutes after fourth stage ignition. The contamination reached a maximum 15 minutes after ignition, remained on the surface for about 43-1/2 minutes, decreased slightly, and then remained constant for the remainder of the experiment life. The effect was a change in normal absorptance of the experiment surface from about 10 to 23.5 percent. The contamination was associated with residual gases from the spent stage or with outgassing of materials due to the increased stage temperature. It was concluded that the spacecraft should have been shielded from contamination deposits on sensitive surfaces and that the fourth stage motor casing should have been jettisoned as soon as practical after firing.

h) SAS - The SAS-A and B spacecraft used the FW-4 motor as a fourth stage for the Scout launch vehicle. Because of concern that the fourth stage would outgas and contaminate the solar cell surfaces as well as the spacecraft silverized teflon thermal coatings, a series of tests were conducted at GSFC to obtain semi-qualitative information. These tests were conducted in a bell jar using samples from an FW-4 rocket motor casing. After the contamination test, most samples were exposed to 500 hours of simulated sunlight in a vacuum. Test data showed that there were contamination effects on the cover glass and on the solar cells. The samples located further away from the contamination source exhibited greater effects. This was probably due to the cooler temperature which one would expect because of the geometry. Overall conclusions were that the cover glass transmittance might be degraded by about 10% following motor firings plus 500 hours of solar exposure.

Reduction of the solar cell output from the same tests was about 6%. Examination of the solar cell characteristic curves showed that the entire curve was degraded which is the type of behavior one would expect from a decreased energy input. No attempt was made to draw conclusions from the test because of the limited nature of the investigation.

i) SERT-II - Ion thrusters have been flown on the SERT-II spacecraft. Solar cell sensors were located near the exhaust of two ion thrusters so that effluent effects could be studied. The sensors indicated about 50% opacity in 6 to 12 hours, irrespective of the temperature. The contamination was not due to the mercury ions because they would have evaporated at the higher temperature. Therefore, it was concluded that it was due to the deposition of molybdenum which came from the grid structure of the thruster. The danger with this type of contaminant is that the effect is permanent. The metallic

deposit has a very low vapor pressure and for practical purposes will not evaporate. Experiments were also conducted with SERT-II to find the effects of a neutralizer bias. There was no problem with a positive bias, but when they attempted to bias the neutralizer negatively, they found increased neutralizer currents. It was not immediately determined if this was due to flow of electrons from space or due to a loop current from the neutralizer cathode to a nearby positive surface.

j) Lincoln Experiment Satellites (LES) - Contact was made with Mr. P. Waldren of Lincoln Laboratories, Cambridge, Mass., the Project Manager for the LES series of communication satellites, concerning the possible degradation of any of their satellites due to contamination.

Mr. Waldren stated that to their knowledge no degradation has occurred to any of the six satellites now on orbit due to contaminations; however, they stated that the solar cell efficiency was quite low and that they could be quite dirty and still function normally. In general, the satellites are covered with solar cells and the areas that are not are covered with mylar coated aluminum or gold. In addition, the orbit for these satellites is equatorial synchronous thus increasing the molecule mean free path to where reflected flux is minimal.

The LES series of satellites were put on orbit by the Titan III transtage which uses N_2H_4/N_2O_4 propellant for both the main propulsion system and the RCS. Although this propellant is relatively dirty, steps were taken to assure that the satellites were never in an engine firing plume. The feeling was that there was no degradation due to the TIII propulsion system.

k) Manned Programs - Optical contamination problems were first encountered in the Mercury program, and have continued in the Gemini and Apollo flights. Initial problems were attributed to materials flowing from the nose cone. The viewing windows were covered during launch to eliminate the problem. During the later Gemini flights, an oil-like deposit formed on the windows. These were attributed to outgassing of non-metallic materials in the window area, principally silicones from the window gaskets, and were later minimized by prelaunch vacuum and heat cure cycles. In addition, "fireflies" were noted by the astronauts which were later attributed to particulates.

Micrometeorite experiments conducted on the Gemini program also revealed a number of contaminants including materials deposited on surfaces, surface pitting due to high velocity thruster debris, chemical interaction with corrosive materials, and gouging by cohesive particles in a combined vibration and accelerating environment.

A semi-quantitative analysis of the window contaminant material from the Gemini GT-4-7, 9-12 space capsules allowed estimation of the percent of each element present. Examination of the possible sources and assignment of the probable importance has been performed and tabulated. The major contamination sources include: the control engine throat ablator, propellant impurities, waste dumps, window seals, and the sea.

A comparison of the Gemini results with those from Apollo has also been performed. The results are similar with the exception of an additional source in the case of the Apollo -- the launch escape system. The Apollo windows in the apex of the cone remained relatively clean. The hatch and side windows were flush with the conical vehicle surface and have been reported as being the most vulnerable to contamination in flight.

APPENDIX C

Review of Available Aircraft Programs

The NASA CV-990 Airborne Laboratory was an experiment operational program sponsored by NASA using a Convair jet passenger transport. The cabin was modified for adaption of a multitude of experiments in standardized racks with standard electrical power, data recording, and communication systems furnished. The airplane had minimum modifications made for the NASA airborne program. For instance, no changes were made to the air conditioning system. In discussions with NASA personnel at Ames Research Center, they stated that the "Experimenters" never indicated concern about the particulate cleanliness in the cabin. If they had a cleanliness requirement, it was their responsibility to provide the necessary protection. NASA did, at times, provide flexible air conditioning ducts to a specific payload station window area for potential window defogging if requested prior to a flight by the Experimenter. The duct was a 2 inch flexible hose that would be connected to the standard cabin air condition plenum running along the ceiling. The duct would be taped or affixed to the experiment and pointed toward the window over which it directed normal air conditioning air.

A number of special ports were installed in the fuselage at various elevations and longitudinal locations. In addition, several of the standard passenger windows were modified for special purpose use. These special ports and windows were used previously for the installation of optical quality glass, defrosting systems, and safety features.

Traces of engine oil vapor was often present in the air conditioning duct, especially when the system was first activated. A satisfactory air filtering system was not found to eliminate this contaminant. However, a remedy, although somewhat inconvenient, was to cover the inside surface of the windows with paper until observation time. Such protective covering could be removed for periods of one to two hours during which time no significant deposits of oil were formed. In any event, the inside surfaces of the windows were readily accessible for cleaning during flight.

All of the outside nadir windows and seven of the 65° elevation windows had sliding shutters for protection of the external surface of the optical windows. The shutters on the 65° windows were pneumatically sealed. These shutters could be cranked out of the field-of-view during flight. The remaining optical ports were kept clean while on the ground by taping plastic sheets over the windows.

In addition to the 990 aircraft, Ames now has a Lear Jet Infrared Astronomical Program and a C141 one meter Infrared Astronomical Program. They stated that on both the programs that the telescopes were open to the atmosphere and that the infrared detectors were separated by seals. Thus far they have had no contamination problem with these infrared telescope systems.

In conclusion, Ames has had no significant contamination problem in their aircraft programs. They feel that with the short duration of experiment exposure that the Experimenters have provided the necessary contamination control. Ames plans no contamination control measures for their aircraft in the future. Based on the short time duration of the 990 experiment exposure and the responsibility of the Experimenter for contamination control, it is felt that this program is not correlatable with the Shuttle Program.

APPENDIX D

Contamination Considerations for a 1 Meter Class Infrared Telescope

The following contamination considerations are based upon available design and planning information for contamination control of a 1 meter class infrared telescope such as that envisioned to be used for the Shuttle Infrared Telescope Facility. As design and planning changes occur during the development of such a facility, these considerations may change and require further analysis. Two principle design considerations for the infrared telescope will minimize any contamination potential. These are the Vacuum End Cap Assembly (VECA) and the vacuum jacket. These will be discussed along with other considerations such as the potential for anomolous conditions to arise for the telescope which may tend to present a contamination impact to this type of system.

After manufacture and final cleaning, a Vacuum End Cap Assembly (VECA)is planned to be placed over the aperture of the telescope and the complete telescope assembly placed in an aluminum canister. The VECA forms an airtight seal that precludes the entrance or exit of any gases or vapors. The VECA will remain in place from this time until the telescope has been placed on orbit and is ready for operation.

Approximately 13 days prior to launch, the telescope inner tube and vacuum jacket are pumped down to vacuum and tested for leakage over a three day period. Approximately 10 days prior to launch, cooldown is started by pumping supercritical helium into the cryogen dewar. Cooling and testing for leakage and instrument operation is completed within 3 days. Between 60 and 70 hours before launch, the cryogen tank is topped to replace any loss in helium. Final topping of the cryogen occurs at the latest access to the instrument which is presently expected to be about 8 hours prior to launch. During the remaining prelaunch environment and launch, the entire telescope is protected by the vacuum jacket and the VECA from condensible vapors and particulates.

Any ingested vapors will not condense on the telescope external walls since these surfaces will follow the ambient payload bay temperatures fairly closely. The free particulates incurred during boost will have an opportunity to migrate away from the Shuttle Orbiter during on orbit pre-operation conditioning of the telescope and should be no problem.

When suitable on orbit environment conditions have been obtained, the VECA will be backed off and the telescope will be deployed for operation. During operation, the telescope may use any or all of 3 contamination control devices; these are:

a) A low-contamination window located within the tube just ahead of the secondary mirror (this window folds in half when not in use and is occulted by the secondary mirror support strut);

b) A low-contamination cover located on a rotatable ring outside the telescope and near the outer end of the fore baffle. (This cover will be transparent and can be rotated over the open end of the fore baffle to protect the internal optical elements and permit continued operation (though slightly degraded) during periods when contaminant emissions may be a problem but the threat is low); and

c) A heavy-contamination cover mounted on the same ring as the low-contamination cover but displaced 120° from it. (This cover is a machined aluminum plate fitted with a face gasket to insure a good seal against contaminant entry when contaminant levels are too high to allow viewing).

The rotatable ring upon which the two covers are located also supports the sunshield which is the reason for it being rotatable. The sunshield will also provide some small amount of contaminant shielding.

These operational covers and protective windows will provide protection for the cooled infrared telescope surfaces depending upon their usage in relationship to the contamination impact analysis presented in section 3.4.

At the end of the infrared telescope mission, the telescope will be retracted into the Shuttle Orbiter payload bay and the VECA emplaced. The bay doors will be closed and the bay vents will remain closed through the high heat reentry period and until the Shuttle Orbiter has reached the 70,000 foot altitude. At this time, the bay vents will be opened to permit pressurization of the bay. However, because of the VECA seal, the telescope tube will maintain the on orbit vacuum and internal cooling will continue until the cryogen is exhausted, either by depletion or being vented. External telescope surfaces will be permitted to attain near ambient temperatures because of the vacuum jacket isolation around the inner tube. As in the launch period, the vacuum jacket and the VECA provide ample protection for the infrared telescope providing that they maintain their integrity. Should these protective measures fail, potential contingency effects could occur.

Two contingency situations may occur that would permit the telescope optics to become contaminated to varying degrees. One of these is leakage of the VECA seal and the other is complete failure of the VECA closure mechanism.

In case of complete failure of the closure mechanism, the telescope will start pressurizing with the payload bay. Because of the extremely low telescope inner surface temperatures, nearly all gases ingested will start condensing on these surfaces. If sufficient cryogen is available, the condensation will continue until the telescope is placed in its shipping container or the cryogen is vented and the telescope permitted to warm. This period could encompass reentry and 17 hours on the ground before the payload bay is opened. Because of the continuous condensation occurring new air will be continuously drawn into the telescope during the waiting period. The maximum amount of air that can be condensed by this process is a mass equal to about 5% of the remaining cryogen plus what can be condensed by the cooled aluminum bulk of the telescope in rising from -269°C to -218°C.

The logical action to take after the bay doors are opened, is to vent the cryogen as soon as possible and permit the telescope to warm up. The VECA should not be closed and probably couldn't be because of frost buildup. A warm clean gas purge should be started and continued until all the condensation has been removed.

Condensation buildup within the instrument will automatically be limited by the insulating characteristics of the frozen condensate. As the external condensate surface becomes farther and farther separated from the cryogen source by the buildup, it will become warmer and sequentially reject one gas after another as it exceeds their freezing point until, eventually only water vapor will be condensing on it. The remaining load of condensed materials should be removed and the telescope completely dried before sealing it in its shipping container. This is the purpose of the warm, dry gas purge. The amount of condensed buildup cannot be calculated accurately under these conditions as it is dependent upon the cooling capacity characteristics and the insulating quality and crystalization characteristics of the multifluid condensate.

In the case where the VECA can be closed on orbit but a leak in the seal developes, condensation will occur at a much slower rate dependent upon the leak size. If the leak is small, a greater majority of the condensation will occur in the heavier

gases at lower altitudes and a higher percentage of H_2O and CO_2 can be expected in the condensate.

Even if the cryogenic supply should be depleted shortly before or shortly after re-entry starts, there is sufficient bulk heat capacity in the telescope tube, internal support structures, enclosures, and optical elements to condense a considerable amount of gases during reentry and landing. The open volume of the 1.5 meter telescope, will be in the vicinity of 800 ft^3. Total cooled bulk in the liner, support structures, enclosures, and optical elements is expected to exceed 30,000 in^3 (492,000 cm^3). The specific heat of aluminum for various temperatures is:

Temp °C	p Ht Cal/gm
-250	0.0039
-240	0.0092
-233	0.0165
-200	0.076
-150	0.1367
-100	0.1676
- 50	0.1914
0	0.2079

The sum of the products of specific heats and degrees for aluminum between -269°C and 0°C is approximately 33.56 calories/gram. Total cooled aluminum volume in the telescope is approximately 1.33×10^6 grams. The total heat capacity is therefore sufficient to freeze 5.6×10^5 grams (1234 lbs) of 0°C water vapor or 4.26×10^5 (939 lbs) of 25°C water vapor. This mass of water is equivalent to the amount of vapor to be found in 2121 and 1614 telescope internal volumes of 100% relative humidity air respectively. However, this amount of air and vapor cannot possibly be ingested as will be shown later. The sum of the products of specific heats and degrees for air from +25°C to freezing at -218.4°C is approximately 123 cal/gram. The sum of the products of specific heats and degrees for aluminum between -269°C and -218°C is approximately 0.801 cal/gram. The total heat capacity for the cooled aluminum between these temperatures is 1.07×10^6 calories. The aluminum could therefore freeze out 8.7×10^3 grams of air or about 1/3 the warm air (25°C) mass in the tube, liquify 1.42×10^4 grams or 80% of the remaining air

and still have sufficient excess heat capacity to freeze 4.05 x 10^5 grams of water (the equivalent of the water vapor in 1534 telescope volumes of air at 25°C, 100% relative humidity.

What would actually happen though is that the air in liquifying and freezing would keep the pressure in the telescope tube below the external pressure until a sufficient volume of warm air had entered to raise the telescope inner surfaces to just above the temperature of liquid air. The condensed air would then boil off and raise the pressure in the tube to or slightly above external pressure excluding any entry of external air for a while. This stalemate could last for a very long time depending upon the rate at which heat could be conducted through the telescope insulation. As the telescope gradually warmed, the inner volume of air would gradually expand and, in leaking back out of the tube, continue to exclude entry of any new air that would otherwise assist in the warming. The frigid air escaping could cause condensation of water vapor on surfaces near the leak exit. This somewhat stagnant condition could easily persist throughout the 17-hour waiting period until the payload bay doors are opened and the telescope removed. There would be no indication that a leak had occurred except for perhaps a slight frosting and/or water condensation around the leak area. An internal pressure gauge would provide a good positive indication of the seal integrity. However, there is nothing the ground crew can do at this time because handling procedures will require that the telescope be placed in its shipping container and returned to the owner. If the return requires a long period of time, the gradually warming telescope could generate a considerable pressure within the sealed canister unless a pressure relief valve is incorporated in the canister.

Under the preceding conditions, only a very small amount of water vapor will be ingested, perhaps the amount in two telescope volumes of 25°C, 100% humidity air at a maximum. This would amount of 528 grams (1.16 lbs) at the most.